UNIVERSITÄT OSNABRÜCK

Photolithographic surface functionalization for spatio-temporally controlled protein immobilization

Dissertation

Presented to the department of Biology/Chemistry, University of Osnabrueck
in partial fulfillment of the requirements for the degree of
'*Doctor Rerum Naturalium*'

Maniraj Bhagawati

Osnabrueck

December 2011

Table of Contents

1 INTRODUCTION 1

1.1 AIMS AND STRATEGIES 2

1.2 SURFACE BIOCOMPATIBILITY 4

1.3 FUNCTIONAL PROTEIN IMMOBILIZATION 7

1.3.1 Biotin/ streptavidin 9

1.3.2 Histidine tag/ transition metal ions 10

1.3.3 HaloTag/HaloTag ligand 11

1.3.4 ybbR tag/ Coenzyme A 13

1.4 PATTERNING 15

1.5 PHOTOLITHOGRAPHY 16

1.5.1 Principles of photolithography 17

1.5.2 Methodology 18

1.5.3 Photo-induced Fenton reaction 21

1.5.4 Nitroveratryloxycarbonyl-based caging 21

1.6 TECHNIQUES FOR ANALYSIS 22

1.6.1 Reflectometric interference spectroscopy (RIfS) 22

1.6.2 Total internal reflection fluorescence spectroscopy (TIRFS) 24

1.6.3 Confocal Laser Scanning Microscopy (CLSM) 25

1.7 REFERENCES 27

2 PATTERNING OF HIS-TAGGED PROTEINS BY PHOTODESTRUCTION OF TRIS-NTA 35

2.1 INTRODUCTION 35

2.2 MATERIALS AND METHODS 36

2.2.1 Materials 36

2.2.2 Protein biochemistry 37

2.2.3 Surface modification 37

2.2.4 Protein binding experiments through Reflectance Interference (RIf) 38

2.2.5 Confocal Laser Scanning Microscopy 38

2.2.6 Motility assays 39

2.3 RESULTS AND DISCUSSION 39

2.3.1 Characterization of the photodestruction process 39

2.3.2 Functional protein patterning 42

2.3.3 Protein patterning in a CLSM 43

2.3.4 Gliding of microtubules on kinesin patterns 46

2.4 CONCLUSIONS 48

2.5 SUMMARY 48

2.6 REFERENCES 48

3 BINARY PROTEIN PATTERNING BY NVOC-BASED CAGING 53

3.1 INTRODUCTION 53

3.2 MATERIALS AND METHODS 54

3.2.1 Materials 54

3.2.2 Protein production, purification and labeling 55

3.2.3 Surface chemistry 55

3.2.4 Surface patterning 55

3.2.5 Binding assays 56

3.2.6 Fluorescence imaging 56

3.3 RESULTS AND DISCUSSION 57

3.3.1 NVOC-based caging and uncaging 57

3.3.2 Binary protein patterning 58

3.4 CONCLUSIONS 60

3.5 SUMMARY 61

3.6 REFERENCES 61

4 MULTIPLEXED PROTEIN PATTERNING BY PHOTO-FRAGMENTATION OF HISTIDINE PEPTIDES 65

4.1 INTRODUCTION 65

4.2 MATERIALS AND METHODS 66

4.2.1 Materials 66

4.2.2 Proteins 66

4.2.3 Surface modification 67

4.2.4 Surface binding by real-time solid phase detection 67

4.2.5 Φ-His photocleavage in solution 68

4.2.6 Photolithography and fluorescence imaging 68

4.3 RESULTS AND DISCUSSION 68

4.3.1 Blocking efficiency of peptide and photo-fragmentation in solution 68

4.3.2 Patterning using a photomask 70

4.3.3 Patterning using a confocal UV laser 72

4.3.4 Multiplexed patterning in a CLSM 74

4.4 CONCLUSIONS 75

4.5 SUMMARY 76

4.6 REFERENCES 76

5 COMBINED PEPTIDE TAGS FOR IMPROVING IMMOBILIZATION EFFICIENCIES AND MICROPATTERNING OF PROTEINS 79

5.1 INTRODUCTION 79
5.2 MATERIALS AND METHODS 81
5.2.1 Materials 81
5.2.2 Proteins 81
5.2.3 Surface modification 81
5.2.4 Surface binding by real-time solid phase detection 82
5.2.5 Photolithography and fluorescence imaging 82
5.3 RESULTS AND DISCUSSION 83
5.3.1 Photo-fragmentation of His_{NVOC} *and patterning of His-tagged proteins 83*
5.3.2 Surface immobilization of His-Halo-tagged proteins 84
5.3.3 Surface immobilization of His-ybbR-tagged proteins 87
5.3.4 Patterning of H6-Halo-mEGFP 89
5.3.5 Patterning of H6-ybbR-EGFP 90
5.3.6 Functionality of patterned proteins 91
5.3.7 Multiplexed protein patterning 92
5.4 CONCLUSIONS 93
5.5 SUMMARY 93
5.6 REFERENCES 94

6 CONCLUSIONS 97

6.1 HIS-TAGGED PROTEIN PATTERNING BY PHOTODESTRUCTION OF TRIS-NTA 97
6.2 BINARY PROTEIN PATTERNING BY NVOC-BASED CAGING 98
6.3 MULTIPLEXED PROTEIN PATTERNING BY PHOTO-FRAGMENTATIONS OF HISTIDINE PEPTIDES 98
6.4 COMBINING PEPTIDE TAGS FOR IMPROVING IMMOBILIZATION EFFICIENCIES AND MICROPATTERNING OF PROTEINS 99
6.5 REFERENCES 100

7 SUMMARY 103

8 APPENDIX 105

8.1 PUBLICATIONS 105
8.2 LIST OF FIGURES AND TABLES 105
8.3 ABBREVIATIONS 107

1 Introduction

The biological functions of proteins are extraordinarily diverse and include catalysis, force generation, signaling and sensing. Controlling the spatial and temporal organization of proteins on surfaces becomes essential for harnessing their powerful capabilities for analytical, technological and medical applications. Protein patterning technology was first used by MacAlear and Wehrung in 1978 for fabrication of bioelectronic microcircuits [1]. However, of late its applications in biological assays and the biotechnology industry have proven to be especially crucial.

Traditionally, protein microarrays have been used for immunological assays, to study protein–protein interactions, or to identify targets of biologically active small molecules [2-4]. Antibody microarrays have long been used for the discovery and analysis of several clinically relevant disease biomarkers. A more recent application of protein patterns has been for the construction of biotechnological and biomedical devices. These applications mostly include chemical and biological sensors for the detection of environmental contaminants or diagnostically important analytes in biological fluids such as blood [5-8]. Very exciting possibilities for combining the enormous potential of proteins with the huge advances made in the field of microelectromechanical systems promise the development of very complex and diverse microdevices. With the recent development of advanced fluorescence microscopy techniques the use of protein micropatterns in fundamental biophysical research has also become common. Here microscopy is used to acquire not only spatial but also temporal information about the dynamics of protein complexes either in *vitro* or in cells. Therefore, methods to control organization of proteins on surfaces in a spatially as well as temporally defined manner are required.

Another recently developed application for patterned proteins has been in the field of tissue engineering. Several studies have demonstrated that lineage selection of stem cells is not only dependent on soluble cues such as growth factors, but is also strongly controlled by the insoluble extracellular matrix (ECM) which regulate a host of microenvironmental parameters such as cell adhesion sites and rigidity [9-11]. Therefore, the creation of complex tissue architectures will be highly facilitated by ability to pattern ECM proteins in order to mimic the natural ECM. Similar ECM-based control is also hypothesized to be active for neoplastic transformation [12, 13], and future therapeutic solutions might be based on controlling the tumor extracellular microenvironment instead of destroying tumor cells. All these applications make the development of new and more powerful methods for protein patterning not only of interest for basic research but also invaluable for the development and improvement of clinically and technologically relevant devices.

1.1 Aims and strategies

During the course of my PhD research I aimed to develop generic protein micropatterning strategies that could be widely applied for biochemical and biophysical studies. The primary objective during this process was that patterned proteins retain a high degree of functionality.Towards this goal, photolithography was chosen as a general patterning strategy as it allows surface structuring without exposing proteins to denaturing conditions. In addition, micropatterning strategies were based on a biocompatible surface functionalization layer that inhibits non-specfic protein-surface interactions and further preserves the integrity of immobilized proteins. Furthermore, in order to have optimal protein functionality it is necessary that patterned proteins be accessible to their soluble interaction partners. Therefore, specific peptide or protein tags that can be recombinantly fused to target proteins, and that can selectively react with their surface-bound ligands were used for protein immobilization. Therefore, micropatterning strategies were developed and optimized such that they were compatible with such protein targeting schemes. Finally, in order to make the techniques readily applicable in biology-focused laboratories it was ensured that they are not too technology-intensive and patterning could be carried out using easily accessible equipment.

As must be already evident from the above discussion, very special surface functionalization comprising of the following layers was needed in order to achieve these goals (Figure 1.1):

1. Biocompatible layer: This was needed to prevent non-specific protein-surface interactions which might cause proteins to adsorb on substrates leading to denaturation and loss of protein activity.
2. Protein capturing layer: This layer consisted of special moieties that could be used for immobilizing target proteins through interactions with specific peptide or protein tags.
3. Patternable layer: This comprised of photosensitive groups that could be used for lithography. While these functional groups might be available as a part of the first two layers, they could also be separately introduced into the surface functionalization scheme.

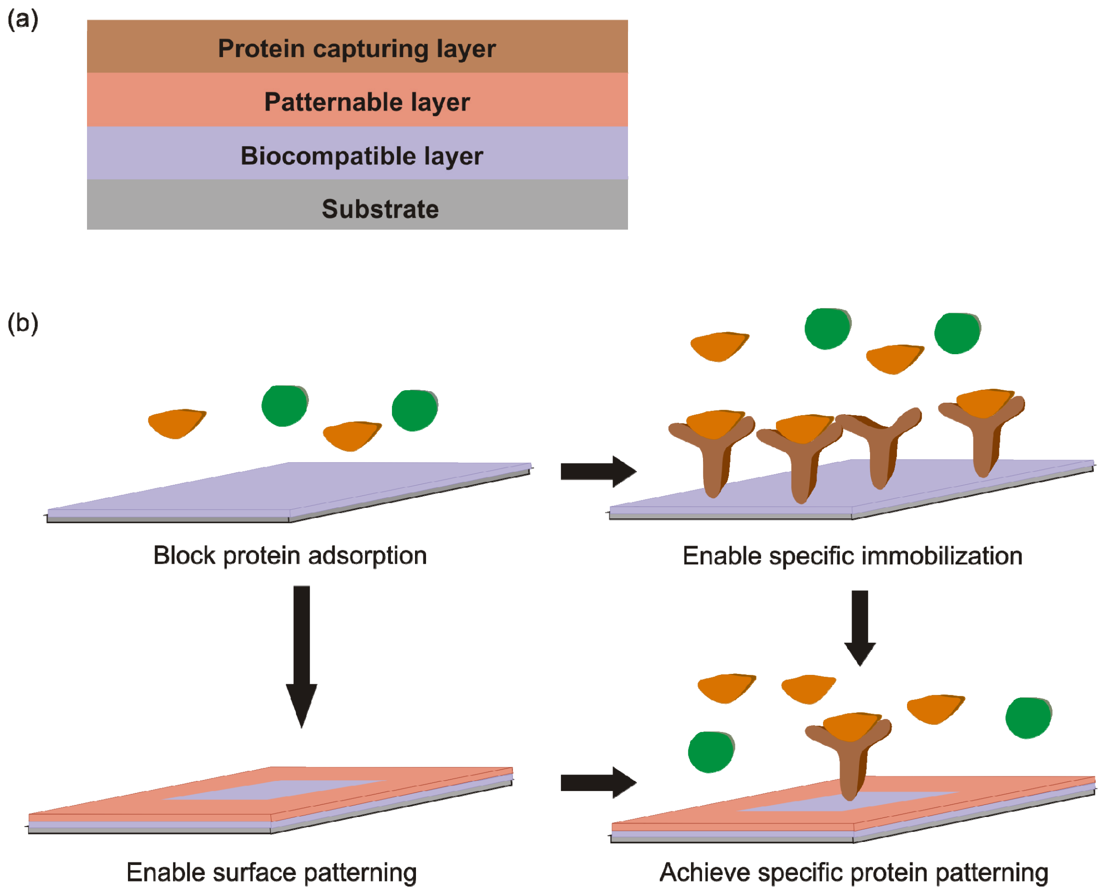
(a)
Protein capturing layer
Patternable layer
Biocompatible layer
Substrate
(b)
Block protein adsorption
Enable specific immobilization
Enable surface patterning
Achieve specific protein patterning

Figure 1.1 Surface architecture. (a) The different functional layers needed to achieve specific protein patterning on surfaces. (b) Cartoon depiction of the functions of the different layers. The same colour codes are used as in (a).

In the following sections each surface layer will be discussed in detail and the intricacies of fabricating such complicated surface architectures will be reviewed.

1.2 Surface biocompatibility

Proteins have a tendency to physically adsorb onto substrates even in the absence of specific recognition partners. Protein adsorption is a complex process, and the factors determining adsorption efficiency is controlled by surface, protein and solvent properties. Several kinds of protein-surface forces, including van der Waals, hydrophobic and electrostatic forces play a major role in this process [14, 15]. An adsorbed protein forms new bonds with the surface, often at the expense of interactions between amino acid residues, thus leading to denaturation and subsequent loss of protein activity. This is not a problem for many traditional techniques such as ELISA assays which can still function with the minor fraction of the immobilized protein which is still active. However, new developments such as fabrication of sensitive biosensors that require very low sample volumes or construction of complex biotechnological nanodevices require that most of the surface immobilized proteins retain their activity. Apart from loss of protein functionality, another drawback of non-specific adsorption is that it reduces the selectivity of several assays. For example, recent advances in microscopy have lead to applications of highly sensitive techniques based on single molecule detection, the efficacy of which is also often thwarted by unwanted background caused by non-specific protein adsorption.

Protein adsorption has been a subject of scientific study for quite some time, and several methods to reduce it have been established. The most commonly used method to prevent protein adsorption is to use a blocking solution containing a protein such as bovine serum albumin (BSA) that resists binding of other proteins. However, this suffers from the disadvantage that the blocking protein might denature and desorb over time thus reducing the blocking efficacy. A further limitation of this strategy is its inability to present other groups (e.g., ligands, antibodies) at the surface in a controlled manner [16]. Another strategy for passivation of surfaces utilizes lipids as a biocompatible surface layer [17, 18]. Lipids can form mono- or bilayers on a variety of surfaces and have been shown to efficiently block protein adsorption. This approach also facilitates the introduction of a variety of protein capturing moieties at easily controllable densities in the form of diverse lipid head groups. However, such lipid layers are quite sensitive to surfactants as well as to air thus reducing their durability. Over the years, the most robust and widely used approaches that have been developed have utilized hydrophilic polymers such as poly(ethylene glycol) (PEG) and polysaccharides, which can be covalently coupled to surfaces [19-22].

Early work had shown that the major contributor to protein repulsion for such polymers is their hydrophilic nature [23]. According to this theory, adsorption of a protein could take place only after the loss of the strong hydration shell of the polymer, which would be energetically unfavorable. However, recent simulations indicate that the dominant effect in protein repulsion might be the high degree of flexibility in the polymer chains which in thermodynamic terms is seen as high conformational entropy. Penetration of a protein into the chains decreases the chain entropy, giving rise to a sharp increase in the polymer-particle interaction energy [23]. According to this theory, efficient blocking of surfaces is achieved only when polymer chains acquire a so-called ‘brush’-like conformation (Figure 1.2).

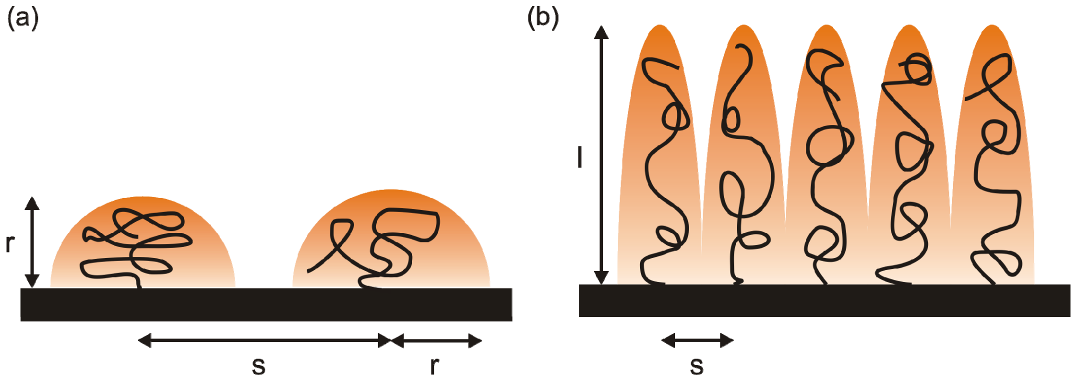

Figure 1.2 ‘Mushrooms’ versus ‘polymer brushes’. A sketch illustrating how surface-tethered polymer chains can take on either ‘mushroom’-like or ‘brush’-like molecular conformations depending upon the polymer packing density. The mushroom regime (a) occurs when the distance between neighboring chains s, is greater than twice the radius of gyration of the polymer r. The brush regime (b) is encountered when $s < 2r$ and the polymer chains are extended away from the surface at a height of l. The shaded areas indicate the probability of the polymer chains to occupy all positions within the shown volume. Modified from [24] .

As evident from Figure 1.2, the transition from a ‘mushroom’-like to a ‘brush’-like conformation can only occur at high surface density of polymers. Although physisorption has been used with some success for polymer-deposition, it has been observed that polymers can desorb over time leading to loss of biocompatibility. In order to have stable coupling of polymer chains, several techniques have been developed to activate substrates in order to make the surface reactive to the polymers. The most widely used among these techniques utilize self-assembled monolayers (SAMs).

SAMs are surfaces made from a thin molecular film of biological or chemical moieties and have stimulated much interest due to their flexibility of processing, molecular order, versatility and simplicity. Many systems undergo self-assembly including long-chain carboxylic acids on metal oxides, organosulfur compounds on noble metal surfaces and organosilane species on hydroxylated glass and silicon oxides [25].

For formation of SAMs on glass, the hydroxylated surface is reacted with a solution of alkyltrichlorosilane [26], alkyltrimethoxysilane [27, 28] or alkyltriethoxysilane [28]. The reactive silane groups first undergo a fast hydrolysis to form silanols, followed by slow condensation to oligomers, which then hydrogen bond to the surface hydroxyl groups and lead to the formation of covalent bonds [16]. The head group of the siloxane can be utilized to subsequently graft polymers (Figure 1.3).

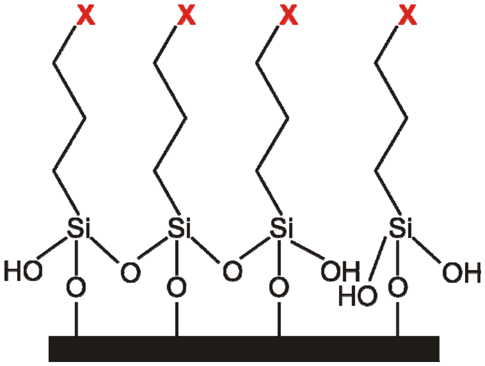

Figure 1.3 Schematic depiction of an alkylsiloxane SAM on glass. The terminal group ‘X’ can be used for grafting protein repelling polymers on the surface.

After activation with SAMs there are several techniques available to get high density polymer brushes on surfaces. Surface initiated polymerization (SIP) utilizes SAMs in which the terminal group ‘X’ can function as an initiator for a specific polymerization reaction [29]. The initiator surfaces are then exposed to solutions containing catalyst and monomer. By the right choice of monomers and by using controlled polymerization reactions such as atom transfer radical polymerization (ATRP) highly biocompatible polymer brushes can be formed on surfaces. As an alternative to ‘assembling’ polymer chains on surfaces via SIP, preformed polymers with reactive end groups can be grafted to the terminal functionality of the SAM. This is a comparatively simpler approach which nevertheless achieves very good polymer surface coverage. Polymers carrying diverse terminal groups are available which makes it very easy to introduce new functionalities on the surface in the same step. Since the micro- or nano-structuring of surfaces often happens at this stage of the surface architecture, the ability to flexibly choose the teminal group at this stage becomes important. Moreover, as the surface has been rendered protein repulsive, it has to be subsequently functionalized with protein binding groups that will enable the selective targeting of proteins to the surface. The terminal moiety offered by the polymer chains hence becomes necessary for the coupling of such groups as well.

1.3 Functional protein immobilization

Immobilization of proteins on surfaces while maintaining a high degree of functionality is of utmost necessity in most applications. However, before discussing specific details about different protein immobilization protocols it would be helpful to briefly review the requirements that guide our selection of techniques. Thus, the major characteristics which determine the suitability of an immobilization approach are enumerated below:

1. Binding stability: Stability of protein immobilization over time is required for both fundamental research as well as for technological applications. Covalent coupling of proteins is preferred when stability in the presence of mechanical forces or for very long durations is a requirement. However, for many experimental systems non-covalent, reversible protein immobilization is advantageous as it allows the reuse of substrates for multiple experimental cycles, of course provided that the interactions are stable over experimental durations.

2. Protein orientation: Proteins have very specific structural sites for interaction with their ligands which might become inaccessible after surface coupling. Therefore, immobilization techniques are required which enable protein capturing in a site-selective manner and thus ensure that protein orientation is uniform and appropriate for optimal functionality.
3. Kinetics: Since protein expression and purification is a time consuming and elaborate procedure it is helpful if low concentrations of proteins can provide high surface densities. This can of course be achieved by increasing the contact times between protein and surface, but this is not always possible because proteins are generally fragile and denature over time even at room temperature. Therefore, approaches that have a high reaction rate constant are always preferred..
4. Bioorthogonality: It is advantageous if proteins can be targeted to surfaces without going through arduous protein purification protocols. This means that the immobilization reaction has to be bioorthogonal, i.e. it has to be specific for the target protein even when it is present in low concentration in a complex physiological mixture such as a cell lysate.

Traditionally preferred methods for protein immobilization utilized either non-specific physical adsorption or chemical cross-linking of amine, thiol or carboxylic acid groups from amino acid residues onto suitable reactive groups on the surface. However, these techniques often cause denaturation of proteins, and at best lead to protein immobilization in random orientations. Moreover, these techniques are not bioorthogonal. One of the ways to address these issues is by immobilizing monoclonal antibodies (mAb) on surfaces as protein capturing agents. mAbs are very specific in terms of their recognition sites and thus guarantee selective protein immobilization in fixed orientations along with ensuring bioorthogonality. They can also function as a protein compatible layer that helps in maintaining protein structure. In spite of these advantages, production of high affinity mAbs for every individual target protein is quite arduous and hence this approach is not optimal.

A much more rational and effective strategy is site-specific immobilization which utilizes special amino acid sequences that can be recombinantly expressed as fusion tags with proteins of interest [30]. These peptide tags undergo very specific reactions with their ligands which can be chemically bound to surfaces. Such approaches not only lead to proteins being arranged in a definite, orderly fashion but also allow the use of spacers and linkers to help minimize steric hindrances between the protein and surface. Diverse peptide and protein tags are now available that satisfy many of the criteria that have been listed. Some of the approaches widely used for site-specific protein immobilization are discussed next.

1.3.1 Biotin/ streptavidin

Capturing proteins on surfaces by interaction of co-factor biotin with the proteins avidin/streptavidin and their derivatives is a classic approach in solid-phase assays [31]. Biotin rapidly binds to avidin/streptavidin in a 4:1 stoichiometry in a quasi-irreversible, non-covalent interaction (Figure 1.4). The binding stoichiometry of the biotin/streptavidin complex enables sandwich binding architectures on surfaces, where biotinylated surfaces are reacted with streptavidin, and the remaining biotin binding sites are used to capture biotinylated proteins. Alternatively, as streptavidin is a comparatively robust protein it can also be immobilized on surfaces via reaction of its amino acid residues to surface moieties (Figure 1.4). Biotin, being a small molecule does not usually affect protein function and reaction of biotin to amines, thiols or carboxylic acid groups in proteins has been traditionally the choice method for biotinylation. However, now several enzymatic processes utilizing petide tags such as the AviTag and the SNAP-tag are often used for site-specifically introducing biotin to target proteins thus further ensuring protein functionality [32, 33]. The biotin-streptavidin interaction has very high reported association rate constants between 3×10^6 - 4.5×10^7 $M^{-1}s^{-1}$ [34]. This, coupled with a very low dissociation constant of around 10^{-6} s^{-1} implies that the interaction is almost irreversible under normal conditions [35]. However, since biotin is needed as a coenzyme in the metabolism of fatty acids and amino acids such as valine and isoleucine, it is present in all cells. Therefore this immobilization strategy is not bioorthogonal.

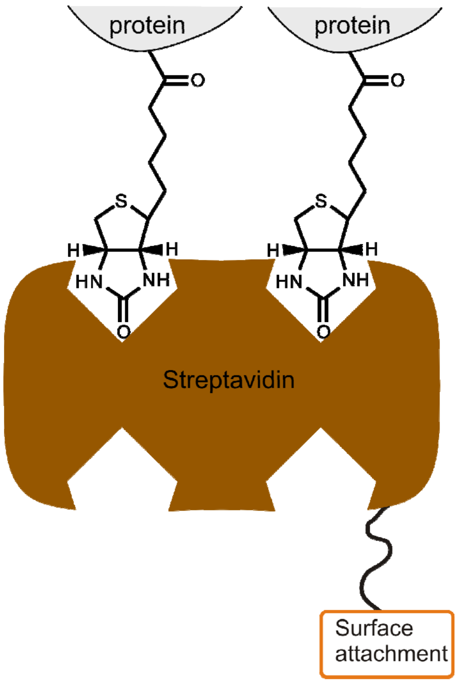

Figure 1.4 Biotin/ streptavidin-based immobilization. Streptavidin can be immobilized on surfaces either via biotins or by reacting residues such as lysines with surface moieties. Free biotin binding sites can be used to capture biotinylated proteins.

1.3.2 Histidine tag/ transition metal ions

Complexation of histidine residues with immobilized transition metal ions was originally studied as a strategy for affinity chromatography of histidine-rich proteins, but has been now systematically extended for the purification of recombinant proteins fused to a 6-10 histidine long peptide sequence [36]. Transition metal ions such as Zn(II), Cu(II), Ni(II), or Co(II) are immobilized by chelating agents such an iminodiacetic acid or nitrilotriacetic acid (NTA), thus maintaining 2 or 3 coordination sites free for histidines (Figure 1.5a). This interaction can be very efficiently disrupted by competing coordinators such as imidazole, which selectively and rapidly remove the protein from the chelator under mild conditions. Chemical strategies for functionalizing various kinds of surfaces by NTA have been developed and widely used for studying His-tagged proteins [37, 38]. However, a major problem with using NTA is that His-tagged proteins often slowly dissociate from the surface. This problem was recently overcome by synthesis of multivalent chelator head (MCH) groups, supramolecular entities with 2–4 NTA moieties incorporated onto branched and cyclic scaffolds (Figure 1.5b) [39]. These

MCHs, which recognize oligohistidine-tags by multivalent interactions (Figure 1.5c), were shown to bind His-tagged proteins with a high stability. Based on high association rate constants of around 10^5 $M^{-1}s^{-1}$ and dissociation rate constants as low as 5 x 10^{-5} s^{-1}, subnanomolar affinities of such MCHs for His-tagged proteins has been demonstrated [39]. Since histidine is a relatively rare amino acid in native proteins, recombinantly expressed proteins fused to His-tags can be preferentially immobilized on MCHs even in the presence of native proteins in the background. The binding selectivity can be further improved by immobilizing in the presence of a low concentration of a competitor such as imidazole, thus making this technique almost bioorthogonal in nature.

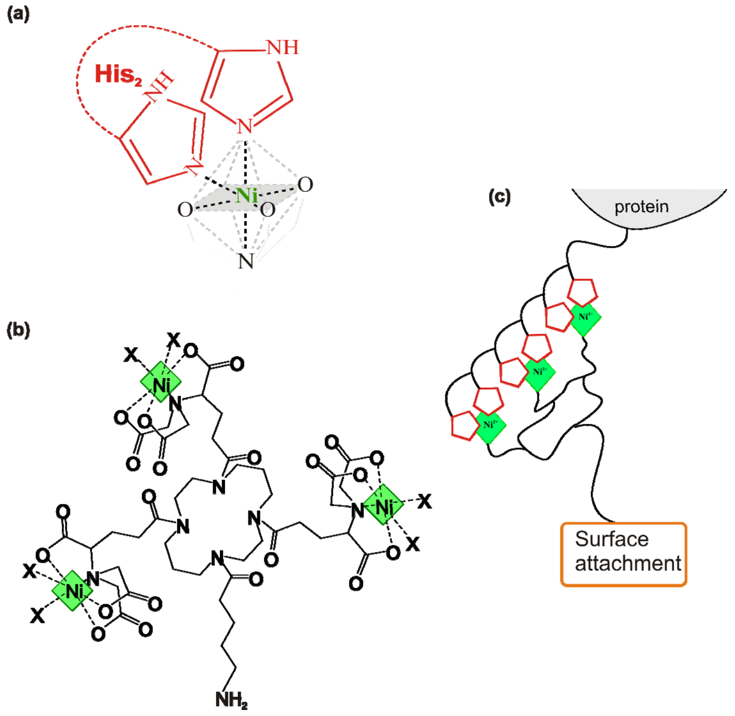

Figure 1.5 His-tag/ transition metal ion-based immobilization. (a) An NTA molecule can occupy four coordination sites of Ni(II), leaving two coordination sites vacant for histidines. (b) Tris-NTA consists of three NTA groups on a cyclic scaffold and has the capacity to coordinate three Ni(II) ions at once. (c) A surface immobilized MCH with three NTAs can theoretically coordinate six histidines at a time, leading to high affinity binding.

1.3.3 HaloTag/HaloTag ligand

The HaloTag protein (HTP) is a commercially available engineered form of the haloalkane dehalogenase DhaA which is found in some haloalkane utilizing strains of

Rhodococcus. The native enzyme is a monomeric protein (MW 33 KDa) that cleaves carbon halogen bonds in aliphatic halogenated compounds [40]. Upon nucleophilic attack by the Asp 106 of the enzyme to the haloalkane, the halogen atom is displaced and an ester bond is formed. Base catalyzed hydrolysis of this covalent intermediate, which is mediated by a conserved histidine located near the aspartate nucleophile, subsequently releases the hydrocarbon as an alcohol and regenerates the aspartate nucleophile for additional rounds of catalysis. HTP contains a critical mutation in the catalytic triad (His 272 to Phe) so that the ester bond formed between HTP and HaloTag ligand (chlorohexane, HTL) cannot be further hydrolyzed (Figure 1.6) [41]. HaloTag ligands labeled with small organic dyes have been developed for *in vivo* fluorescent labeling of target proteins [41]. Recombinant proteins carrying the HTP either at the N- or C-terminus can be thus efficiently labeled using this strategy. Recently, HTL has been fused to surfaces of luminescent nanoparticles and their targeting to intracellular proteins in cells has been demonstrated [42]. This study also clearly showed that the rate constant for the HTP-HTL reaction is highly dependent on the type of HTL-conjugate. Highest rate constants of ~ 10^6 $M^{-1}s^{-1}$ were observed for HTL conjugated to hydrophobic and positively charged residues, while the rate constant for the PEG-HTL conjugate was ~ 10^3 $M^{-1}s^{-1}$. Inspite of this low reaction rate constant, this immobilization strategy has the advantage that it is bioorthogonal in all cell lines that are routinely used for recombinant protein expression.

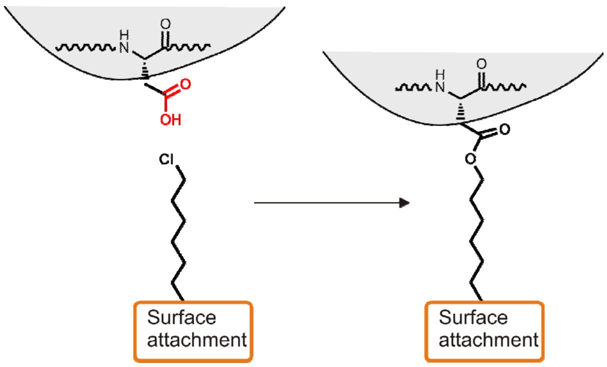

Figure 1.6 HaloTag/ HaloTag ligand-based immobilization. An aspartate residue in the HaloTag of a recombinantly expressed target protein displaces the chlorine atom from surface immobilized HaloTag ligand and forms a covalent ester bond with it.

1.3.4 ybbR tag/ Coenzyme A

The ybbR tag is an 11-residue peptide which was identified from a genomic library of *Bacillus subtilis* by phage display as an efficient substrate for phosphopantetheinyl transferase Sfp [43]. In nature, the 4'-phosphopantetheinyl moiety of coenzyme A (CoA) is transferred to a serine residue conserved in all peptidyl carrier proteins [44]. It was demonstrated that under mild physiological conditions, Sfp catalyses the transfer of the phosphopantetheinyl group from CoA to a serine residue on the ybbR tag fused to a protein of interest, resulting in a site-specific and covalent bond between the protein and CoA (Figure 1.7). This strategy was originally developed for site-specific fluorescent labeling of proteins using CoA-fluorophore conjugates, but has been since extended for covalent immobilization of ybbR-tagged proteins to a variety of CoA functionalized substrates [45]. The short length of the tag makes it very attractive for recombinant expression and it has been demonstrated that the ybbR tag can be fused to the N or C termini of target proteins or even inserted in a flexible loop in the middle of a target protein [43]. However, as CoA is ubiquitously present in all cells, this immobilization approach requires prior protein purification. Kinetic information for this enzymatic reaction is given by the Michaelis-Menten constant (K_m) which is around 140 μM [43]. Since much lower protein concentrations are generally used for immobilization, the ratio k_{cat}/K_m can be used as an estimate for the second order rate constant for the reaction. A low value of $\sim 10^3$ $M^{-1}s^{-1}$ for this ratio implies that this approach requires comparatively higher protein concentrations for achieving desired surface densities.

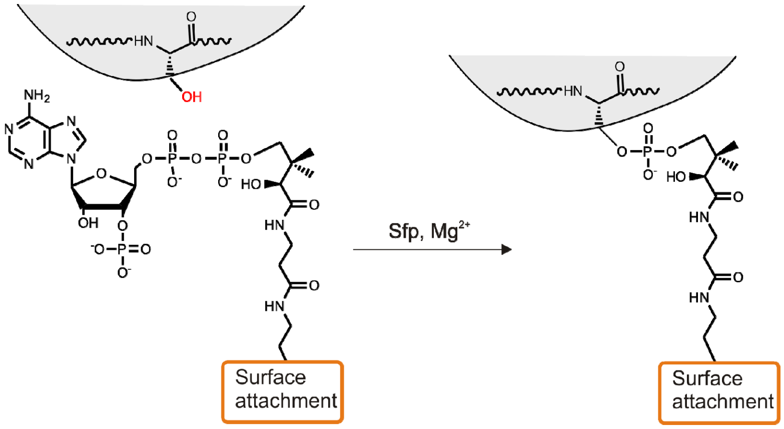

Figure 1.7 ybbR tag/ CoA-based immobilization. Sfp in the presence of Mg(II) catalyzes the formation of a covalent bond between surface bound CoA and a serine residue in the ybbR tag of a target protein.

These techniques provide simple and generic means to immobilize recombinantly expressed proteins on surfaces. They ensure that proteins are captured in fixed orientations, and can be easily combined with a biocompatible polymer layer thus maintaining a high degree of protein activity. Before progressing to the next section which will discuss some important elements of protein patterning, I have summarized the salient features of the different immobilization strategies in the table below.

Table 1.1 Attributes of the different protein immobilization approaches.

	Biotin/streptavidin	**His-tag/Ni^{2+}**	**HaloTag/HTL**	**ybbR-tag/CoA**
Nature of bond	Non-covalent, irreversible	Non-covalent, reversible	Covalent	Covalent
Association rate constant ($M^{-1}s^{-1}$)	3×10^6 - 4.5×10^7	10^5	10^3 - 10^6, depends on HTL-conjugate	10^3
Bioorthogonality	No	Yes	Yes	No

1.4 Patterning

The first attempts to pattern proteins were motivated by the aim to incorporate biomolecules into miniature electronic devices. Hence, it was but natural that the techniques to achieve this were also borrowed from the electronics industry. In 1978 MacAlear and Wehrung used photoresist technology from the semiconductor industry to create patterns on an underlying compressed proteinaceous layer [1]. Since this ‘primitive’ attempt at protein patterning, several different methods, more suited to the sensitive nature of proteins have been developed.

In this context, the most important requirements for a patterning technique are

1. They should be compatible with site-specific functional protein immobilization strategies like the ones described, and
2. They should not expose proteins to non-physiological conditions.

Techniques so far applied for protein patterning can be grouped into three families.

1. Patterning by physically controlled deposition: These techniques include micro contact printing (MCP) [46], ink-jet printing [47] and dip pen nanolithography (DPN) [48] among others. In these techniques the material to be patterned is deposited on a homogenous surface using spatially-controlled deposition strategies. For example, in MCP a soft stamp with patterned relief is used to deposit materials on surfaces, while in DPN an atomic force microscope tip coated with the chemical molecule desired to be deposited is used as a nano-pen for ‘writing’ patterns on a surface. These techniques have been used to pattern diverse chemical molecules including proteins [49, 50] and DNA [51, 52] on a variety of substrates. Surface structures measuring tens of nanometers up to hundreds of micrometers can be fabricated over large surface areas using these strategies.
2. Patterning by self-assembly: These techniques include interfacial self-assembly [53] and molecular self-assembly [54] approaches for acquiring surface patterns. Molecular self-assembly utilizes chemical or physical forces operating at the nanoscale to assemble basic units into larger structures. The most complex nanostructures fabricated using this strategy utilize the high programmability of DNA

self-assembly. Using DNA as a structural element, diverse structures such as two-dimensional periodic lattices and three-dimensional structures in the shapes of polyhedra have been fabricated [55] which have then been used as templates to control the assembly of other molecules such as proteins [56]. Apart from DNA, these approaches have been used to pattern diblock copolymers [57] and nanoparticles [58] on surfaces. These strategies allow patterning with a nanometer resolution; however they offer very little flexibility with respect to pattern configuration.

3. Patterning by high-energy irradiation: In these techniques, structures on surfaces are created by locally initiating chemical reactions using high-energy radiation like light (photolithography), electrons (electron beam lithography) [59] and extreme UV (extreme UV lithography) [60]. Patterns can be defined by using lithographic masks or by using a scanner for spatially controlling irradiation geometry. These strategies have been used for patterning proteins on a variety of substrates in dimensions ranging from tens of nanometers to hundreds of micrometers.

The methods for protein patterning that have been developed and that will be described in this thesis are all based on photolithography. Hence, the following is a brief description of the principles and methodology adopted for photolithography, with an emphasis on its application for protein patterning.

1.5 Photolithography

Photolithography has long been used in the semiconductor industry for metal patterning in electronic circuits. Traditionally photolithography has involved the transfer of geometric shapes on a mask to the surface of a substrate using the photosensitivity of suitable molecules. However, recent developments utilizing laser scanners and micro-mirror systems have made possible the creation of patterns on surfaces without the need of a mask [61]. Although photolithography is highly flexible and easy to use, one disadvantage is the inherent diffraction limitation of light, which restricts patterned structures to hundreds of nanometers. Nevertheless, recent applications using near field techniques for surface irradiation have demonstrated the fabrication of structures below this limit [62].

1.5.1 Principles of photolithography

In a photolithographic process, chemical reactions are locally activated on a surface by using light as a source of energy. The first step in any photochemical reaction is the absorption of a photon by a molecule and its resultant excitation to a higher electronic state. Multiple excited states are likely to exist for a molecule, the relations between which are best described by a Jablonski diagram (Figure 1.8) [63].

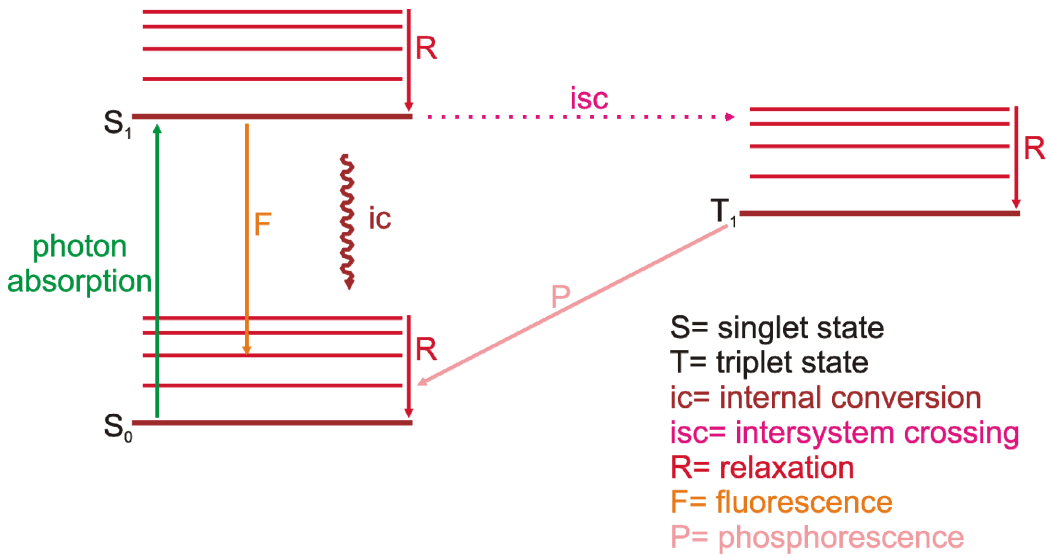

Figure 1.8 Jablonski diagram. Absorption of a photon excites an electron from the ground state (S_0) to an excited state (S_1). More than one electronic excited state is likely to exist for a given molecule. Each electronic state will have a group of vibrational (and rotational) states, depicted by red lines above each state marker. Transitions between electronic states often occur to higher vibrational levels which then relax to lower levels by collisional loss of energy. Internal conversion of excited states to lower energy states of the same multiplicity takes place rapidly with loss of heat energy. An excited state may also return to the ground state by emitting a photon (fluorescence). Conversion of a singlet state to a lower energy triplet state is termed intersystem crossing. Radiative decay from a triplet state is called phosphorescence and is generally quite slow.

A photochemical reaction occurs when internal conversion and relaxation of an excited state (**S_1** or **T_1** in Figure 1.8) leads to a ground state isomer of the initial substrate molecule, or when an excited state undergoes a chemical reaction such as addition or dissociation forming products at their individual ground states. For some photochemical reactions, the molecule which is excited by photons is not of interest, but its only function is to couple the light energy into a non-absorbing molecule. In such cases, the **$T_1 \rightarrow S_0$**

transition of the absorbing molecule takes place in a non-radiative manner by intermolecular energy transfer to a different molecule. This collisional process is termed sensitization. Photochemical sensitization commonly occurs by a $\mathbf{T_1} + S_0 \rightarrow \mathbf{S_0} + T_1$ reaction, thus exciting a new species to a triplet state which can then undergo characteristic reactions of its own [64].

1.5.2 Methodology

The most important equipment for photolithography is the light source. Traditionally, photolithography in the context of protein patterning has used UV light from gas-discharge lamps using mercury, sometimes in combination with noble gases such as xenon. These lamps produce light across a broad spectrum with several strong peaks in the ultraviolet range, the most important being the spectral lines at 436 nm ("g-line"), 405 nm ("h-line") and 365 nm ("i-line"). The required line(s) can be selected using optical filters. Patterns are created by irradiating through a photomask, which is a transparent quartz substrate with opaque regions defined by chromium patterns. A recently developed technique, termed virtual mask photolithography, now allows the creation of patterns even without a photomask. In this process, a digitally controlled micromirror array is used to define regions that should be irradiated using a mercury or xenon lamp [61]. In recent times however, lasers have also become a light source of choice for photolithography. Confocal laser scanning microscopes equipped with UV lasers combine the flexibility offered by the laser scanning device with the high resolution of the objective lens and provide a user-friendly approach towards photolithography, especially in biology-focused laboratories [65].

In addition to the light source, the other important element in photolithography is of course the photosensitive moiety. Light can be used to activate surfaces modified with such moieties to locally bind target molecules, or to deactivate surfaces to render them non-reactive. The following general strategies are mostly used in the context of protein patterning [1]:

1. Photoactivation: Here a photosensitive moiety is used to block the surface. Upon irradiation, the ‘cage’ is removed and target proteins are captured into irradiated

regions. One approach is to cage protein binding groups on the surface. Upon irradiation, the cage is removed and proteins can bind to the unblocked regions. If uncaging can be carried under physiological conditions, this strategy can allow not only spatial but also temporal control over protein immobilization as the photoactivation reaction can be carried out with target proteins in the background (Figure 1.9a). As an alternative, if the protein capturing group is not amenable to photosensttive caging, the terminal moieties of the biocompatible polymer layer can be blocked with a photolabile group. Upon irradiation, exposed regions are unblocked and can capture proteins after reaction with suitable protein binding groups (Figure 1.9b). In another approach, protein capturing groups with terminal photoactivable moieties can be immobilized into suitably functionalized surfaces only in irradiated regions (Figure 1.9c). This requires that the protein capturing group by itself is insensitive to irradiation.

2. Photodeactivation: Here the surface is rendered unreactive or incapable of protein binding in irradiated regions due to the photosensitive nature of surface moieties. As in photoactivation, this approach can also be carried out at two different levels. If the terminal moieties presented on a surface functionalized with the biocompatible polymer layer are photosensitive and can be destroyed by irradiation, then the protected regions can be further reacted with protein binding groups and used to capture target proteins (Figure 1.9d). Alternatively, if the protein capturing group is itself photosensitive then it can be destroyed by irradiation and non-irradiated regions can bind selected proteins normally (Figure 1.9e).

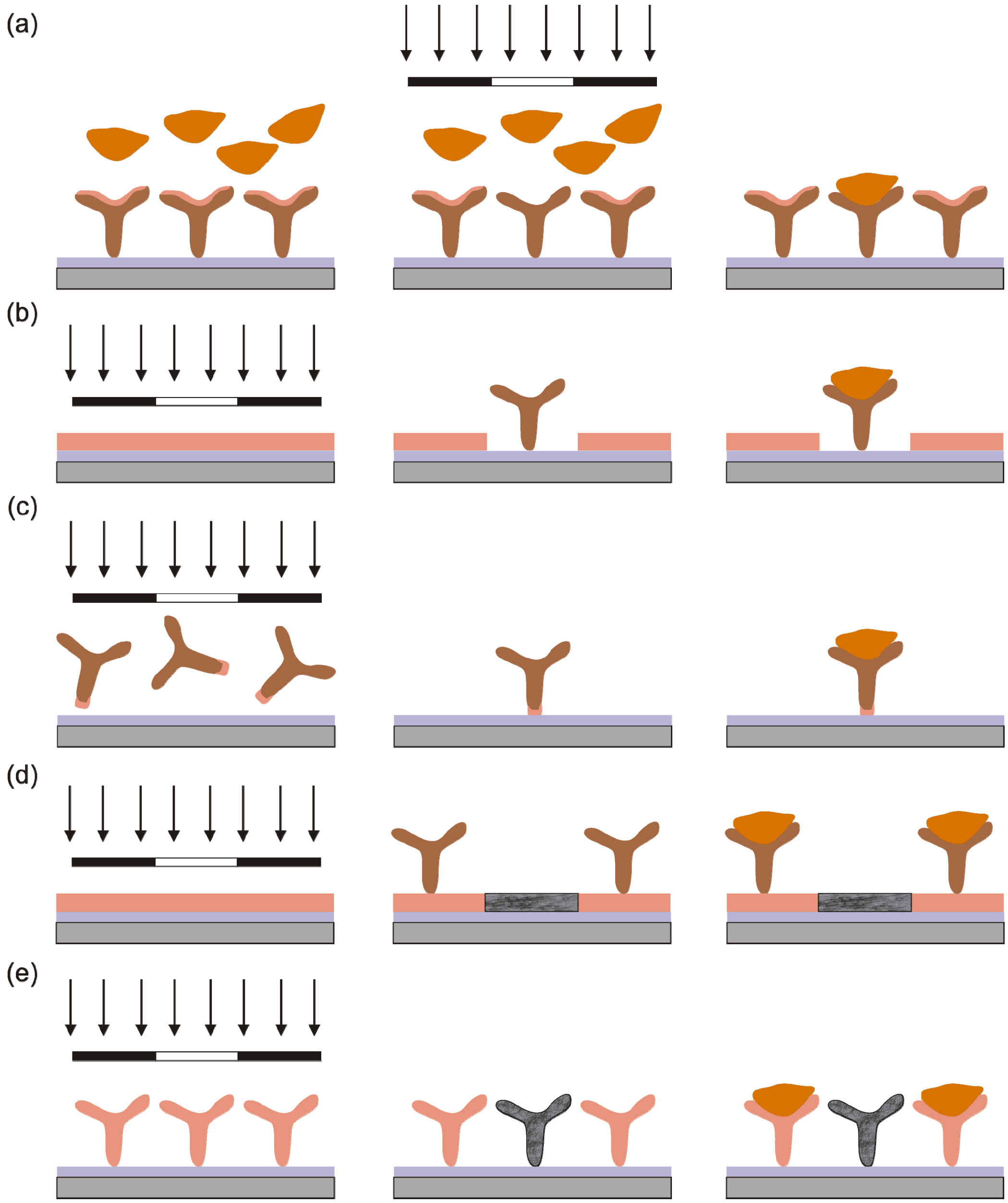

Figure 1.9 Strategies for photochemical protein patterning. (a) Surface immobilized protein capturing groups (PCGs) caged with a photo-sensitive moiety are incubated with the target protein. Upon irradiation, the cage is removed and protein binds to exposed regions. (b) Reactive groups on the surface are caged by a photosensitive moiety. Upon irradiation, the cage is removed, and the exposed regions are reacted with PCGs which can subsequently bind target proteins. (c) Surface is incubated under PCG having photoactivable terminal moieties which react with the surface upon irradiation. Target proteins are captured in exposed regions. (d) Surface is functionalized with a reactive photo-sensitive moiety that is destroyed upon irradiation. PCGs are reacted to covered regions and subsequently used for capturing target proteins. (e) Photo-sensitive surface immobilized PCGs are rendered incapable of protein binding upon irradiation. Target proteins bind to covered regions upon incubation.

In all these approaches it is imperative that patterning be carried out at a level above the biocompatible layer as it is essential to have high polymer coverage in order to prevent non-specific protein binding. Moreover, it should also be noted that the biocompatible layer should be insensitive to irradiation so that it maintains its integrity and surface protection ability.

As is clearly evident from this discussion, the photo-sensitive group is of utmost importance in any photolithographic strategy. Although numerous such groups are available, several of which have also been used for protein patterning, the two photochemical reactions most relevant to this thesis are described below.

1.5.3 Photo-induced Fenton reaction

The Fenton reaction which uses hydrogen peroxide and iron catalyst for generation of hydroxyl radicals was developed in the 1890s and has been since mostly utilized for oxidation of a variety of organic contaminants in water [66]. The photo-induced Fenton reaction can take place in the absence of hydrogen peroxide making use of atmospheric oxygen and the property of certain transition metal ions to be reduced under UV irradiation [67-69]. The reaction takes place along the following steps.

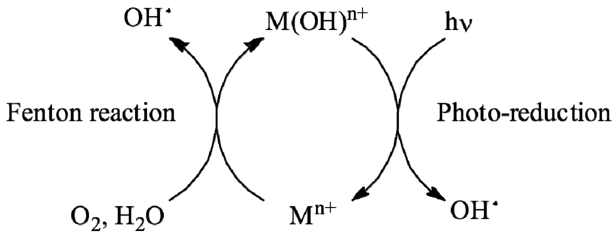

Here ‘M’, ‘n’ and ‘n+1’ represent a transition metal ion and its oxidation states respectively. Hydroxyl radicals which are generated during this reaction can oxidize functional groups on the surface. The metal ion shuttles between n and (n+1) oxidation states and can thus take part in the reaction indefinitely.

1.5.4 Nitroveratryloxycarbonyl-based caging

The nitroveratryloxycarbonyl (NVOC) group is a photo-labile protection group that has been used to cage alcohols, amines and phosphates for a variety of applications. The photolysis of NVOC-derivatives proceeds according to the following reaction mechanism [70].

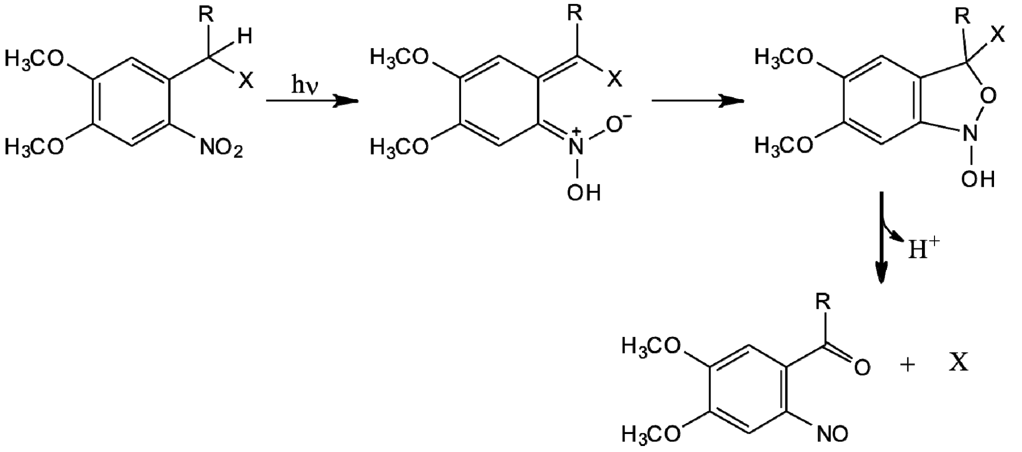

1.6 Techniques for analysis

Most of the experiments that will be discussed in this thesis are conducted on surfaces. Therefore, special surface-sensitive techniques are required for analysis and characterization of these experiments. This section is a brief description of three such tools that will be frequently used for these studies.

1.6.1 Reflectometric interference spectroscopy (RIfS)

RIfS is a technique for label free-detection and quantification of molecular interactions on a surface [71]. It is based on an interference layer obtained by coating a glass substrate (n ~ 1.52) with a silica layer (d = 300-500 nm, n ~1.45). Owing to the differences in refractive index between the glass substrate and the silica layer, as well as the silica layer and the environment (n ~ 1.33 for buffer), a light beam is partially reflected at these interfaces (Figure 1.10a). The reflected beams have different optical path lengths and therefore a phase difference is formed.

$$\Delta\phi = 2\frac{nd}{\lambda} + \phi_{refl}$$

Where $\Delta\phi$ is the phase difference, ϕ_{refl} is the phase shift upon reflection, n is the refractive index, d is the layer thickness and λ is the wavelength.

Superposition of the two light beams leads to an interference pattern that depends on the phase shift between the two beams. At an incidence angle of zero (illumination perpendicular to the surface) the total reflected intensity is given by

$$I = I_R + I_1 + I_2 + 2\sqrt{I_1 I_2}\cos\left(4\pi\frac{nd}{\lambda}\right)$$

Where I_R, I_1, I_2 are the reflected beam intensities as depicted, n and d are the refractive index and the thickness of the interference layer, respectively, and λ is the wavelength of the light beam. At constant optical thickness ($n{\cdot}d$) of the interference layer, the reflected intensity as a function of λ is modulated yielding an interference spectrum with maxima for constructive interference and minima for destructive interference. Changes in the optical thickness upon protein binding on the silica layer result in a shift of the interference spectrum, which can be probed by monitoring the position of an extremum or reflected intensity at a fixed wavelength in real time (Figure 1.10b).

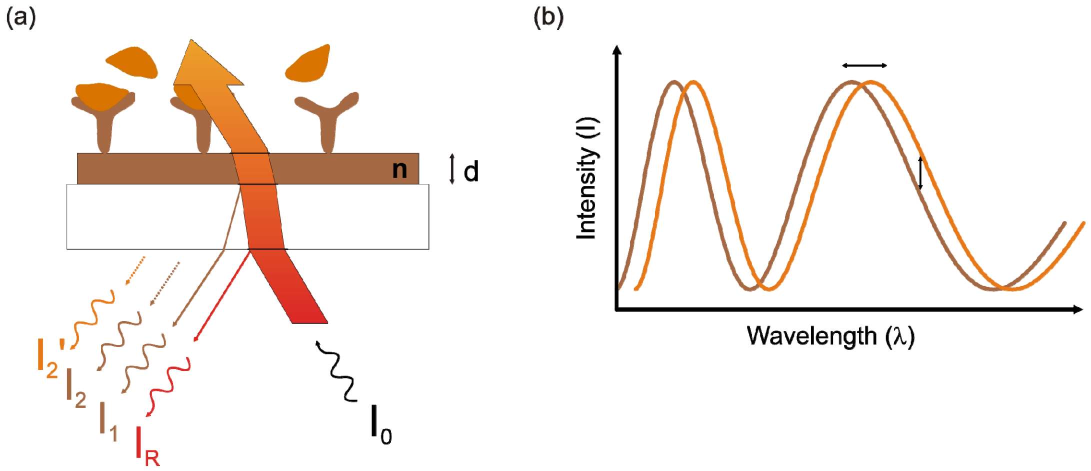

Figure 1.10 Principle of RIfS detection. (a) A glass chip with a thin silica layer is illuminated with a white light beam that is partially reflected at each interface. (b) An interference pattern (intensity vs. wavelength) is obtained, which changes (brown vs. orange curve) upon binding of molecules to the silica layer.

Therefore, by knowing the change in the interference pattern, the change in optical thickness ($n.d$) as a result of surface binding can be calculated. Knowing the refractive index (n) of the molecule that is bound to the surface, the change in the thickness of the physical layer (d) upon binding can be ascertained. From this data, very quantitative information such as the molecular surface density of analytes can be inferred. RIfS can measure surface binding in terms of mass/unit area (ng/mm^2) in real time with a sensitivity of ~ 0.02 ng/mm^2 (~ 6×10^{11} $molecules/mm^2$ for a 20 kDa protein) [72].

1.6.2 Total internal reflection fluorescence spectroscopy (TIRFS)

As described above, RIfS gives highly quantitative information about surface density of bound molecules However, some surface binding measurements such as analysis of very low affinity interactions requires much higher sensitivities than what is offered by RIfS. Also, since RIfS is only sensitive to changes in optical thickness, it is not possible to differentiate between different surface-bound species. These limitations can be conveniently overcome by using fluorescent probes. Thus, combining RIfS with fluorescence measurement offers the ability to conduct highly sensitive quantitative analysis of surface binding [73]. In order to make fluorescence analysis surface sensitive, a technique known as TIRF is used for illumination.

When light reaches the interface between two media, it is reflected and refracted. The incidence and refraction angles are related by Snell's law:

$$n_1 \sin\theta_1 = n_2 \sin\theta_2$$

Where n_1 and n_2 are refractive indices of the two media, θ_1 is the angle of incidence and θ_2 is the angle of refraction.

If the refractive index of the first medium is higher than that of the second ($n_1 > n_2$), then $\theta_1 < \theta_2$. The incidence angle when $\theta_2 = 90°$ is called the critical angle θ_c.

$$\theta_c = \sin^{-1}(n_2 / n_1)$$

If the angle of incidence is higher than θ_c, then the light is totally internally reflected and does not propagate into the second medium. However, some of the light still penetrates the medium of lower refractive index as an electromagnetic field called an 'evanescent wave'. A key characteristic of an evanescent wave is that it propagates parallel to the interface, vanishing exponentially with distance. The decay length (d_p) of the evanescent wave along the depth of field depends on the incident angle (θ), the wavelength of the excitation beam (λ) and the refractive indices of both media:

$$I_z = I_0 \exp(-z / d_p)$$

$$d_p = \frac{\lambda}{4\pi\sqrt{{n_1}^2 \sin^2\theta - {n_2}^2}}$$

This means that using TIRF, only fluorophores that are very close (~100 nm) to the interface will be excited. Thus fluorescent species that are bound to the surface contribute to the major fluorescence, and unbound fluorophores in the background are not detected.

1.6.3 Confocal Laser Scanning Microscopy (CLSM)

CLSM is an invaluable tool for imaging thin optical sections in living and fixed specimens ranging in thickness up to 100 μm. When compared to widefield microscopy, confocal microscopy offers a better spatial resolution, especially in the z-dimension. This is accomplished by the placement of a pinhole aperture in front of the detector which only allows fluorescent light from the objective focal plane to reach the detector. The significant amount of fluorescence emission that occurs at points above and below the focal plane is not confocal with the pinhole and is thus prevented from reaching the detector (Figure 1.11). Refocusing the objective shifts the excitation and emission points on a specimen to a new plane that becomes confocal with the pinhole aperture. This offers the capability to collect serial optical sections from thick specimens.

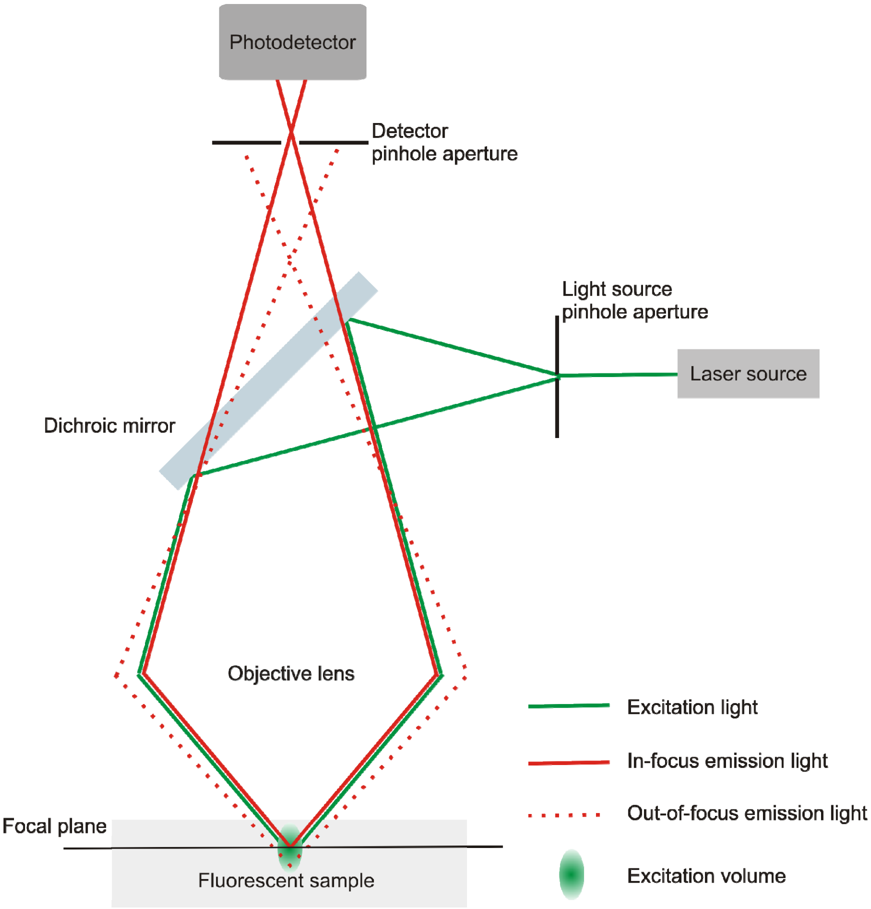
Photodetector
Detector pinhole aperture
Light source pinhole aperture
Laser source
Dichroic mirror
Objective lens
Focal plane
Fluorescent sample
Excitation light
In-focus emission light
Out-of-focus emission light
Excitation volume

Figure 1.11 Confocal laser scanning microscopy. Schematic diagram of the optical pathway and principal components in a confocal laser scanning microscope. Modified from [74].

In addition to the pinhole, further improvement in resolution is achieved by the small size of the illumination spot that ranges from approximately 0.25 to 0.8 µm in diameter (depending upon the objective numerical aperture) and from 0.5 to 1.5 µm in depth at the brightest intensity. The laser spot is scanned across a defined area in order to generate the image of an extended sample. Besides enabling the acquisition of high resolution fluorescent images, these attributes make a CLSM an invaluable tool for photolithography. The very small illumination spot size that is achieved by using a high numerical aperture objective allows photochemical reactions to be conducted with a very high spatial resolution. As the illumination spot can be freely moved all over the sample using the scanning unit, versatile patterns can be defined on the surface. Therefore, this thesis will include applications of this microscopy system as a tool for imaging as well as for photolithography.

1.7 References

1. Blawas, A.S. and W.M. Reichert, *Protein patterning.* Biomaterials, 1998. **19**(7-9): p. 595-609.

2. Marsden, D.M., et al., *Discovery of a quorum sensing modulator pharmacophore by 3D small-molecule microarray screening.* Org Biomol Chem, 2010. **8**(23): p. 5313-23.

3. Nicholson, R.L., et al., *Small-molecule screening: advances in microarraying and cell-imaging technologies.* ACS Chem Biol, 2007. **2**(1): p. 24-30.

4. Zhou, H., et al., *Solution and chip arrays in protein profiling.* Trends Biotechnol, 2001. **19**(10 Suppl): p. S34-9.

5. Ligler, F.S., et al., *Array biosensor for detection of toxins.* Anal Bioanal Chem, 2003. **377**(3): p. 469-77.

6. Rowe, C.A., et al., *Array biosensor for simultaneous identification of bacterial, viral, and protein analytes.* Anal Chem, 1999. **71**(17): p. 3846-52.

7. Sun, S., et al., *Lab-on-a-chip for botulinum neurotoxin a (BoNT-A) activity analysis.* Lab Chip, 2009. **9**(22): p. 3275-81.

8. Taitt, C.R., et al., *A portable array biosensor for detecting multiple analytes in complex samples.* Microb Ecol, 2004. **47**(2): p. 175-85.

9. Hung, H.S., et al., *Novel approach by nanobiomaterials in vascular tissue engineering.* Cell Transplant, 2011. **20**(1): p. 63-70.

10. Teo, B.K., et al., *Nanotopography/mechanical induction of stem-cell differentiation.* Methods Cell Biol, 2010. **98**: p. 241-94.

11. Yang, F., et al., *High throughput optimization of stem cell microenvironments.* Comb Chem High Throughput Screen, 2009. **12**(6): p. 554-61.

12. Burness, M.L. and D.A. Sipkins, *The stem cell niche in health and malignancy.* Semin Cancer Biol, 2010. **20**(2): p. 107-15.

13. Lathia, J.D., et al., *Deadly teamwork: neural cancer stem cells and the tumor microenvironment.* Cell Stem Cell, 2011. **8**(5): p. 482-5.

14. Mrksich, M., *Tailored substrates for studies of attached cell culture.* Cell Mol Life Sci, 1998. **54**(7): p. 653-62.

15. Mrksich, M. and G.M. Whitesides, *Using Self-Assembled Monolayers to Understand the Interactions of Man-made Surfaces with Proteins and Cells.* Annual Review of Biophysics and Biomolecular Structure, 1996. **25**(1): p. 55-78.

16. Senaratne, W., L. Andruzzi, and C.K. Ober, *Self-assembled monolayers and polymer brushes in biotechnology: current applications and future perspectives.* Biomacromolecules, 2005. **6**(5): p. 2427-48.

17. Knoll, W., et al., *Functional tethered lipid bilayers.* J Biotechnol, 2000. **74**(3): p. 137-58.

18. Knoll, W., et al., *Solid supported lipid membranes: new concepts for the biomimetic functionalization of solid surfaces.* Biointerphases, 2008. **3**(2): p. FA125.

19. Banerjee, I., R.C. Pangule, and R.S. Kane, *Antifouling coatings: recent developments in the design of surfaces that prevent fouling by proteins, bacteria, and marine organisms.* Adv Mater, 2011. **23**(6): p. 690-718.

20. Jones, B.J. and M.A. Hayes, *Surface modification methods for enhanced device efficacy and function.* Methods Mol Biol, 2006. **339**: p. 49-56.

21. Lundberg, P., et al., *Poly(ethylene glycol)-based thiol-ene hydrogel coatings-curing chemistry, aqueous stability, and potential marine antifouling applications.* ACS Appl Mater Interfaces, 2010. **2**(3): p. 903-12.

22. Yu, L., et al., *Flow-through functionalized PDMS microfluidic channels with dextran derivative for ELISAs.* Lab Chip, 2009. **9**(9): p. 1243-7.

23. Steels, B.M., J. Koska, and C.A. Haynes, *Analysis of brush-particle interactions using self-consistent-field theory.* Journal of Chromatography B: Biomedical Sciences and Applications, 2000. **743**(1-2): p. 41-56.

24. Backmann, N., et al., *Sensing surface PEGylation with microcantilevers.* Beilstein J Nanotechnol, 2010. **1**: p. 3-13.

25. Ulman, A., *Formation and Structure of Self-Assembled Monolayers.* Chem Rev, 1996. **96**(4): p. 1533-1554.

26. McGovern, M.E., K.M.R. Kallury, and M. Thompson, *Role of Solvent on the Silanization of Glass with Octadecyltrichlorosilane.* Langmuir, 1994. **10**(10): p. 3607-3614.

27. Piehler, J., et al., *A high-density poly(ethylene glycol) polymer brush for immobilization on glass-type surfaces.* Biosens Bioelectron, 2000. **15**(9-10): p. 473-81.

28. Lyubchenko, Y., et al., *Atomic force microscopy of long DNA: imaging in air and under water.* Proc Natl Acad Sci U S A, 1993. **90**(6): p. 2137-40.

29. Edmondson, S., V.L. Osborne, and W.T. Huck, *Polymer brushes via surface-initiated polymerizations.* Chem Soc Rev, 2004. **33**(1): p. 14-22.

30. Camarero, J.A., *Recent developments in the site-specific immobilization of proteins onto solid supports.* Biopolymers, 2008. **90**(3): p. 450-8.

31. Wilchek, M. and E.A. Bayer, *The avidin-biotin complex in bioanalytical applications.* Anal Biochem, 1988. **171**(1): p. 1-32.

32. Beckett, D., E. Kovaleva, and P.J. Schatz, *A minimal peptide substrate in biotin holoenzyme synthetase-catalyzed biotinylation.* Protein Sci, 1999. **8**(4): p. 921-9.

33. Keppler, A., et al., *A general method for the covalent labeling of fusion proteins with small molecules in vivo.* Nat Biotechnol, 2003. **21**(1): p. 86-9.

34. Srisa-Art, M., et al., *Monitoring of Real-Time Streptavidin−Biotin Binding Kinetics Using Droplet Microfluidics.* Analytical Chemistry, 2008. **80**(18): p. 7063-7067.

35. Piran, U. and W.J. Riordan, *Dissociation rate constant of the biotin-streptavidin complex.* J Immunol Methods, 1990. **133**(1): p. 141-3.

36. Ueda, E.K., P.W. Gout, and L. Morganti, *Current and prospective applications of metal ion-protein binding.* J Chromatogr A, 2003. **988**(1): p. 1-23.

37. Kang, E., et al., *Specific adsorption of histidine-tagged proteins on silica surfaces modified with Ni2+/NTA-derivatized poly(ethylene glycol).* Langmuir, 2007. **23**(11): p. 6281-8.

38. Trammell, S.A., et al., *Orientated binding of photosynthetic reaction centers on gold using Ni-NTA self-assembled monolayers.* Biosens Bioelectron, 2004. **19**(12): p. 1649-55.

39. Lata, S., et al., *High-affinity adaptors for switchable recognition of histidine-tagged proteins.* J Am Chem Soc, 2005. **127**(29): p. 10205-15.

40. Dick B, J., *Evolving haloalkane dehalogenases.* Current Opinion in Chemical Biology, 2004. **8**(2): p. 150-159.

41. Los, G.V., et al., *HaloTag: a novel protein labeling technology for cell imaging and protein analysis.* ACS Chem Biol, 2008. **3**(6): p. 373-82.

42. Lisse, D., et al., *Selective Targeting of Fluorescent Nanoparticles to Proteins Inside Live Cells.* Angew Chem Int Ed Engl, 2011. **50**(40): p. 9352-9355.

43. Yin, J., et al., *Genetically encoded short peptide tag for versatile protein labeling by Sfp phosphopantetheinyl transferase.* Proc Natl Acad Sci U S A, 2005. **102**(44): p. 15815-20.

44. Reuter, K., et al., *Crystal structure of the surfactin synthetase-activating enzyme sfp: a prototype of the 4'-phosphopantetheinyl transferase superfamily.* EMBO J, 1999. **18**(23): p. 6823-31.

45. Wong, L.S., J. Thirlway, and J. Micklefield, *Direct site-selective covalent protein immobilization catalyzed by a phosphopantetheinyl transferase.* J Am Chem Soc, 2008. **130**(37): p. 12456-64.

46. Kumar, A., et al., *Patterned Self-Assembled Monolayers and Meso-Scale Phenomena.* Accounts of Chemical Research, 1995. **28**(5): p. 219-226.

47. Schena, M., et al., *Quantitative monitoring of gene expression patterns with a complementary DNA microarray.* Science, 1995. **270**(5235): p. 467-70.

48. Piner, R.D., et al., *"Dip-Pen" nanolithography.* Science, 1999. **283**(5402): p. 661-3.

49. Wilson, D.L., et al., *Surface organization and nanopatterning of collagen by dip-pen nanolithography.* Proc Natl Acad Sci U S A, 2001. **98**(24): p. 13660-4.

50. Bieri, C., et al., *Micropatterned immobilization of a G protein-coupled receptor and direct detection of G protein activation.* Nat Biotechnol, 1999. **17**(11): p. 1105-8.

51. Demers, L.M., et al., *Direct patterning of modified oligonucleotides on metals and insulators by dip-pen nanolithography.* Science, 2002. **296**(5574): p. 1836-8.

52. Tan, H., S. Huang, and K.-L. Yang, *Transferring Complementary Target DNA from Aqueous Solutions onto Solid Surfaces by Using Affinity Microcontact Printing.* Langmuir, 2007. **23**(16): p. 8607-8613.

53. Ma, H. and J. Hao, *Ordered patterns and structures via interfacial self-assembly: superlattices, honeycomb structures and coffee rings.* Chem Soc Rev, 2011. **40**(11): p. 5457-71.

54. Whitesides, G., J. Mathias, and C. Seto, *Molecular self-assembly and nanochemistry: a chemical strategy for the synthesis of nanostructures.* Science, 1991. **254**(5036): p. 1312-1319.

55. Douglas, S.M., et al., *Self-assembly of DNA into nanoscale three-dimensional shapes.* Nature, 2009. **459**(7245): p. 414-418.

56. Yan, H., et al., *DNA-templated self-assembly of protein arrays and highly conductive nanowires.* Science, 2003. **301**(5641): p. 1882-4.

57. Hosoi, A.E., et al., *Two-dimensional self-assembly in diblock copolymers.* Phys Rev Lett, 2005. **95**(3): p. 037801.

58. Choi, S., et al., *Coffee-Ring Effect-Based Three Dimensional Patterning of Micro/Nanoparticle Assembly with a Single Droplet.* Langmuir, 2010. **26**(14): p. 11690-11698.

59. Zhang, G.-J., et al., *Nanoscale Patterning of Protein Using Electron Beam Lithography of Organosilane Self-Assembled Monolayers.* Small, 2005. **1**(8-9): p. 833-837.

60. Städler, B. and et al., *Nanopatterning of gold colloids for label-free biosensing.* Nanotechnology, 2007. **18**(15): p. 155306.

61. Lee, K.-N., et al., *Micromirror array for protein micro array fabrication.* Journal of Micromechanics and Microengineering, 2003. **13**(3): p. 474.

62. Kingsley, J.W., et al., *Optical nanolithography using a scanning near-field probe with an integrated light source.* Applied Physics Letters, 2008. **93**(21): p. 213103-3.

63. Harris, D.C. and M.D. Bertolucci, *Symmetry and spectroscopy : an introduction to vibrational and electronic spectroscopy*. Dover classics of science and mathematics. 1989, New York: Dover. xii, 550 p.

64. Gilbert, L., *Molecular mechanisms of photosensitization.* Biochimie, 1986. **68**(6): p. 771-778.

65. Jonkheijm, P., et al., *Photochemical surface patterning by the thiol-ene reaction.* Angew Chem Int Ed Engl, 2008. **47**(23): p. 4421-4.

66. Chedeville, O., A. Tosun-Bayraktar, and C. Porte, *Modeling of fenton reaction for the oxidation of phenol in water.* J Autom Methods Manag Chem, 2005. **2005**: p. 31-6.

67. Ciesla, P., et al., *Homogeneous photocatalysis by transition metal complexes in the environment.* Journal of Molecular Catalysis a-Chemical, 2004. **224**(1-2): p. 17-33.

68. Leonard, S., et al., *Cobalt-mediated generation of reactive oxygen species and its possible mechanism.* Journal of Inorganic Biochemistry, 1998. **70**(3-4): p. 239-244.

69. Urbanski, N.K. and A. Beresewicz, *Generation of (OH)-O-. initiated by interaction of Fe2+ and Cu+ with dioxygen; comparison with the Fenton chemistry.* Acta Biochimica Polonica, 2000. **47**(4): p. 951-962.

70. Corrie, J.E.T., et al., *Photoremovable Protecting Groups Used for the Caging of Biomolecules*, in *Dynamic Studies in Biology*. 2005, Wiley-VCH Verlag GmbH & Co. KGaA. p. 1-94.

71. Proll, G., et al., *Reflectometric interference spectroscopy.* Methods Mol Biol, 2009. **503**: p. 167-78.

72. Piehler, J. and G. Schreiber, *Fast transient cytokine-receptor interactions monitored in real time by reflectometric interference spectroscopy.* Anal Biochem, 2001. **289**(2): p. 173-86.

73. Lamken, P., et al., *Ligand-induced Assembling of the Type I Interferon Receptor on Supported Lipid Bilayers.* Journal of Molecular Biology, 2004. **341**(1): p. 303-318.

74. Paddock, S.W., *Principles and practices of laser scanning confocal microscopy.* Mol Biotechnol, 2000. **16**(2): p. 127-49.

2 Patterning of His-tagged proteins by photodestruction of tris-NTA

2.1 Introduction

Functional protein immobilization onto solid supports is a key prerequisite for solid phase-based bioanalytical techniques which are rapidly gaining importance in fundamental and applied biosciences. Further applications include dissection of protein-protein interaction networks using protein chips, high-throughput functional characterization of protein function and drug screening, as well as the development of biomedical devices [1]. These applications frequently require miniaturization with the goal to enable massive parallelization, to minimize sample consumption and to integrate functions into miniaturized biomedical and biotechnological devices. Molecular motor proteins such as kinesin and myosin, which are responsible for ATP- or GTP-based directional transport in cells, are particularly attractive building blocks for the construction of such devices. Numerous approaches to organize motor proteins into functional micro- and nanostructures have been reported [2-8], which have inspired development of novel bioanalytical devices [9-13].

For these purposes, techniques for functional organization of proteins on surfaces into micrometer and sub-micrometer sized assemblies are demanded. Despite substantial developments in this field such as soft lithography techniques, piezodispensing, photolithography and light-controlled surface chemistry, simple and generic techniques for functional protein patterning are scarce [14]. A key challenge for protein micropatterning is to maintain the structure, and thus function, of proteins immobilized to the surface, many of which denature upon interacting with solid supports. Thus, surface modifications are required to render the surface biocompatible, which is achieved by thin protein-repellent polymer layers. Moreover, suitable, spatially resolved functionalization of these layers is required for site-specific capturing of target molecules onto surfaces [14].

Recently, multivalent nitrilotriacetic acid heads have been developed as generic, high-affinity adapters for oligohistidine-tagged proteins [15]. These multivalent chelators have proven powerful for stable, yet reversible protein binding in solution and for immobilization onto various supports [16-18]. In combination with a dense PEG polymer brush, oriented and highly functional capturing of kinesin onto glass type surfaces and ATP-dependent transport of microtubules on such surfaces were demonstrated [19].

Here, we present a generic method for functional micropatterning of such surface architectures. This method is based on selective photodestruction of surface-immobilized tris(nitrilotriacetic acid) (tris-NTA) by a light-induced Fenton reaction with suitable transition metal ions being complexed by the NTA moieties. We analysed the influence of the coordinated metal ion species and the wavelength of light on the photodestruction process. Subsequently, we implemented this approach both by using UV illumination through a mask and by using the UV laser of a standard confocal microscope for patterning His-tagged proteins. Interferon-α2 receptor, Ifnar2 was micropatterned using this strategy and activity of patterned protein was confirmed by investigating its interaction with Interferon-α2. Finally, kinesin was immobilized along microstructures in the form of lines and the fidelity of mictotubule transport as a function of line-width was studied.

2.2 Materials and methods

2.2.1 Materials

Diamino(polyethylene glycol) with MW 2000 Da (PEG2000) was purchased from Rapp Polymere. Diamino(polyethylene glycol) with MW 897.1 Da (PEG18) and and 468.6 Da (PEG 6) were purchased from Polypure. Other chemicals were purchased from Sigma Aldrich and used as obtained. Microstructured masks were designed as a 5” commercially available chrome-on-glass (COG) positive photomasks (desired structures are chromium), which was diced into 70 partial masks (10mm x 15mm) with different design variations. The width of these structures was varied between 1 µm and 10 µm and the spaces between 10 µm and 100 µm. A 75 W and a 150 W Xenon arc lamp and 280-400 nm dichroic mirror for irradiation were purchased from Newport Spectra-Physics.

2.2.2 Protein biochemistry

Maltose Binding Protein with decahistidine tag (MBP-H10), Interferon α2 (IFNα2), and its receptor ifnar2 with a decahistidine tag (ifnar2-H10) were expressed in *E. coli*, purified and site-specifically labeled with Oregon Green 488 (OG488) maleimide as described previously [15, 17, 20]. Kinesin-H10 contained the N-terminal 612 amino acids of Drosophila Kinesin-1 followed by a C-terminal decahistidine tag was expressed in *E. coli* and purified as described [19]. The purification of tubulin from pig brain, Alexa-568 labeling of tubulin, and the polymerization of microtubules was performed as described in the literature [21, 22].

2.2.3 Surface modification

Transducer slides for reflectance interference (RIf) detection and glass coverslips for microscopy were cleaned with 1 M NaOH for 3 minutes followed by overnight incubation in a freshly prepared mixture of one part hydrogen peroxide and two parts concentrated sulfuric acid. After rinsing with water and drying in a nitrogen stream, the surfaces were silanized with glycidyloxypropyltrimethoxysilane (GOPTS). The diamino-polyethylene glycols were reacted with the epoxy groups on the surface as described before [23]. For functionalization with tris-NTA, 5 µL of a solution of O*t*Bu-protected tris-NTA-carboxylic acid in chloroform (100 mg/ml) was applied on the surface. Coupling of the carboxy group with the amine modified surface was started by addition of 5 µL of N,N’-Diisopropylcarbodiimide and the reaction was carried out by incubation for 1 hour at 75 ^{o}C. The excess reaction mixture was washed off with chloroform after the reaction. The substrates were then incubated in trifluoroacetic acid overnight to cleave of the tert-butyl esters and free the NTA head groups.

For photodestruction of the NTA moieties on surfaces, 10 mM solutions of the required metal salt ($NiCl_2 \cdot 6\,H_2O$, $FeSO_4 \cdot 7\,H_2O$, CuCl and $CoCl_2 \cdot 6\,H_2O$) were incubated after removing all traces of transition metal ions with 100 mM HCl. These surfaces were irradiated under a 75 W or 150 W xenon lamp fitted with a 280-400 nm dichroic mirror. Illumination times of 60 min at 75 W and 20 min at 150 W were used for complete destruction of NTA moieties. For surface patterning, irradiation was carried out through a photomask placed on the surface.

In *situ* patterning was carried out in a flow cell with an LSM 510 META from Carl Zeiss equipped with a 20 mW 405 nm laser. A tris-NTA modified coverslip was loaded with Co(II) and ^{OG488}MBP-H10 was immobilized on it. The resulting fluorescence was used to focus the microscope and find the region of interest. The 405 nm laser was then used at 100% power output to irradiate specific patterns on the surface (using the 'bleach' function on the software). Irradiation was carried out at a scan speed of 25.6 µs/pixel for 200 iterations for purposes of patterning and for 10, 50, 100 or 200 iterations for demonstrating control over surface tris-NTA density. In a control experiment irradiation was carried out with Ni(II) coordinated to the chelator heads. Another control experiment was performed using the 488 nm line of a 40 mW argon ion laser for irradiation under the same conditions.

2.2.4 Protein binding experiments through Reflectance Interference (RIf)

Measurements by RIf were carried out with a home-built set-up including continuous flow through conditions as described earlier [24]. Tris-NTA functionalized RIf transducers were treated with 100 mM HCl in the flow cell, followed by equilibration in HEPES buffered saline (HBS (20 mM HEPES, 150 mM NaCl, pH 7.5)). A 10 mM solution of $NiCl_2$ in HBS was injected, followed by injection of a 400 nM solution of MBP-H10 in HBS. The binding was then observed. Surfaces were regenerated by an injection of 500 mM imidazole in HBS to remove the protein and a further wash by 100 mM HCl to remove the bound Ni(II).

2.2.5 Confocal Laser Scanning Microscopy

An LSM 510 META confocal laser scanning microscope (CLSM) from Carl Zeiss was used for imaging. Tris-NTA modified coverslips were treated with 100 mM HCl followed by incubation in 10 mM solution of $NiCl_2$ in HBS. ^{OG488}MBP-H10 (50 nM in HBS) was used for imaging of patterns. For probing of protein activity, 50 nM of ifnar2-H10 in HBS was first incubated on a Ni(II) loaded patterned tris-NTA coverslip. After washing with buffer, ^{OG488}IFNα2 was incubated on the surface and imaged immediately after washing out the excess ligand with HBS.

2.2.6 Motility assays

A flow chamber was built from a Ni(II)-loaded patterned glass and a poly-L-lysine (PLL)-PEG passivated counter glass [25], separated by two strips of double sticky tape (Tesa; Hamburg, Germany). The flow chamber was equilibrated with 30 µL B80 (80 mM K-PIPES, 2 mM $MgCl_2$, 1 mM EGTA, 2 mM MgATP, pH 6.8) while positioned on an ice-cold metal block. The flow chamber was equilibrated with 30 µL B80 containing 1 mg/mL *β*-casein for 5 min. Then 330 nM kinesin-H10 in 30 µL B80 was flowed into the chamber and incubated for 10 min. Unbound motors were washed out with 30 µL B80 after 10 min. For visualization of the patterns, the flow chamber was also incubated after motor immobilization with 100 nM GFP-H10 in B80 for 5 min. The chamber was allowed to warm up to room temperature and five chamber volumes of preformed, taxol-stabilized, AlexaFluor 568-labeled microtubules in motility buffer (B80, 0.02 mM Taxol, 2 mM Mg-ATP, 2 mM mercaptoethanol, pH 6.8) containing ATP and an oxygen scavenger system (20 mM glucose, 40 mg/ml glucose oxidase and 20 mg/mL catalase) were flowed through the chamber. Microtubules were imaged using an IX-71 total internal reflection fluorescence (TIRF) microscope (Olympus) with a ×60/1.45 TIRFM objective (Olympus; Hamburg, Germany) and a Spectra Services Cascade II:512 camera (Roper Scientific GmbH, Germany). The temperature was maintained at 25 ±1 °C. The number of microtubules landing and their travel distances were measured using Image J software.

2.3 Results and discussion

2.3.1 Characterization of the photodestruction process

Fe(II) ions, which have been traditionally used in the Fenton reaction, precipitate and bind irreversibly to tris-NTA functionalized surfaces upon oxidation. Thus, other transition metal ions were tested for their efficiency as catalysts for the light-induced Fenton reaction. For these experiments, the NTA heads were first loaded with the metal ion under study and then the surface was illuminated with UV-light. Subsequently, all metal ions were removed by washing with HCl or EDTA and the remaining NTA groups were loaded with Ni(II) ions prior to protein binding.

Protein binding efficiencies to tris-NTA functionalized surfaces, which were UV-illuminated with the NTA moiety loaded with different transition metal ions are compared in Figure 2.1a. Illumination in presence of Ni(II) ions did not affect the binding capacity of the surface; in contrast, no protein binding could be observed after loading Co(II), Cu(I) or Fe(II) ions. These three transition metal ions mediate photo-induced Fenton reactions [26-28], which is responsible for the destruction of the NTA moieties on the surface. The same effect was observed for mono-NTA functionalized surfaces. Among these metal ions, Co(II) has a high solubility in HBS and also does not precipitate on the surface. Due to these advantages, it was used for all further experiments. Next, as shown in Figure 2.1b, we observed that efficiency of photodestruction on surfaces decreases with decrease in length of the PEG chain which indicates that the surface architecture has some influence on the destruction process. In order to further characterize the photodestruction process, we quantitatively assessed protein binding to surfaces, which were illuminated for shorter durations than required for full destruction of the binding capacity. Under these conditions, unstable protein binding was observed, indicating that the tris-NTA groups were partially destroyed and thus lost binding affinity (Figure 2.1c).

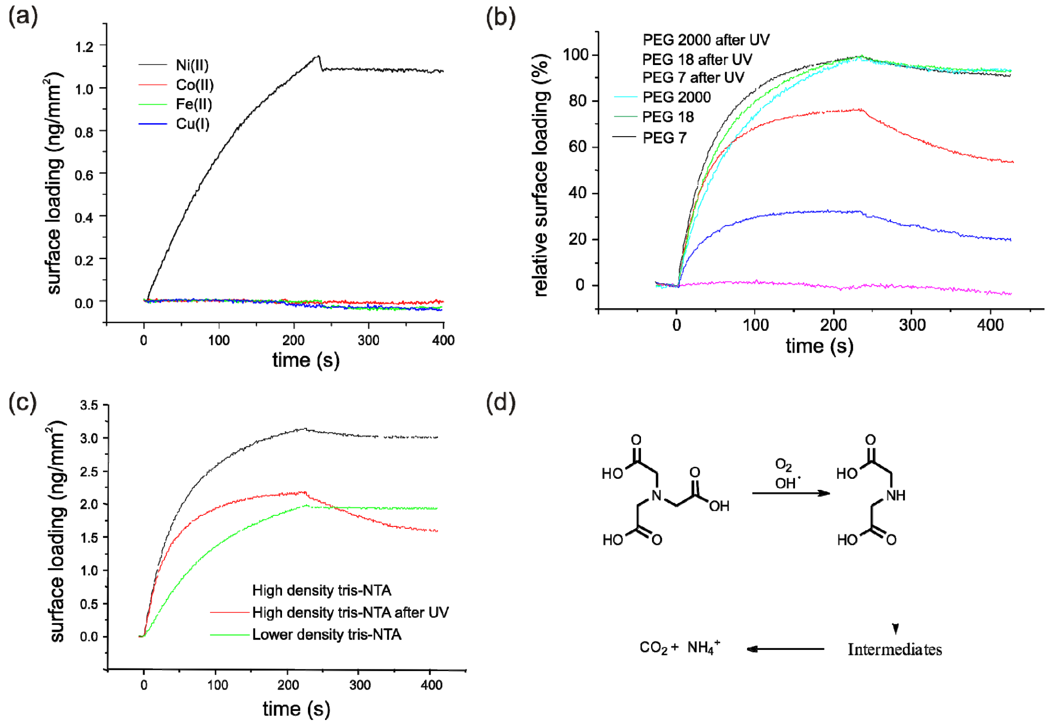

Figure 2.1 Characterization of NTA-photodestruction by the light-induced Fenton reaction. (a) Protein binding to tris-NTA-surfaces after UV-illumination in presence of different transition metal ions and subsequent loading of the remaining NTA groups with Ni(II) ions and binding of His-tagged protein (MBP-H10) as detected by reflectance interference. (b) Normalized RIf curves showing binding of MBP-H10 to tris-NTA surfaces with different lengths of PEG before and after photodestruction. PEG7, PEG18: monodisperse PEG with 7 and 18 ethylene glycol units, respectively. PEG 2000: PEG with an average molecular mass of 2000 g/mol (average of 45 ethylene glycol units). (c) RIf curves showing binding of MBP-H10 to tris-NTA surfaces irradiated for shorter durations than required for complete photodestruction (red curve). As controls, binding of MBP-H10 to a high density (black curve) and low density (green curve) tris-NTA modified surface are shown. (d) Possible mechanism of NTA decomposition by a photo-induced Fenton reaction according to reference [29].

Moreover, leaching out of Ni(II) ions was observed, indicating that the NTA moieties themselves were destroyed by the Fenton reaction. This is in line with studies done into the hydroxyl radical mediated oxidation of chelating agents such as NTA and EDTA. Oxidation of NTA yielded species with weaker metal ion coordination ability such as imidodiacetic acid, glycolic acid, oxalic acid and glycine (Figure 2.1d) [29]. Since the active oxidant in the Fenton reaction is also a hydroxyl radical, a similar oxidation pathway can be assumed. Thus, the metal-ion mediated photodestruction apparently selectively eliminates the transition metal ion binding moieties, but not the protein repelling PEG polymer brush. This was supported by the observation of negligible non-specific protein binding to surfaces after photodestruction (Figure 2.1a).

2.3.2 Functional protein patterning

After the characterization and optimization of the reaction conditions we focused on applying this strategy for patterning His-tagged proteins. For this, we irradiated a tris-NTA functionalized surface with UV light through a photomask in order spatially control regions of photodestruction as demonstrated in Figure 2.2.

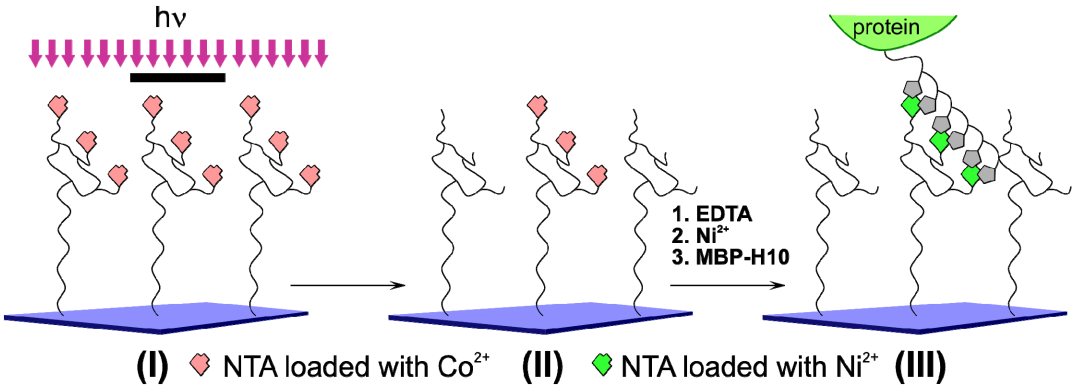

Figure 2.2 Schematic illustration of the patterning process. Surfaces modified with tris-NTA head groups are loaded with Co(II) ions (I), followed by UV-irradiation through a photomask (II). Remaining tris-NTA head groups can capture His-tagged proteins after loading Ni(II) ions (III).

After UV-illumination through a mask, selective and fully reversible binding of fluorescence-labeled, His-tagged maltose binding protein (MBP-H10) to the non-illuminated areas was observed by confocal laser scanning microscopy (CLSM) (Figure 2.3a). We furthermore explored specificity of protein binding as well as functionality of the immobilized protein by a protein-protein interaction assay (Figure 2.3b). For this purpose, the protein interferon-α2 labeled with Oregon Green 488 (^{OG488}IFNα2), which does not carry a His-tag, was incubated on a micropatterned surface with and without prior incubation of its receptor ifnar2 fused to a His-tag (ifnar2-H10). Binding of ^{OG488}IFNα2 into micropatterns was observed only in presence of ifnar2-H10, confirming highly specific protein binding as well as the functional integrity of proteins immobilized into such micropatterns.

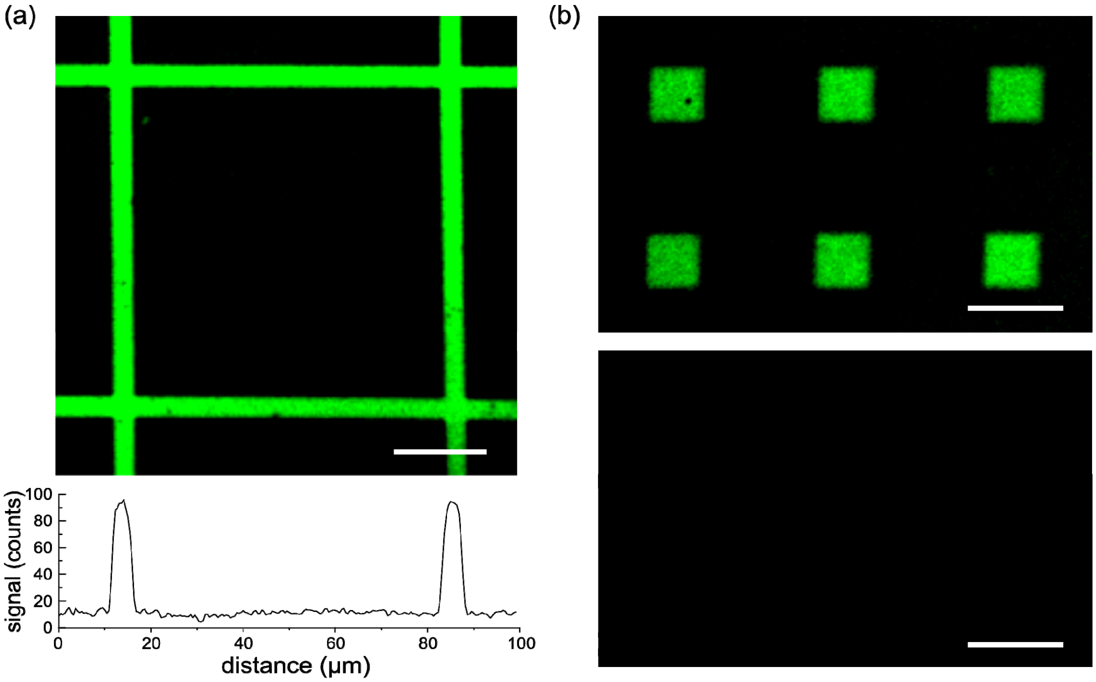

Figure 2.3 Functional surface micropatterning by illumination through a mask. (a) After UV illumination through a photomask, the remaining tris-NTA moieties were loaded with fluorescence-labeled MBP-H10 and imaged by CLSM. The fluorescence intensity profile along the indicated line is shown below. (b) Binding of fluorescence-labeled IFNα2 to micropatterned surfaces with (top) and without (bottom) prior incubation of its His-tagged receptor IFNAR2. The scale bar is 20 µm in all images.

2.3.3 Protein patterning in a CLSM

In a second approach, we explored in *situ* patterning of tris-NTA functionalized surfaces by means of the 405 nm laser beam in a confocal laser scanning microscope (Figure 2.4). Photodestruction of Co(II)-loaded tris-NTA by scanning selected regions of interest with the beam of the 405 nm laser was carried out either in presence of ^{OG488}MBP-H10 for focussing purposes or without protein. After removing Co(II), surfaces were loaded with Ni(II) and binding of ^{OG488}MBP-H10 was imaged.

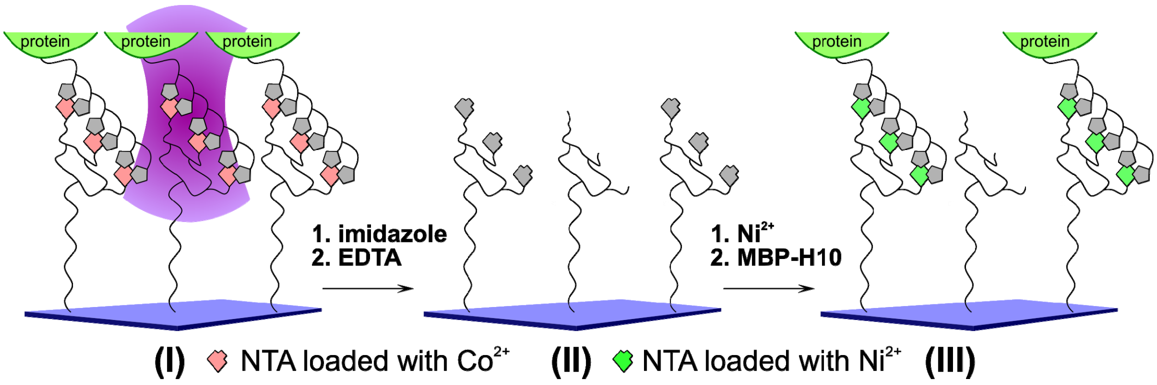

Figure 2.4 Schematic illustration of patterning using the UV laser of a CLSM. Tris-NTA modified surfaces are loaded with Co(II) ions followed by immobilization of a fluorescently labeled His-tagged protein (protein binding is optional). Selected regions are then irradiated with the 405 nm laser line in a CLSM (I). Co(II) ions (and protein, if applicable) is removed by imidazole and EDTA (II) followed by immobilization of proteins into non-destructed areas after loading Ni(II) ions (III).

Selective photodestruction was obtained in the illuminated areas (Figure 2.5a). Varying the number of iteration cycles during exposure to the 405 nm laser yielded different densities of binding sites (Figure 2.5b), providing the possibility to control the surface concentration of immobilized proteins in a spatially resolved manner. However, negligible effect was observed when the surface was irradiated for similar iterations using a 488 nm laser thus confirming that the photodestruction process is wavelength specific (Figure 2.5c). No photodestruction was also observed when the surface was irradiated with the NTA heads coordinated with Ni(II), thus confirming that the effect here is also due to the photo-induced Fenton reaction (Figure 2.5d).

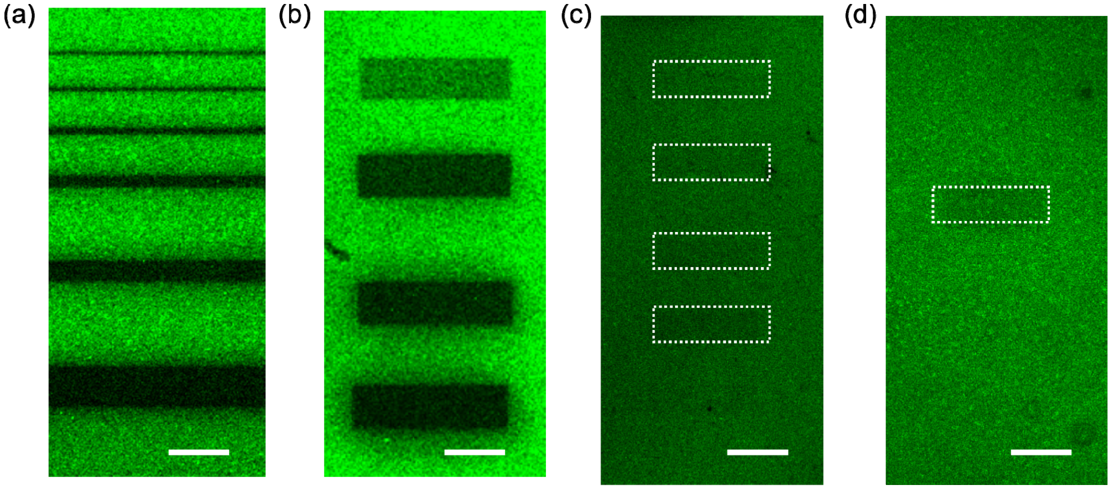

Figure 2.5 In *situ* patterning of tris-NTA surfaces in a CLSM. (a) Binding of fluorescently labeled MBP-H10 to tris-NTA modified surfaces with lines of different width scanned using the 405 nm laser in the presence of NTA-complexed Co(II) ions. (b) Density of fluorescently labelled MBP-H10 binding could be easily manipulated by scanning regions on the surface in the presence of NTA-complexed Co(II) ions with the 405 nm laser for different numbers of iterations (10, 50, 100 and 200). (c) Upon scanning the surface under similar conditions using a 488 nm laser, no photodestruction was effected as negligible difference in protein binding is observed between irradiated and non-irradiated areas. (d) No photodestruction occurred when a tris-NTA surface was scanned with the 405 nm laser under Ni(II) bound conditions. The indicated rectangular regions in (c) and (d) demarcate the regions scanned with the 488 nm and 405 nm laser respectively. The scale bar is 20 µm in all images.

In the next step, we combined the two irradiation strategies in order to demonstrate the flexibility of this patterning technique (Figure 2.6a, b). For this, a tris-NTA modified surface was first patterned with squares of equal sizes by irradiation through a photomask. Subsequently, these patterns were further modified by confocal scanning with a 405 nm laser beam.

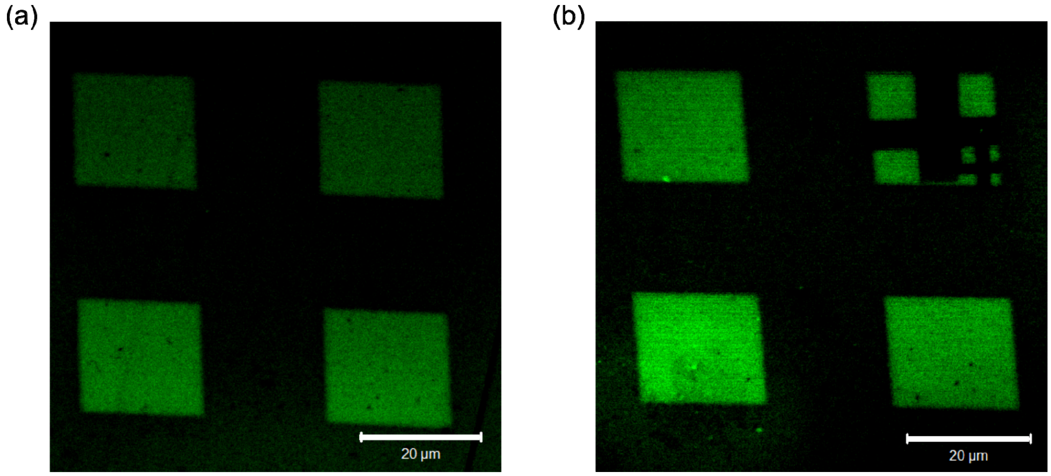

Figure 2.6 Combining photomask- and CLSM- based patterning. (a) A tris-NTA surface was patterned with squares using mask illumination. (b) The square in the upper right corner was further modified by confocal laser scanning. Scale bar is 20 µm in all images.

2.3.4 Gliding of microtubules on kinesin patterns

This work, which was done in collaboration with the group of Dr. Thomas Surrey at EMBL Heidelberg, was aimed towards testing the capability of this photochemical surface patterning method to immobilize molecular motors into microstructures and studying guided filament transport on the obtained patterns. For this purpose, we used a recombinant dimeric kinesin with a C-terminal decahistidine tag (kinesin-H10), which has been shown before to support microtubule gliding on unpatterned tris-NTA surfaces [19]. We co-immobilized decahistidine tagged green fluorescent protein (GFP-H10) as a fluorescent marker for visualizing the tris-NTA lines. Alexa-568 labeled microtubules selectively landed on the kinesin/GFP lines in random orientations (Figure 2.7a, b). In presence of ATP, all microtubules in contact with the lines were transported by the motors, confirming that photochemical patterning followed by subsequent selective tris-NTA-mediated motor immobilization yielded highly active protein patterns.

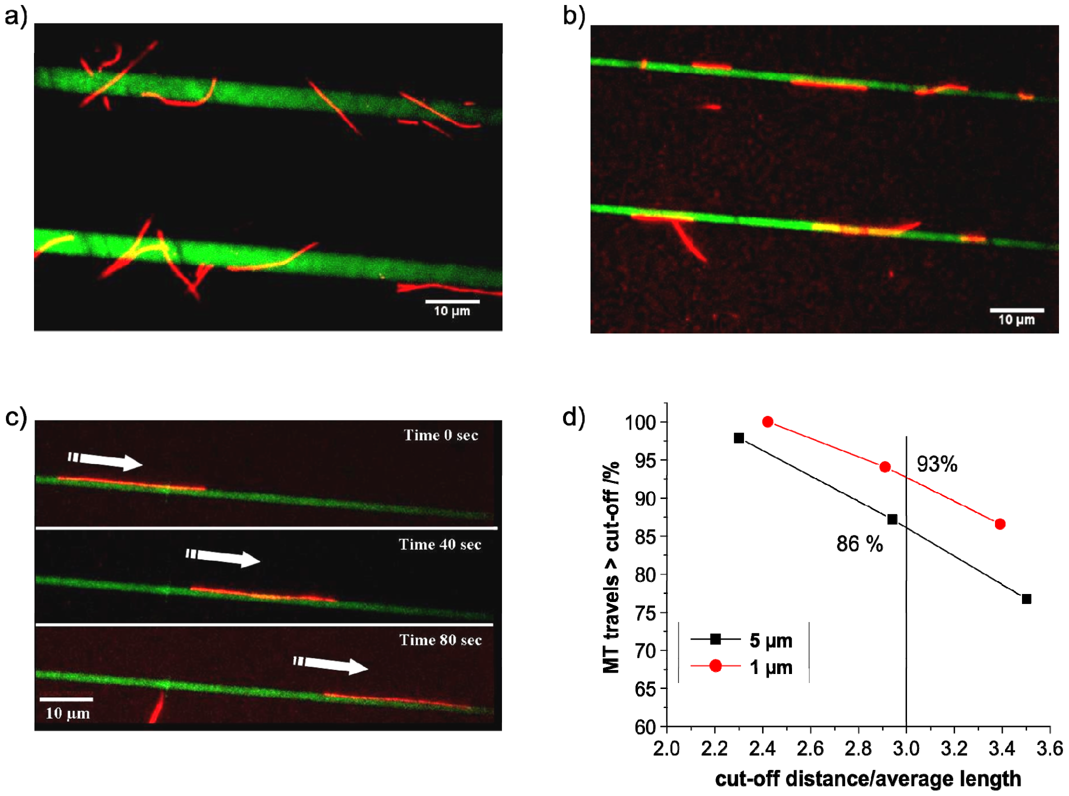

Figure 2.7 Transport of microtubules by patterned kinesin. (a, b) Fluorescence images of Alexa568-labeled microtubules (red) on kinesin-H10 captured onto tris-NTA lines (green) of 5 µm (a) and 1 µm (b) width. (c) Images from a time-lapse movie showing a labeled microtubule (red) on a kinesin-H10 line of 1 µm width (green) at the times indicated. (d) Percentages of microtubules traveling more than the indicated multiples of their average length along lines of 5 µm (black) and 1 µm (red) width. More than 85% and more than 90% of the microtubules travel more than 3 times (vertical line) of their average length along 5 µm and 1 µm lines, respectively.

Microtubules which had landed perpendicularly to the line diffused into solution after having been transported out of the line region. Microtubules with parallel orientation with respect to the line were seen gliding along the line (Figure 2.7c), in most cases for distances longer than multiples of their length. Quantitative analysis revealed that the distance travelled on individual lines was influenced by the characteristics of the pattern. Microtubules were observed to travel systematically slightly longer distances on thinner lines (Figure 2.7d). Insignificant differences in the velocities of the microtubules gliding on both types of lines (360 ± 60 nm/s on 1 µm lines and 370 ± 60 nm/s on 5 µm lines) confirmed similar densities of the motor proteins on both lines. These observations suggest that by further reducing the thickness of these structures into sub-micron dimensions, even higher microtubule transport fidelity could be obtained.

2.4 Conclusions

We have developed a versatile method for functional protein patterning. In contrast to conventional methods such as microcontact printing of proteins, our new method is optimized for highly active protein patterns, because the microstructuring reaction takes place at the level of chemistry and the biomolecules are captured under physiological conditions. This introduces the flexibility to separate pattering and protein immobilization, reducing the danger of protein inactivation during patterning. We have used this method to organize motor proteins into highly functional microstructures. Motility assays established that microtubule transport characteristics depend on geometrical features of the tracks that are defined by the patterning process. The possibility to modify mask-based protein structures using the additional flexibility of confocal laser scanning provides the means for generating complex patterns, which will enable for further exploring the bases of microtubule transport by micropatterned motor proteins. However, generic application of this technique for functional patterning of proteins is ensured by the widespread use of the His-tag for protein purification.

2.5 Summary

We described a method to pattern His-tagged proteins on tris-NTA modified surfaces using a transition metal ion mediated photo-induced Fenton reaction. Local initiation of this reaction by UV irradiation through a photomask led to the production of hydroxyl radicals which destroyed neighboring tris-NTA moieties. Thus, His-tagged proteins could be specifically targeted to the non-irradiated regions. Photo-destruction could also be achieved by scanning selected regions with the UV laser of a confocal laser scanning microscope thus allowing flexible creation and modification of protein patterns. This strategy enabled the functional organization of His-tagged kinesin into micropatterns. Microtubules were selectively captured on the structures, and adenosine triphosphate dependent transport along lines was demonstrated.

2.6 References

1. van den Heuvel, M.G. and C. Dekker, *Motor proteins at work for nanotechnology.* Science, 2007. **317**(5836): p. 333-6.

2. Clemmens, J., et al., *Motor-protein "roundabouts": microtubules moving on kinesin-coated tracks through engineered networks.* Lab Chip, 2004. **4**(2): p. 83-6.

3. Clemmens, J., et al., *Comparison of microtubule guiding on kinesin-coated microfabricated surfaces.* Biophysical Journal, 2003. **84**(2): p. 293A-293A.

4. Hess, H., et al., *Light-controlled molecular shuttles made from motor proteins carrying cargo on engineered surfaces.* Nano Letters, 2001. **1**(5): p. 235-239.

5. Hess, H., et al., *Molecular shuttles operating undercover: A new photolithographic approach for the fabrication of structured surfaces supporting directed motility.* Nano Letters, 2003. **3**(12): p. 1651-1655.

6. Huang, Y.M., et al., *Microtubule transport, concentration and alignment in enclosed microfluidic channels.* Biomed Microdevices, 2007. **9**(2): p. 175-84.

7. Ionov, L., M. Stamm, and S. Diez, *Reversible switching of microtubule motility using thermoresponsive polymer surfaces.* Nano Lett, 2006. **6**(9): p. 1982-7.

8. Reuther, C., et al., *Biotemplated nanopatterning of planar surfaces with molecular motors.* Nano Lett, 2006. **6**(10): p. 2177-83.

9. Fischer, T., A. Agarwal, and H. Hess, *A smart dust biosensor powered by kinesin motors.* Nat Nanotechnol, 2009. **4**(3): p. 162-6.

10. Goel, A. and V. Vogel, *Harnessing biological motors to engineer systems for nanoscale transport and assembly.* Nat Nanotechnol, 2008. **3**(8): p. 465-75.

11. Kim, T., et al., *Biomolecular motor-driven molecular sorter.* Lab Chip, 2009. **9**(9): p. 1282-5.

12. Lin, C.T., et al., *Self-contained, biomolecular motor-driven protein sorting and concentrating in an ultrasensitive microfluidic chip.* Nano Lett, 2008. **8**(4): p. 1041-6.

13. Rios, L. and G.D. Bachand, *Multiplex transport and detection of cytokines using kinesin-driven molecular shuttles.* Lab Chip, 2009. **9**(7): p. 1005-10.

14. You, C., et al., *Affinity capturing for targeting proteins into micro and nanostructures.* Anal Bioanal Chem, 2009. **393**(6-7): p. 1563-70.

15. Lata, S., et al., *High-affinity adaptors for switchable recognition of histidine-tagged proteins.* J Am Chem Soc, 2005. **127**(29): p. 10205-15.

16. Lata, S., M. Gavutis, and J. Piehler, *Monitoring the dynamics of ligand-receptor complexes on model membranes.* J Am Chem Soc, 2006. **128**(1): p. 6-7.

17. Lata, S. and J. Piehler, *Stable and functional immobilization of histidine-tagged proteins via multivalent chelator head-groups on a molecular poly(ethylene glycol) brush.* Anal Chem, 2005. **77**(4): p. 1096 -1105.

18. Tinazli, A., et al., *High-Affinity Chelator Thiols for Switchable and Oriented Immobilization of Histidine-Tagged Proteins: A Generic Platform for Protein Chip Technologies.* Chemistry, 2005. **11**(18): p. 5249-5259.

19. Bieling, P., et al., *Processive kinesins require loose mechanical coupling for efficient collective motility.* EMBO Rep, 2008. **9**(11): p. 1121-7.

20. Gavutis, M., et al., *Lateral ligand-receptor interactions on membranes probed by simultaneous fluorescence-interference detection.* Biophys J, 2005. **88**(6): p. 4289-302.

21. Castoldi, M. and A.V. Popov, *Purification of brain tubulin through two cycles of polymerization-depolymerization in a high-molarity buffer.* Protein Expr Purif, 2003. **32**(1): p. 83-8.

22. Hyman, A., et al., *Preparation of modified tubulins.* Methods Enzymol, 1991. **196**: p. 478-85.

23. Piehler, J., et al., *A high-density poly(ethylene glycol) polymer brush for immobilization on glass-type surfaces.* Biosens Bioelectron, 2000. **15**(9-10): p. 473-81.

24. Piehler, J. and G. Schreiber, *Fast transient cytokine-receptor interactions monitored in real time by reflectometric interference spectroscopy.* Anal Biochem, 2001. **289**(2): p. 173-86.

25. Bieling, P., et al., *Reconstitution of a microtubule plus-end tracking system in vitro.* Nature, 2007. **450**(7172): p. 1100-5.

26. Ciesla, P., et al., *Homogeneous photocatalysis by transition metal complexes in the environment.* Journal of Molecular Catalysis a-Chemical, 2004. **224**(1-2): p. 17-33.

27. Urbanski, N.K. and A. Beresewicz, *Generation of (OH)-O-. initiated by interaction of Fe2+ and Cu+ with dioxygen; comparison with the Fenton chemistry.* Acta Biochimica Polonica, 2000. **47**(4): p. 951-962.

28. Leonard, S., et al., *Cobalt-mediated generation of reactive oxygen species and its possible mechanism.* Journal of Inorganic Biochemistry, 1998. **70**(3-4): p. 239-244.

29. Emilio, C., R. Gettar, and M. Litter, *Mechanism of degradation of nitrilotriacetic acid by heterogeneous photocatalysis over TiO_2 and platinized TiO_2.* Journal of Applied Electrochemistry, 2005. **35**(7): p. 733-740.

3 Binary protein patterning by NVOC-based caging

3.1 Introduction

The previous chapter introduced a strategy for functional patterning of His-tagged proteins on tris(nitrilotriacetic acid) functionalized surfaces with a high resolution. As a demonstration of the utility of such patterns we showed the directional transport of microtubule on patterned kinesin which can be envisioned to have very innovative applications in miniaturized biomechanical devices. However, for many purposes, both in basic research as well as in biotechnology, patterns consisting of two proteins immobilized into separate regions are desired. This requires the use of orthogonal protein immobilization approaches which can ensure the selective targeting of different proteins to specific ligands patterned on a surface while preserving their functional integrity to the highest possible level. Several approaches based on either the interaction between biotin and streptavidin or related proteins [1-4], or on the complexation of immobilized transition metal ions by oligohistidine-tags [5-9] have been successfully utilized to achieve oriented functional protein immobilization. Another group of protein immobilization techniques use chemical approaches such as chemical ligation [10], Staudinger ligation [11], thiol-ene reaction [3] or "Click chemistry" utilizing azide alkyne Huisgen cycloaddition [12]. Recently, enzymatic reactions have found increasing attention for posttranslational labeling and immobilization of proteins and several peptide tags that can be recombinantly expressed with target proteins have developed [13-14]. One such recently developed strategy is based on the ybbR tag. This is an 11 residues long peptide identified from a genomic library of *Bacillus subtilis* by phage display as an efficient substrate for Sfp phosphopantetheinyl transferase (PPT). Sfp catalyzes the transfer of the 4'-phosphopantetheinyl moiety of CoA to a serine residue on the ybbR tag [15-16]. Thus this strategy can be utilized for covalently immobilizing ybbR-tagged proteins onto surface-bound CoA.

In addition to orthogonal protein immobilization, generic patterning techniques that are compatible with such immobilization approaches are also required for achieving binary protein patterning. Here, we have explored nitroveratryloxycarbonyl (NVOC)-based caging of surface amines as a photolithographic strategy to demonstrate patterning of two proteins based on two orthogonal immobilization approaches-biotin and the ybbR tag. NVOC, which is a photo-cleavable protection group for amines and hydroxyls, can be selectively and very mildly cleaved with irradiation by 350 nm light. In this work, glass surfaces were first modified with a dense poly(ethylene glycol) (PEG) brush to render them protein compatible. Amine groups presented by the PEG chains were then uniformly caged by NVOC. Using a photomask, selected regions were UV-irradiated thus freeing the amines, which were subsequently reacted with biotin. The remaining amine groups were uncaged by a second round of irradiation, and were reacted with coenzyme A (CoA). Thus, micropatterns of biotin and CoA were readily achieved using this approach. Subsequently, streptavidin was selectively targeted to the biotinylatyed regions while CoA was used to efficiently capture the interferon-α2 receptor, Ifnar2 which was fused to an ybbR tag. Finally, the immobilized receptor was shown to be highly functional by investigating the interaction with its ligand.

3.2 Materials and methods

3.2.1 Materials

Homofunctional diamino poly(ethylene glycol) (DAPEG) with an average molecular mass of 2000 g/mol was purchased from Rapp Polymere, Tübingen/Germany. 2-Mercaptoethanol, Manganese(II)-chloride tetrahydrat, HEPES and Sodium chloride were purchased from Carl Roth, Karlsruhe/Germany. Oregon Green 488 maleimide was purchased from Invitrogen. Streptavidin labeled with ATTO 565 (^{AT565}SAv) was purchased from ATTO-TEC GmbH, Siegen/Germany. A 75 W Xenon lamp fitted with a 280 – 400 nm dichroic mirror was purchased from Newport Spectra-Physics and microstructured masks for photo-patterning (chrome on quartz) were obtained from NB Technologies, Bremen/Germany. CoA-488 and phosphopantetheinyl transferase Sfp were purchased from Covalys Biosciences, Witterswil/Switzerland. All other chemicals were purchased from Sigma Aldrich.

3.2.2 Protein production, purification and labeling

IFNAR2-EC carrying an N-terminal ybbR-tag (ybbR-IFNAR2) was cloned by insertion of an oligonucleotide linker coding for the ybbR peptide (DSLEFIASKLA) into the *Nde*I restriction site upstream of the IFNAR2-EC gene in the plasmid pT72CR2 [17]. IFNα2 and ybbR-IFNAR2 were expressed and purified following previously published protocols [18]. ybbR-IFNα2 was labeled by PPT using CoA-488 and Sfp according to published protocols [19].

3.2.3 Surface chemistry

Surface chemistry was carried out on transducer slides for reflectance interference detection (a thin silica layer on a glass substrate) [20] as well as standard glass cover slides for fluorescence microscopy. Surface coating with a thin DAPEG polymer brush was carried out as described in detail previously [21]. The surface was incubated under a 50 mM solution of biotinamidohexanoic acid N-Hydroxysuccinimide ester (Biotin-NHS) in dry DMF in order to get biotin functionalized surfaces. For functionalization with maleimide groups, the DAPEG-modified surfaces were incubated under a saturated solution of 3-(Maleimido)propionic acid N-Hydroxy-succinimide ester (MPA-NHS) in dry DMF for 30 min at room-temperature. Reaction with CoA was carried out in *situ* under aqueous conditions in a flow-through format (see below).

3.2.4 Surface patterning

Photolithographic patterning was performed using Nitroveratryloxycarbonyl chloride (NVOC chloride) as a photocleavable amine protecting group. For caging of the surface amine groups, DAPEG functionalized surface were incubated with a saturated solution of NVOC chloride in chloroform for 1 h at 75°C. Uncaging of the amine groups was achieved by irradiation through a photomask for 5 min using a 75 W Xenon lamp equipped with a 280-400 nm dichroic mirror. Irradiation was carried out in the presence of 50 mM semicarbazide in methanol in order to minimize side reactions. Subsequently, deprotected amine groups were reacted with Biotin-NHS. For purposes of binary patterning, the surface was again irradiated as before but without a photomask. This led to the deprotection of the remaining surface amines which were subsequently reacted with MPA-NHS.

3.2.5 Binding assays

Protein immobilization and protein interactions were monitored by reflectance interference spectroscopy (RIfS). The measurements were performed under continuous flow-through conditions using home-built set-ups as described earlier [20, 22]. Maleimide-functionalized RIfS transducer slides (prepared as described above) were equilibrated in HBS (20 mM HEPES pH 7.5, 150 mM sodium-chloride and 0.01% Triton X-100) and then reacted with 1 mM CoA in HBS. Prior to protein immobilization, the remaining maleimide groups were blocked by injection of 10 mM 2-mercaptoethanol in HBS. Subsequently, 1 µM of ybbR-IFNAR2 in HBS was immobilized in the presence of 1 µM Sfp and 10 mM Mn^{2+} ions. Surface-bound metal ions were removed by an injection of 25 mM EDTA. Then, the activity of the immobilized protein was probed by injecting the ligand IFNα2.

3.2.6 Fluorescence imaging

Micropatterns of fluorescence-labeled proteins were imaged by means of a confocal laser-scanning microscope (FluoView 1000, Olympus). A 40 mW multiline Argon ion laser was used for the excitation of AT488 and a 20 mW 559 nm diode laser for the exciation of ATTO 565. All experiments were carried out using a home-built flow cell, and ybbR-IFNAR2 was immobilized on patterned coverslides under the same conditions as described in the previous section. In order to confirm the activity of the immobilized ybbR-IFNAR2-EC, 100 nM fluorescence labeled IFNα2 (^{AT488}IFNα2) was injected. The specificity of the interaction was verified by competition with unlabeled IFNα2. Binary patterns were developed by the injection of 100 nM ^{AT565}SAv, which was captured by the patterned biotin on the surface. Dual color images were obtained by sequential line scanning in order to minimize cross-talk between the two channels.

3.3 Results and discussion

3.3.1 NVOC-based caging and uncaging

Photo-deprotection of caged amine functionalities has been demonstrated to be a versatile approach towards biofunctional surface patterning.[4, 23-25] Based on this approach, we implemented PPT-based functional surface patterning by caging of surface amine groups with NVOC-chloride after coupling of the diamino-PEG. In the first step, the caging reaction on the surface and the uncaging by UV irradiation was analyzed by reacting free surface amines with Biotin-NHS. The amount of immobilized biotin molecules was probed by streptavidin binding using RIfS (Figure 3.1a). Very low streptavidin binding compared to the positive control confirmed efficient protection of surface amines by reaction with NVOC-chloride. Upon UV-irradiation in presence of 50 mM semicarbazide, ~ 75 % recovery of streptavidin binding was observed, confirming successful uncaging of surface amines. The same approach was used for coupling MPA-NHS, followed by reaction with CoA and subsequent PPT-mediated immobilization of ybbR-IFNAR2. The amount of ybbR-IFNAR2 on the surface was quantified by probing the binding of IFNα2 using RIfS (Figure 3.1b). Only insignificant binding of IFNα2 was detected after caging the surface amines with NVOC-chloride prior to the reaction with MPA-NHS, confirming the specificity of the immobilization procedure. Upon uncaging surface amines, strong binding of IFNα2 was observed, reaching ~75 % of the binding amplitude obtained for the positive control.

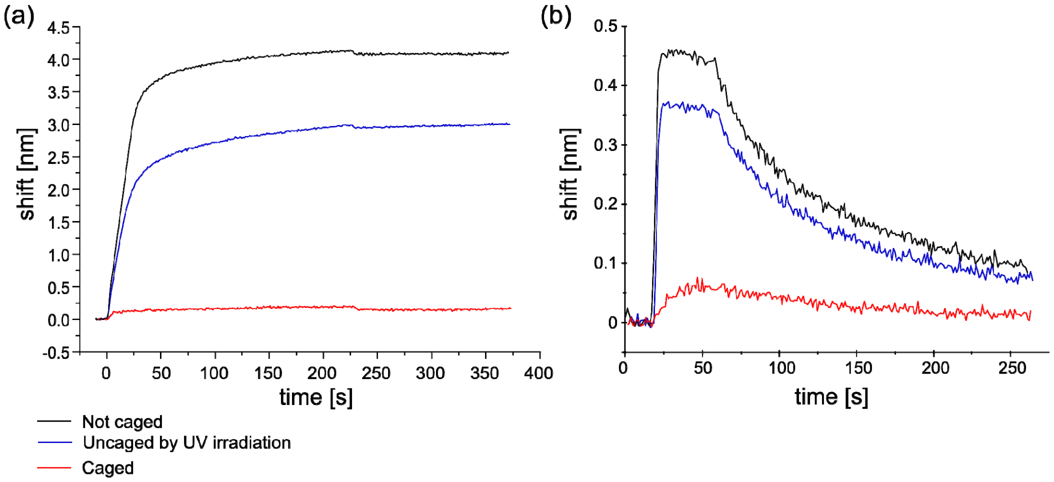

Figure 3.1 Caging of surface amines by NVOC-chloride. (a) Binding of 100 nM streptavidin to surfaces reacted with Biotin-NHS before (black) and after (red) caging with NVOC-chloride, and after UV-illumination of NVOC-caged amines (blue). (b) Binding of 1 µM IFNα2 to ybbR-IFNAR2 immobilized by PPT after caging (red) and after uncaging (blue) of surface amines. For comparison, a positive control without caging the amine groups is shown (black).

3.3.2 Binary protein patterning

With this efficient protocol in hand, we explored photolithographic protein patterning. In order to generate binary protein patterns, we followed a two step illumination scheme (Figure 3.2): After UV-illumination through a photomask, the uncaged amine groups were reacted with Biotin-NHS, followed by another exposure to UV light and coupling of MPA-NHS. The coverslide was then mounted in a flow cell and functionalized with CoA under flow-through conditions followed by coupling of ybbR-IFNAR2 in presence of Sfp.

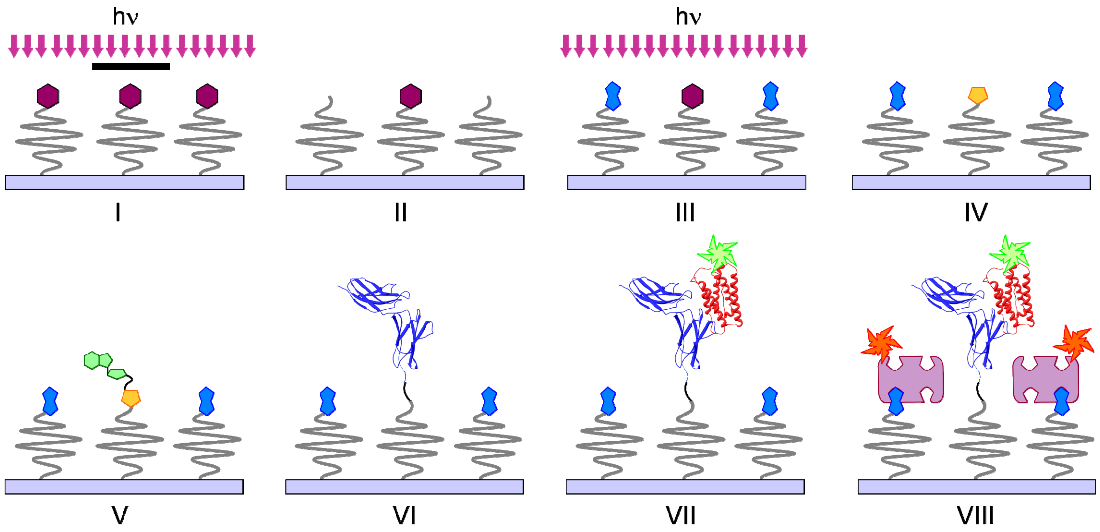

Figure 3.2 Schematic of the patterning process. Figures I-IV show the surface chemistry while the subsequent steps (V-VIII) were carried out in a flow cell. NVOC-caged surfaces were first UV-deprotected through a photomask (I) and the deprotected areas (II) were functionalized with Biotin-NHS, followed by uncaging of the remaining amines with UV light (III). Subsequently, the uncaged amines were functionalized with MPA-NHS (IV). After mounting the coverslide into a flow cell, surfaces were first reacted with CoA (V) followed by PPT-mediated immobilization of ybbR-IFNAR2 (VI). Subsequently, protein binding assays with ^{AT488}IFNα2 (VII) and ^{AT565}SAv (VIII) were carried out.

Upon injection of ^{AT488}IFNα2, patterns of green fluorescence were observed in the areas which were not illuminated during the first illumination cycle, indicating successful immobilization of ybbR-IFNAR2 into the micropatterns (Figure 3.3a). IFNα2 binding proved reversible and complete washout in presence of unlabeled IFNα2 was obtained. Moreover, no binding of ^{AT488}IFNα2 was detectable when incubated in presence of unlabeled IFNα2, confirming binding specificity. In the next step, we tested binding of orange-fluorescent streptavidin ^{AT565}SAv to the surface. Specific targeting of ^{AT565}SAv to the grid, which was UV-illuminated prior to Biotin-NHS coupling, was observed (Figure 3.3b), confirming successful binary protein patterning. Upon addition of unlabeled IFNα2, selective washout of ^{AT488}IFNα2, but not ^{AT565}SAv was observed, confirming highly specific binary protein targeting into microstructures.

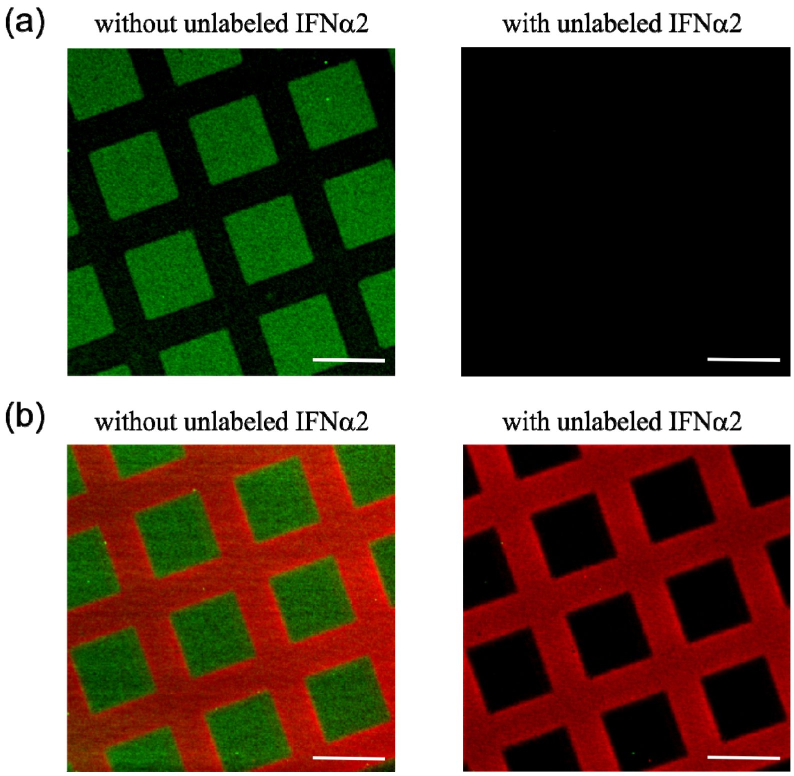

Figure 3.3 Binary protein patterning. (a) CLSM image after binding of ^{AT488}IFNα2 to immobilized ybbR-IFNAR2 in absence (left) and in presence (right) of unlabeled IFNα2. (b) Dual color CLSM image after sequential incubation with 100 nM ^{AT488}IFNα2 and 100 nM ^{AT565}SAv (left), and after exchanging ^{AT488}IFNα2 by 1 µM unlabeled IFNα2 (right). All scale bars represent 20 µm.

3.4 Conclusions

Site-specific covalent immobilization and lateral organization of recombinant protein on planar substrates is highly demanded for numerous analytical and biotechnological applications. Although several strategies are currently available for functional protein immobilization, very generic surface patterning approaches are needed in order to make use of them for such applications. As demonstrated here, NVOC-based photolithography is a very simple and robust method to achieve this aim. Bottom-up surface chemistry was performed in order to modify surfaces with a dense biocompatible PEG brush presenting terminal amine groups that were efficiently caged by NVOC. Under mild UV irradiation upto 75% uncaging was achieved. The generic nature of this approach was demonstrated by using it to pattern biotin and CoA, which were subsequently used to immobilize streptavidin and ybbR-tagged Ifnar2 respectively. The receptor was confirmed to be active by studying the interaction with its ligand IFNα2. Finally, it must be noted that the free amine groups available after UV irradiation can be reacted with a multitude of hetero-functional crosslinkers in order to present reactive groups on the surface that are compatible with the variety of protein immobilization strategies currently available.

3.5 Summary

We presented a generic technique for binary patterning of proteins using the photosensitive amine-protection group nitroveratryloxycarbonyl chloride (NVOC-Cl). Protection and UV-uncaging efficiencies were tested and optimized using solid-phase protein-binding assays. UV irradiation of the surface through a photomask caused localized uncaging of the amine groups. Sequential uncaging and reaction with biotin and coenzyme A (CoA) allowed the patterning of streptavidin and ybbR-tagged proteins into spatially defined regions. Interaction assays using Interferonα2 and its surface immobilized receptor confirmed the high degree of activity of patterned proteins.

3.6 References

1. Christman, K.L., et al., *Submicron streptavidin patterns for protein assembly.* Langmuir, 2006. **22**(17): p. 7444-50.

2. Hyun, J., et al., *Microstamping on an activated polymer surface: Patterning biotin and streptavidin onto common polymeric biomaterials.* Langmuir, 2001. **17**(20): p. 6358-6367.

3. Jonkheijm, P., et al., *Photochemical surface patterning by the thiol-ene reaction.* Angew Chem Int Ed Engl, 2008. **47**(23): p. 4421-4.

4. Alonso, J.M., et al., *Photopatterned Surfaces for Site-Specific and Functional Immobilization of Proteins.* Langmuir, 2008. **24**(2): p. 448-457.

5. Tinazli, A., et al., *High-Affinity Chelator Thiols for Switchable and Oriented Immobilization of Histidine-Tagged Proteins: A Generic Platform for Protein Chip Technologies.* Chemistry, 2005. **11**(18): p. 5249-5259.

6. Klenkar, G., et al., *Piezo Dispensed Microarray of Multivalent Chelating Thiols for Dissecting Complex Protein-Protein Interactions.* Anal Chem, 2006. **78**: p. 3643-3650.

7. Valiokas, R., et al., *Differential protein assembly on micropatterned surfaces with tailored molecular and surface multivalency.* ChemBiochem, 2006. **7**(9): p. 1325-1329.

8. Rakickas, T., et al., *Protein-protein interactions in reversibly assembled nanopatterns.* Nano Lett, 2008. **8**(10): p. 3369-75.

9. Bhagawati, M., et al., *Organization of motor proteins into functional micropatterns fabricated by a photo-induced Fenton reaction.* Angew Chem Int Ed Engl, 2009. **48**(48): p. 9188-91.

10. Camarero, J.A., Y. Kwon, and M.A. Coleman, *Chemoselective attachment of biologically active proteins to surfaces by expressed protein ligation and its application for "protein chip" fabrication.* J Am Chem Soc, 2004. **126**(45): p. 14730-1.

11. Kalia, J., N.L. Abbott, and R.T. Raines, *General method for site-specific protein immobilization by Staudinger ligation.* Bioconjug Chem, 2007. **18**(4): p. 1064-9.

12. Jean-François Lutz, *1,3-Dipolar Cycloadditions of Azides and Alkynes: A Universal Ligation Tool in Polymer and Materials Science.* Angewandte Chemie International Edition, 2007. **46**(7): p. 1018-1025.

13. Johnsson, N. and K. Johnsson, *Chemical tools for biomolecular imaging.* ACS Chem Biol, 2007. **2**(1): p. 31-8.

14. Johnsson, N., N. George, and K. Johnsson, *Protein chemistry on the surface of living cells.* Chembiochem, 2005. **6**(1): p. 47-52.

15. Yin, J., et al., *Genetically encoded short peptide tag for versatile protein labeling by Sfp phosphopantetheinyl transferase.* Proc Natl Acad Sci U S A, 2005. **102**(44): p. 15815-20.

16. Zhou, Z., et al., *Genetically Encoded Short Peptide Tags for Orthogonal Protein Labeling by Sfp and AcpS Phosphopantetheinyl Transferases.* ACS Chem Biol, 2007.

17. Piehler, J. and G. Schreiber, *Biophysical analysis of the interaction of human ifnar2 expressed in E-coli with IFN alpha 2.* J Mol Biol, 1999. **289**(1): p. 57-67.

18. Piehler, J., L.C. Roisman, and G. Schreiber, *New structural and functional aspects of the type I interferon- receptor interaction revealed by comprehensive mutational analysis of the binding interface.* Journal of Biological Chemistry, 2000. **275**(51): p. 40425-40433.

19. Yin, J., et al., *Site-specific protein labeling by Sfp phosphopantetheinyl transferase.* Nat Protoc, 2006. **1**(1): p. 280-5.

20. Schmitt, H.-M., et al., *An integrated system for optical biomolecular interaction analysis.* Biosensors and Bioelectronics, 1997. **12**(8): p. 809-816.

21. Piehler, J., et al., *A high-density poly(ethylene glycol) polymer brush for immobilization on glass-type surfaces.* Biosensors & Bioelectronics, 2000. **15**(9-10): p. 473-481.

22. Piehler, J. and G. Schreiber, *Fast transient cytokine-receptor interactions monitored in real time by reflectometric interference spectroscopy.* Analytical Biochemistry, 2001. **289**(2): p. 173-186.

23. Jonas, U., et al., *Colloidal assemblies on patterned silane layers.* Proc Natl Acad Sci U S A, 2002. **99**(8): p. 5034-9.

24. Stegmaier, P. and A. del Campo, *Photoactive branched and linear surface architectures for functional and patterned immobilization of proteins and cells onto surfaces: a comparative study.* Chemphyschem, 2009. **10**(2): p. 357-69.

25. Chen, S. and L.M. Smith, *Photopatterned thiol surfaces for biomolecule immobilization.* Langmuir, 2009. **25**(20): p. 12275-82.

4 Multiplexed protein patterning by photo-fragmentation of histidine peptides

4.1 Introduction

The last chapter presented a strategy based on photosensitive caging of amine groups as a means to obtain binary patterns of proteins utilizing two orthogonal immobilization strategies. While this is very useful and quite sufficient for several biophysical and biochemical assays, it has a limitation that only two proteins can be patterned on the surface. Moreover, surfaces have to be pre-patterned prior to protein immobilization thus leaving no further opportunity to modify patterns. Much higher flexibility would be offered if multiple proteins could be patterned in *situ* under physiological conditions. Uncaging of caged biotin has been successfully employed for these purposes in different ways for protein micropatterning [1-4]. These methods, however, either require modification of target proteins with caged biotin, or a sandwich-based format for protein immobilization. Also, a caged benzylguanine derivative has been employed for photolithography of alkylguanine-DNA-alkyltransferase-tagged proteins [5]. The slow association kinetics of this reaction, however, obstructs efficient writing of protein microstructures in *situ* as well as multiplexed protein organization. Thus, no efficient generic method for in *situ* protein organization in microstructures is currently available. Here, we have established a versatile approach for directly controlling site-specific immobilization of oligohistidine-tagged proteins in *situ* by means of a confocal laser beam.

This approach is based on a photocleavable oligohistidine-tag for blocking the free coordination sites of Ni(II) ions immobilized through tris(nitrilotriacetic acid) (tris-NTA) moieties [6], which are covalently attached to glass surfaces through a highly biocompatible poly(ethylene glycol) (PEG) polymer brush [7]. Upon photocleavage of the oligohistidine peptide by means of UV light, the fragments rapidly dissociate from the surface because of a dramatic loss of binding affinity due to reduced multivalency. Thus tris-NTA moieties are efficiently uncaged and capable of capturing oligohistidine-tagged proteins. UV irradiation could be performed either through a photomask, or by using a

UV laser in a confocal laser scanning microscope. This not only allowed a high degree of control over irradiation geometry but also over the surface density of patterned protein. Functionality of immobilized protein was confirmed by studying the interaction between interferon-α2 and its receptor. Finally, this strategy was used to pattern multiple His-tagged proteins in a sequential fashion thus validating the capability of this approach to achieve multiplexed, spatio-temporally controlled protein immobilization.

4.2 Materials and methods

4.2.1 Materials

Diamino-polyethylene glycol with MW 2000 Da (PEG2000) was purchased from Rapp Polymere. OtBu-protected tris-NTA-carboxylic acid was synthesized as described previously [6]. Oligohistidine peptides containing the photocleavable building block 3-amino-3- (2 nitrophenyl) propionic acid in different positions were custom-made by EMC microcollections. ATTO655 labeled streptavidin was purchased from ATTO-TEC. Other chemicals were purchased from Sigma Aldrich and used as obtained. Microstructured masks were obtained from NB Technologies. The width of these structures was varied between 1 µm and 10 µm and the spaces between 10 µm and 100 µm. A 75 W Xenon arc lamp fitted with a 280-400 nm dichroic mirror for UV irradiation was purchased from Newport Spectra-Physics.

4.2.2 Proteins

MBP-H6 was expressed in *E. coli* and purified as described previously [7] and labeled with Dy649 maleimide yielding an average degree of labeling of ~1. EGFP-H6 cloned in the plasmid pET21a was expressed in *E. coli* and purified by immobilized metal ion chromatography and size exclusion chromatography by standard protocols. For binding experiments with crude cell lysates, cells were sonicated in 20 mM HEPES pH 7.5 and 150 mM sodium-chloride (HBS) containing protease inhibitor and 1 mM EDTA followed by centrifugation at 40,000 g. The EGFP concentration in the supernatant was determined from its absorption at 480 nm and for surface binding experiments the supernatant was further diluted to a concentration of 1 M in HBS buffer. IFN 2 carrying an N-terminal

YbbR-tag (YbbR-IFNα2) for posttranslational labeling using phosphopantetheinyl transfer (PPT) from Coenzyme A (CoA) derivatives [8] was expressed and purified like wildtype IFNα2. YbbR-IFNα2 was labeled with ATTO 488 conjugated to CoA (CoA-488, Covalys Biosciences) by means of the PPTase Sfp (Covalys Biosciences) according to the protocol from the manufacturer. After the labeling reaction, $_{\text{AT488}}$IFN 2 was further purified by size exclusion chromatography. IFNAR2-H10 was expressed in *E. coli* and refolded from inclusion bodies and purified as described before [9-10].

4.2.3 Surface modification

Glass surfaces were coated with a molecular PEG polymer brush and functionalized with tris-NTA as described earlier [7]. For functionalization with tris-NTA, 5 µL of a solution of OtBu-protected tris-NTA-carboxylic acid in chloroform (100 mg/ml) was applied on the surface. Coupling of the carboxy group with the amine modified surface was started by addition of 5 µL of N,N'- diisopropylcarbodiimide and the reaction was carried out by incubation for 1 h at 75 °C. The excess reaction mixture was washed off with chloroform after the reaction. The substrates were then incubated in trifluoroacetic acid overnight to cleave of the tert-butyl esters and free the NTA head groups.

4.2.4 Surface binding by real-time solid phase detection

Peptide and protein binding to tris-NTA functionalized surfaces was probed using label-free detection by reflectance interference spectroscopy (RIfS) and total internal reflection fluorescence spectroscopy (TIRFS). The measurements were performed under continuous flow through conditions using home-built set-ups described earlier [11-13]. GFP was excited with the 488 nm line of an Argon ion laser, Dy649 was excited by a 640 nm diode laser. The excitation laser power was ~100µW illumination a 1 mm spot, excluding photobleaching during binding experiments. All binding experiments were carried out in HBS (20 mM HEPES pH 7.5 and 150 mM sodium-chloride) supplemented with 0.01% Triton X-100. Prior to binding experiments, tris-NTA functionalized surfaces were sequentially treated with 100 mM HCl, 10 mM $NiCl_2$ and 250 mM imidazole. This was followed by injections of either 1 µM -His or 100 nM GFP-H6 as required.

4.2.5 Φ-His photocleavage in solution

Φ-His at a concentration of 1 M in HBS was irradiated under a 75 W Xenon lamp for varying durations of time to achieve photocleavage in solution.

4.2.6 Photolithography and fluorescence imaging

Tris-NTA modified coverslips were sequentially treated with 100 mM HCl, 10 mM $NiCl_2$ and 250 mM imidazole, followed by incubation with 1 M Φ-His. The surfaces were subsequently incubated under 10 mM 1,4-benzoquinone followed by profuse washing with HBS. Offline photolithography was achieved by irradiation of such surfaces through a microstructured photomask using a 75 W Xenon arc lamp for 5 min. Fluorescence imaging and *in situ* photolithography were carried out with a confocal laser scanning microscope (Fluoview 1000, Olympus). The microscope was equipped with a 40 mW multiline Argon ion laser and a 20 mW 635 nm diode laser and a 50 mW 405 nm diode laser used for photo-fragmentation. Tris-NTA modified coverslips preconditioned as described above were used. The cleavage of the Φ-His peptide was achieved by scanning regions of interest (ROIs) with the 405 nm laser (at 10% laser power) at a scan speed of 8 µs/pixel for 50 iterations (unless specified otherwise). The surface was subsequently incubated with the protein of interest at a concentration of 1 µM for 5 min, rinsed with HBS and imaged by excitation with the respective laser (488 nm for of GFP and 635 nm for Dy649/AT655). Sequential line mode imaging was applied for dual color imaging in order to minimize the spectral crosstalk.

4.3 Results and discussion

4.3.1 Blocking efficiency of peptide and photo-fragmentation in solution

Photocleavable oligohistidine peptides were obtained by solid phase synthesis using 3-amino-3-(2-nitrophenyl)-propionic acid (Φ) as a photocleavable building block [14]. Different sequences were tested for efficient blocking of the surface. The structure of the photocleavable portion of the peptides is shown in Figure 4.1.

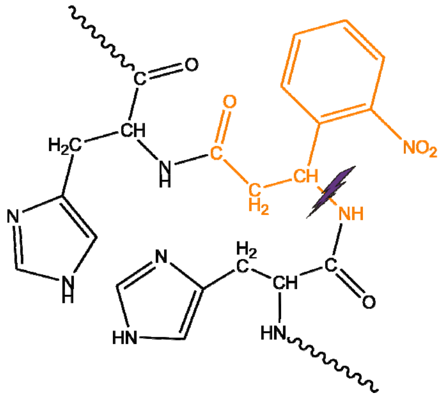

Figure 4.1 The photocleavable peptide. Structure of the photo-cleavable unit comprising of Histidines (black) connected via 3-amino-3-(2-nitrophenyl)-propionic acid (orange). The bond that is cleaved upon UV-irradiation is indicated.

The peptide with the sequence (HHHΦ)$_3$HHH turned out to be very efficient for blocking of tris-NTA functionalized surfaces as detected by probing surface binding by label-free detection using reflectance interference (RIf) (Figure 4.2a). This peptide (Φ–His) was used throughout this study. Upon UV-irradiation of this peptide in a cuvette, reduced binding of the peptide to tris-NTA was observed (Figure 4.2b). The decrease in peptide binding was accompanied by a substantial increase in subsequent binding of a His-tagged protein (Figure 4.2c).

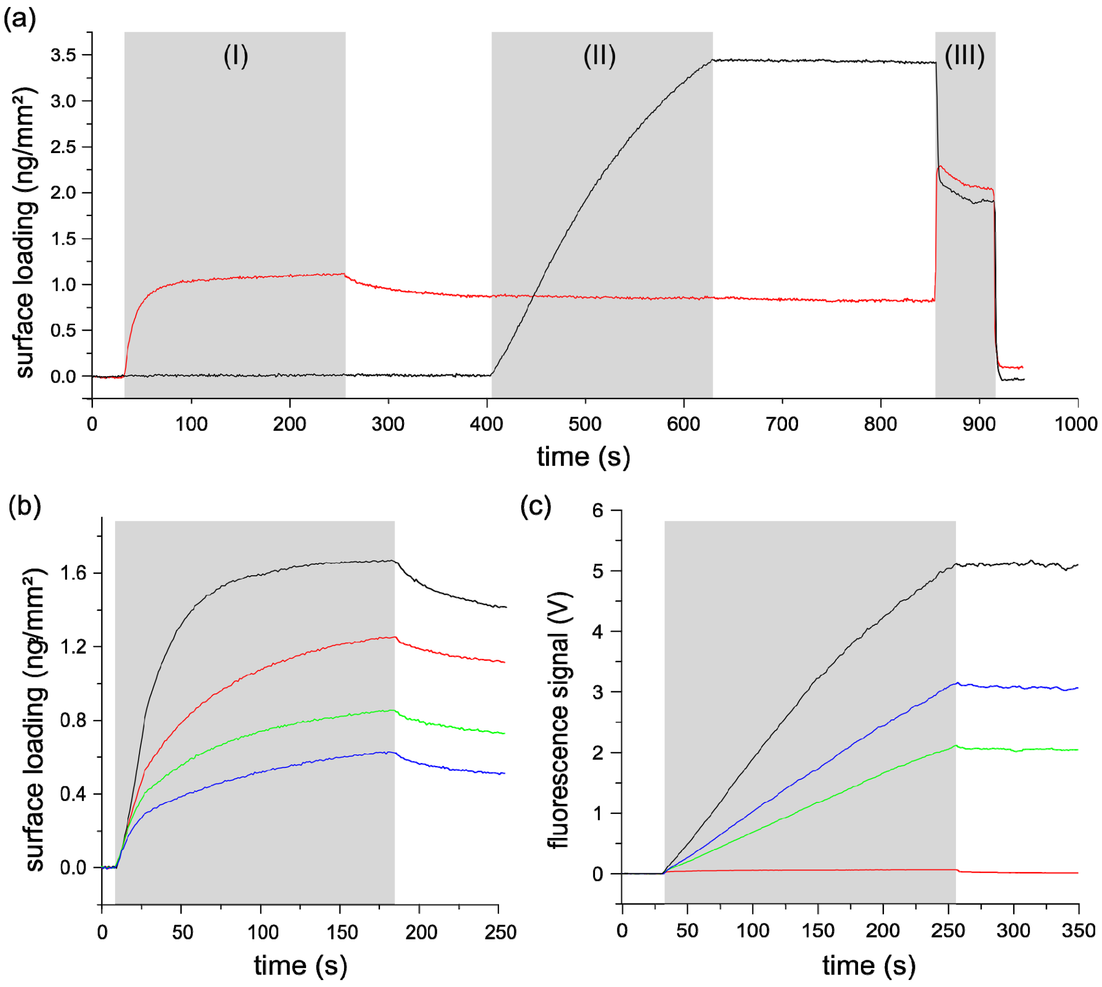

Figure 4.2 Blocking of tris-NTA functionalized surfaces by the Φ-His-peptide. (a) Blocking of surface tris-NTA groups by injection of 1 µM Φ-His-peptide (I) followed by injection of 200 nM GFP-H6 (II) and regeneration with imidazole (III) as detected by RIfS (red curve). For comparison, binding of GFP-H6 to the same surface without prior blocking with the Φ–His-peptide is shown (black curve). (b) Binding signal for the Φ-His-peptide before (black) and after UV irradiation for 100 s (red), 1,000 s (green) and 10,000 s (blue). (c) Binding of GFP-H6 to tris-NTA surfaces blocked with Φ-His-peptide before (red curve) and after irradiation for 3,000 s (green) and 10,000 s (blue) as detected by TIRFS. Binding of GFP-H6 to non-blocked surfaces is shown in comparison (black). The grey bars mark the injection periods.

4.3.2 Patterning using a photomask

Uncaging of Φ–His complexed on a tris-NTA functionalized surface was explored by illumination through a photomask. The scheme for these experiments is shown in Figure 4.3: tris-NTA modified surfaces were loaded with Ni(II) and subsequently incubated under a solution of Φ–His in order to completely saturate the remaining coordination sites of Ni(II) (I). Upon exposure to UV light Φ-His was fragmented and therefore dissociated from the Ni(II) ions due to loss of multivalency (II). Ni(II) coordination sites were thus freed in order to bind His-tagged proteins from solution (III).

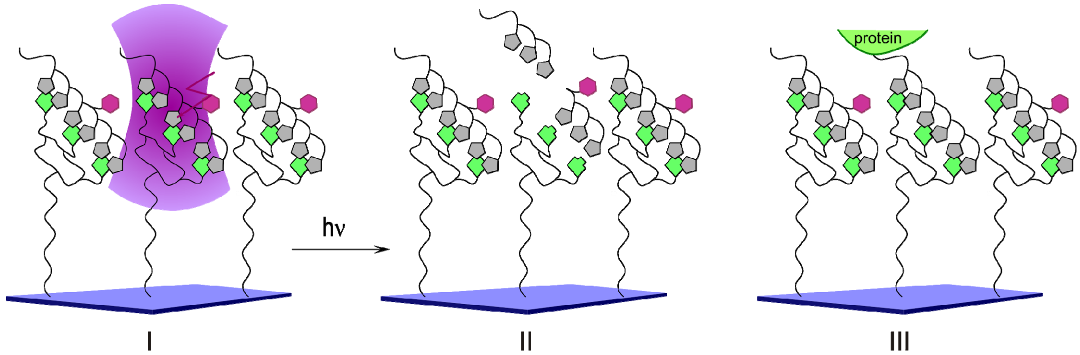

Figure 4.3 Schematic illustration of the patterning method. After saturating surface tris-NTA moieties with Φ-His, the peptide is locally cleaved by UV illumination either through a mask or by means of a confocal UV laser (I). Upon cleavage of the peptide, the multivalency of interaction with tris-NTA is substantially reduced, leading to rapid dissociation of the peptide fragments (II). His-tagged proteins can now bind to the free tris-NTA moieties (III). The Φ-His-peptide is shown only partially for better clarity.

However, insignificant protein binding and irreversible loss of binding capacity was observed upon UV illumination of the surface loaded with Φ–His. This could be explained by photodestruction of tris-NTA groups by photo-oxidation through radicals formed during photocleavage, or by side-reactions of the photocleaved nitrobenzyl groups with surface nucleophiles. In order to reduce these non-specific effects, we treated the surface with 1,4-benzoquinone as an electron scavenger. Binding of 1,4-benzoquinone to the surface was observed by label-free detection (Figure 4.4a). Thus, protein binding experiments did not require the presence of this compound in solution.

Indeed, uncaging of tris-NTA by photo-fragmentation of complexed Φ–His was possible after treatment with 1,4-benzoquinone: under these conditions, strong binding of GFP-H6 into micro-structures was observed after UV-illumination of the surface through a photomask (Figure 4.4b). Protein binding was specific to His-tagged proteins and immobilized proteins could be quantitatively removed by imidazole.

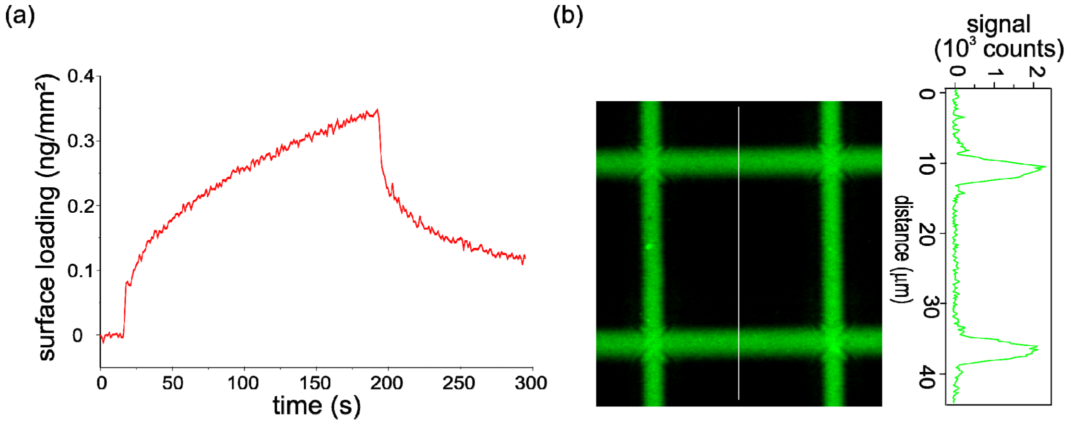

Figure 4.4 Protein patterning by UV irradiation through a photomask. (a) Binding signal of 10 mM benzoquinone to a tris-NTA surface as observed by RIfS. (b) CLSM image of a tris-NTA surface blocked with Φ-His, which was uncaged by UV illumination through a photomask followed by incubation of GFP-H6. The profile shows the fluorescence intensity across the indicated line.

4.3.3 Patterning using a confocal UV laser

Uncaging of surface tris-NTA groups was also possible by laser lithography using a 405 nm laser in a confocal fluorescence microscope: Upon scanning regions of interest (ROI) with the laser, specific binding of His-tagged proteins to these areas was detected (Figure 4.5a). Depending on the number of iterations, different levels of protein binding were observed until saturation was reached. In order to confirm specificity of protein targeting, His-tagged green fluorescent protein (GFP) was incubated along with ATTO655 labeled streptavidin at a concentration ratio of 1:50. Even under this condition, only GFP signal could be observed in the UV irradiated region (Figure 4.5b). This method enabled the fabrication of very high resolution protein micropatterns and microstructures close to the diffraction limit of light (~300 nm FWHM) could be obtained (Figure 4.5c, d).

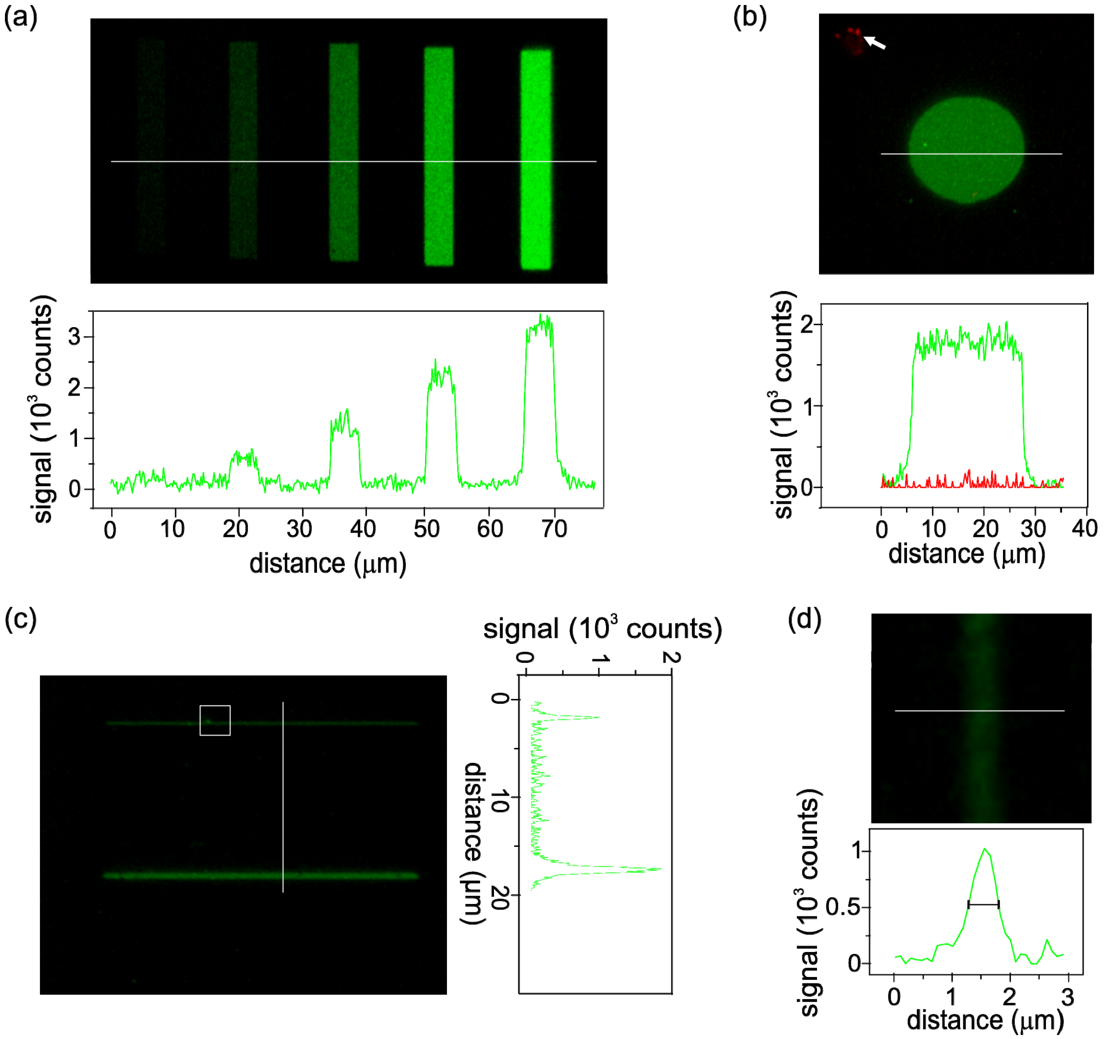

Figure 4.5 Protein patterning by laser lithography. (a) After uncaging different ROIs by scanning with the confocal beam of a 405 nm laser for different numbers of iterations (1, 3, 10, 30 and 100), the surface was incubated with GFP-H6. (b) GFP-H6 was selectively targeted to irradiated regions even in the presence of 50 times higher concentration of red labeled streptavidin. In order to demonstrate the capability to detect streptavidin, an area was chosen where nonspecific binding of the protein to a surface defect was detectable (in the upper left corner, indicated by an arrow). (c) CLSM image of a Φ-His blocked tris-NTA functionalized surface on which single lines were scanned with a 405 nm laser for different number of iterations (10 and 100) followed by incubation with GFP-H6. (d) Enlarged view corresponding to the square indicated in panel (c). The profiles show the fluorescence intensity along the indicated lines.

A very powerful application of this patterning technique is demonstrated in Figure 4.6a where His-tagged GFP from a crude *E. coli* lysate was specifically targeted to a microstructure fabricated by this strategy. This possibility will enable the micropatterning of diverse proteins without the need to go through cumbersome and time-consuming purification protocols.

In order to confirm the activity of immobilized proteins, the extracellular domain of IFNAR2 fused to a decahistidine-tag (IFNAR2-H10) was immobilized by laser lithography. Specific targeting of this protein into the scanned ROIs was confirmed by injection of its ligand Interferon-α2, which was labeled with ATTO 488 (^{AT488}IFNα2). Binding of ^{AT488}IFNα2 was detected exclusively in the pre-scanned ROIs only after incubation of IFNAR2-H10 (Figure 4.6b).

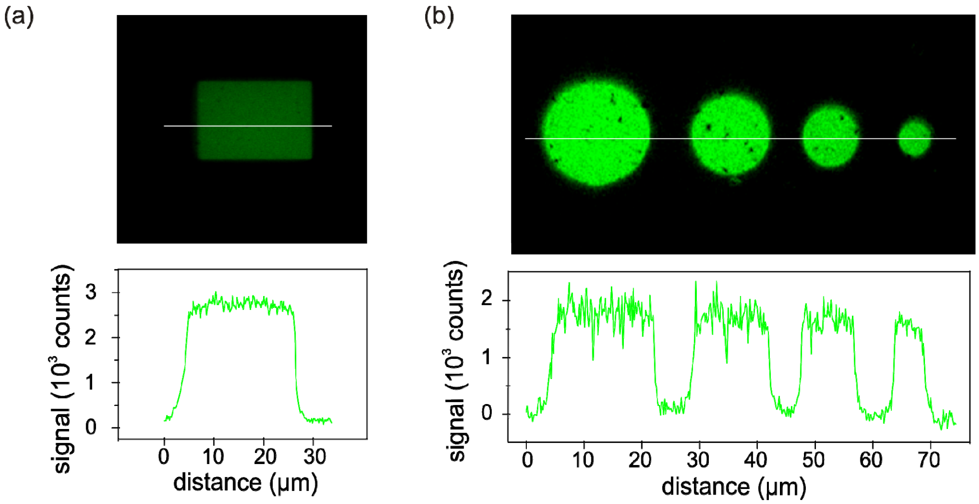

Figure 4.6 Protein patterning by laser lithography. (a) Protein patterning from crude cell lysate. After uncaging of tris-NTA groups by the 405 nm laser, a crude lysate from *E. coli* expressing GFP-H6 diluted into HBS was incubated on the surface. (b) Activity of patterned proteins. After uncaging circular ROIs with different diameters, unlabeled IFNAR2-H10 was immobilized, followed by incubation of green labeled IFNα2. The profiles show the fluorescence intensity along the indicated lines.

4.3.4 Multiplexed patterning in a CLSM

Next to the flexibility to freely design protein patterns by laser lithography, this method also enables for iterative writing of different proteins. In order to demonstrate this capability, we sequentially targeted two different proteins with different fluorescence labels in *situ*. To this end, a grid obtained by mask illumination followed by immobilization of GFP-H6 was sequentially decorated with GFP-H6 and DY-649 labeled maltose binding protein with a hexahistidine tag (^{Dy649}MBP-H6). The overlay of the green and red fluorescence channels are shown in Figure 4.7. The high fidelity of protein targeting into different ROIs is confirmed by intensity profiles of the red and green channels.

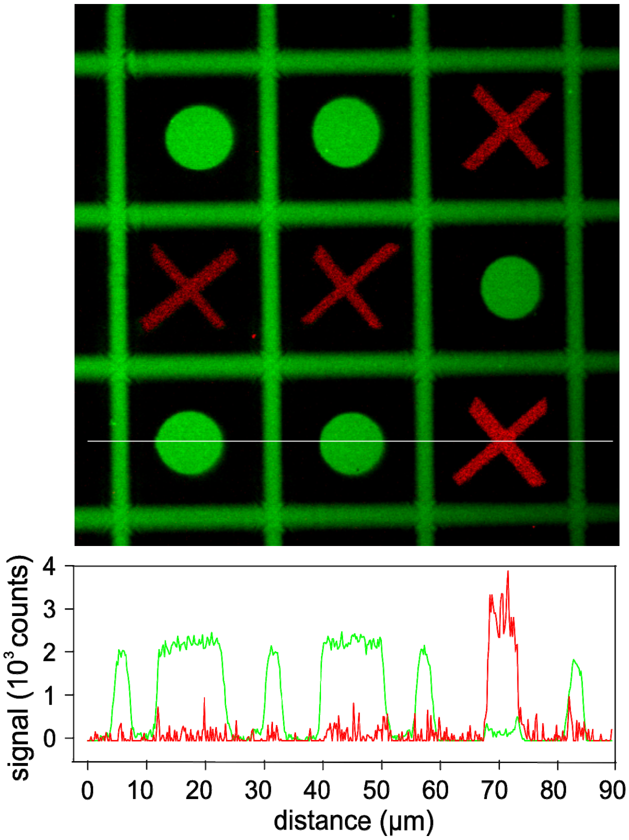

Figure 4.7 Sequential patterning of multiple proteins . Multiplexed protein immobilization by combining illumination through a photomask and in *situ* laser lithography using GFP-H6 and red labeled MBP-H6 for sequentially “writing” protein structures into the grid. The cross-section shows the fluorescence intensity across the indicated lines.

4.4 Conclusions

These examples demonstrate the versatile capabilities of our approach for iterative “writing” of different recombinant proteins into functional microstructures using a non-covalent caging approach. Owing to rapid protein binding, multiplexed protein organization into complex microstructures by combination with micro-fluidics will be feasible. Using near field optical techniques for local uncaging should enable to create structures below the diffraction limited resolution of light. Another interesting feature of our approach is the non-covalent nature of the caging/uncaging mechanism, which is based on modulation of the multivalency of the interaction. Thus, proteins and photocleavable peptides can be removed by imidazole, enabling for a complete erase of proteins pattern and multiple use of the substrate. With the His-tag being by far the most frequently used affinity-tag for protein purification and the relatively simple compounds used for surface modification, highly generic application of the technique can be envisioned.

4.5 Summary

We presented a generic approach for targeting proteins into micropatterns by in *situ* laser lithography. To this end, we designed a photocleavable oligohistidine peptide for caging tris-NTA groups on surfaces by multivalent interactions. Local photofragmentation of the peptide by UV illumination through a photomask or by a confocal laser beam uncaged tris-NTA, thus generating free binding sites for rapid, site-specific capturing of His-tagged proteins into micropatterns. Iterative writing of proteins by laser lithography enabled for assembly of multiplexed functional protein microstructures on surfaces. Thus, versatile, user-defined protein micropatterns could be assembled under physiological conditions with a standard confocal laser-scanning microscope.

4.6 References

1. Choi, H.J., et al., *Micropatterning of biomolecules on glass surfaces modified with various functional groups using photoactivatable biotin.* Anal Biochem, 2005. **347**(1): p. 60-6.

2. Hengsakul, M. and A.E. Cass, *Protein patterning with a photoactivatable derivative of biotin.* Bioconjug Chem, 1996. **7**(2): p. 249-54.

3. Pirrung, M.C. and C.Y. Huang, *A general method for the spatially defined immobilization of biomolecules on glass surfaces using "caged" biotin.* Bioconjug Chem, 1996. **7**(3): p. 317-21.

4. Sundberg, S.A., et al., *Spatially-addressable immobilization of macromolecules on solid supports.* J Am Chem Soc, 1995. **117**(49): p. 12050-12057.

5. Banala, S., A. Arnold, and K. Johnsson, *Caged substrates for protein labeling and immobilization.* Chembiochem, 2008. **9**(1): p. 38-41.

6. Lata, S., et al., *High-affinity adaptors for switchable recognition of histidine-tagged proteins.* J Am Chem Soc, 2005. **127**(29): p. 10205-15.

7. Lata, S. and J. Piehler, *Stable and functional immobilization of histidine-tagged proteins via multivalent chelator head-groups on a molecular poly(ethylene glycol) brush.* Anal Chem, 2005. **77**(4): p. 1096 -1105.

8. Yin, J., et al., *Genetically encoded short peptide tag for versatile protein labeling by Sfp phosphopantetheinyl transferase.* Proc Natl Acad Sci U S A, 2005. **102**(44): p. 15815-20.

9. Lamken, P., et al., *Ligand-induced assembling of the type I interferon receptor on supported lipid bilayers.* J Mol Biol, 2004. **341**(1): p. 303-18.

10. Piehler, J. and G. Schreiber, *Biophysical analysis of the interaction of human ifnar2 expressed in E. coli with IFNalpha2.* J Mol Biol, 1999. **289**(1): p. 57-67.

11. Gavutis, M., et al., *Lateral ligand-receptor interactions on membranes probed by simultaneous fluorescence-interference detection.* Biophys J, 2005. **88**(6): p. 4289-302.

12. Gavutis, M., S. Lata, and J. Piehler, *Probing 2-dimensional protein-protein interactions on model membranes.* Nat Protoc, 2006. **1**(4): p. 2091-103.

13. Piehler, J. and G. Schreiber, *Fast transient cytokine-receptor interactions monitored in real time by reflectometric interference spectroscopy.* Anal Biochem, 2001. **289**(2): p. 173-86.

14. Grunwald, C., et al., *In situ assembly of macromolecular complexes triggered by light.* Proc Natl Acad Sci U S A, 2010. **107**(14): p. 6146-51.

5 Combined peptide tags for improving immobilization efficiencies and micropatterning of proteins

5.1 Introduction

The last chapter introduced an approach towards obtaining high resolution functional patterns of His-tagged proteins on tris(nitrilotriacetic acid) (tris-NTA) functionalized surfaces. While this enabled the in *situ* patterning of multiple proteins on a surface using a confocal laser scanning microscope, it suffers from a limitation inherent to the immobilization scheme. This was that the interaction of a His-tag with Ni(II) ions is quite sensitive to transition metal ions and their chelators, as well as to other proteins displaying histidine tags. Therefore, previously immobilized proteins leach out every time the surface is exposed to a new His-tagged protein in solution. This problem can be solved by using peptide tags such as the Halo- or ybbR-tag that enable the irreversible covalent coupling of fusion proteins to surfaces modified with their specific ligands [1-5]. However, these tags offer very low binding rate constants (~ 10^3 $M^{-1}s^{-1}$), meaning that high amounts of fusion protein are needed to get required surface densities. In contrast, the His-tag enables protein immobilization at low concentrations due to a high association rate constant (~ 10^5 $M^{-1}s^{-1}$) [6]. Therefore, combined tags consisting of a His-tag and either a ybbR- or a Halo-tag were conceived as a solution to the limitations of the individual peptide tags.

This concept was based on the hypothesis that the His-tag would first target proteins onto surfaces. As a result of its high rate constant, this would be a fast process even at comparatively low protein concentrations. Once the protein is captured onto the surface, the effective volume available for the Halo- or the ybbR-tag would become very low, thus increasing the effective local concentration of the tag significantly (Figure 5.1). This would thus increase the rate of the reaction of these tags with their surface-immobilized ligands to a huge extent. Furthermore, it was envisaged that patterning approaches for His-tagged proteins could be extended for proteins carrying such combined tags in order to enable site-specific covalent targeting into mico- and nano-structures.

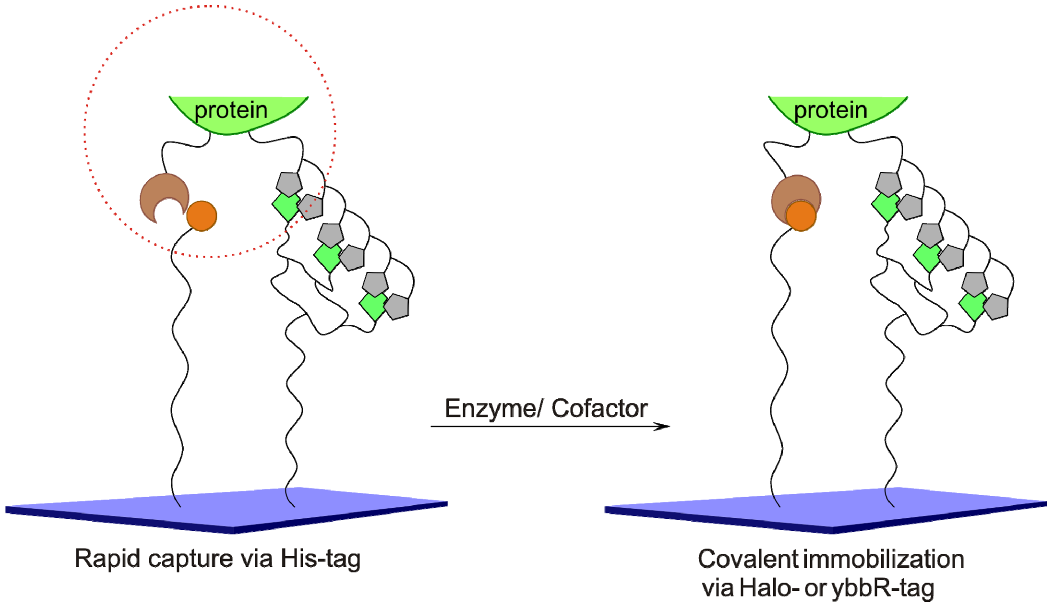
protein
protein
Enzyme/ Cofactor
Rapid capture via His-tag
Covalent immobilization via Halo- or ybbR-tag

Figure 5.1 Combined peptide tags. Fusion proteins first get rapidly captured via the interaction of its His-tag with Ni(II) ions on the surface. This decreases the volume accessible to the Halo- or ybbR-tag (indicated by the red circle) thus increasing its effective concentration. Therefore the covalent reaction of the peptide tag with its specific ligand on the surface occurs rapidly.

Towards these ends, approaches for simultaneously functionalizing substrates with tris-NTA [6], together with ligands for either the ybbR-tag (coenzyme A, CoA) or Halo-tag (Halo-tag ligand, HTL) were developed. Solid phase surface-binding experiments were conducted to demonstrate that proteins fused to the combined His-ybbR and His-Halo tags were targeted to surfaces at much higher efficiencies than the individual ybbR- or Halo-tagged proteins at equal concentrations. Furthermore, micropatterning of such proteins was shown to be possible by using a photofragmentable Histidine peptide based on the peptide used in the previous chapter. Protein functionality was confirmed by investigating the interaction of Interferonα2 with its patterned receptor Ifnar2 carrying a combined His-ybbR tag. Finally, multiplexed patterning of His-ybbR tagged proteins was shown to be possible using this approach.

5.2 Materials and methods

5.2.1 Materials

Diamino-polyethylene glycol with MW 2000 Da (DAPEG) was purchased from Rapp Polymere. OtBu-protected tris-NTA-carboxylic acid was synthesized as described previously [6]. Oligohistidine peptide containing the photocleavable building block 3-amino-3- (4,5-dimethoxy-2-nitrophenyl) propionic acid was obtained from our collaborator Dr. Aranzazu del Campo. Other chemicals were purchased from Sigma Aldrich and used as obtained.

5.2.2 Proteins

H6-EGFP, H6-ybbR-EGFP and H6-ybbR-mCherry cloned in the plasmid pET21a were expressed in *E. coli* and purified by immobilized metal ion chromatography and size exclusion chromatography by standard protocols. H6-Halo-mEGFP was expressed and purified as previously described [1]. Sfp was expressed as an MBP fusion protein in *E. coli* and purified on an amylase column. IFNα2 mutant YNS carrying an N-terminal ybbR-tag (ybbR-IFNα2) for posttranslational labeling using phosphopantetheinyl transfer (PPT) from Coenzyme A (CoA) derivatives [5] was expressed and purified like wildtype IFNα2. YbbR-IFNα2 was labeled with OG 488 conjugated to CoA (CoA-OG 488) by means of the PPTase Sfp (Covalys Biosciences) according to the protocol from the manufacturer. After the labeling reaction, IFNα2-YNS^{OG488} was further purified by size exclusion chromatography. YbbR-IFNAR2-H10 was expressed in *E. coli* and refolded from inclusion bodies and purified as described before [7-8].

5.2.3 Surface modification

Transducer slides for reflectance interference (RIf) detection and glass coverslips for microscopy were functionalized with DAPEG as described previously [9]. Amine groups on the surface were then reacted with 50 mM 6-Maleimidohexanoic acid N-hydroxysuccinimide ester in DMF for 30 minutes at room temperature in order to get maleimide groups. Surfaces simultaneously modified with tris-NTA and CoA (tris-NTA+CoA) were obtained by reacting a solution of 500 μM tris-NTA-SH [10] and 125 μM CoA in the presence of 10 mM $MgCl_2$ in HBS on the surface for 1 hour at room temperature. Surfaces functionalized with tris-NTA and HTL (tris-NTA+HTL) were obtained by first reacting maleimide functionalized surfaces with 500 μM tris-NTA-SH in the presence of 10 mM $MgCl_2$ for in HBS for 5 minutes at room temperature, followed by further reaction with a 500 μM solution of HTL-SH in HBS for 30 minutes at room temperature.

5.2.4 Surface binding by real-time solid phase detection

Peptide and protein binding to tris-NTA functionalized surfaces was probed using label-free detection by reflectance interference (RIf). The measurements were performed under continuous flow through conditions using home-built set-ups described earlier [11-13]. All binding experiments were carried out in HBS (20 mM HEPES pH 7.5 and 150 mM sodium-chloride) supplemented with 0.01% Triton X-100. Prior to binding experiments, tris-NTA+CoA and tris-NTA+HTL functionalized surfaces were sequentially treated with 250 mM EDTA, 10 mM $NiCl_2$ and 500 mM imidazole in order to load the tris-NTA chelators with Ni(II) ions, unless specified otherwise. This was followed by injections as described in the relevant text.

5.2.5 Photolithography and fluorescence imaging

Tris-NTA+CoA and tris-NTA+HTL modified coverslips were sequentially treated with 250 mM EDTA, 10 mM $NiCl_2$ and 500 mM imidazole, followed by incubation with 1 μM His_{NVOC}. Fluorescence imaging and photolithography were carried out with a confocal laser scanning microscope (Fluoview 1000, Olympus). The microscope was equipped with a 40 mW multiline Argon ion laser, a 20 mW 559 nm diode laser and a 50 mW 405 nm diode laser used for photo-fragmentation. Cleavage of the His_{NVOC} peptide was achieved by scanning regions of interest (ROIs) with the 405 nm laser (at 100% laser power) at a scan speed of 8 μs/pixel for 1 iteration. The surfaces were subsequently treated as described in the relevant text. EGFP and mEFGP were imaged by excitation with the 488 nm laser line, while mCherry was imaged by excitation with the 559 nm laser line. Sequential line mode scanning was applied for dual color imaging in order to minimize the spectral crosstalk.

5.3 Results and discussion

5.3.1 Photo-fragmentation of His$_{NVOC}$ and patterning of His-tagged proteins

Photocleavable oligohistidine peptide with the sequence (HHHν)$_3$HHH, where ν stands for 3-amino-3- (4,5-dimethoxy-2-nitrophenyl) propionic acid (Figure 5.2) was obtained from our collaborator Dr. Aranzazu del Campo. Of note here is the photocleavable group 4,5-dimethoxy nitrobenzene, which has a red shifted absorption spectrum as compared to nitrobenzene (λ_{max} ~ 260 nm) which was used in the last chapter.

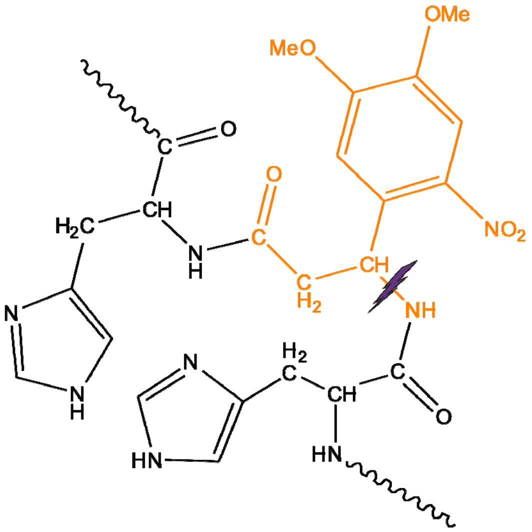

Figure 5.2 The photocleavable peptide. Structure of the photo-cleavable unit comprising of Histidines (black) connected via 3-amino-3-(4,5-dimethoxy-2-nitrophenyl)-propionic acid (orange). The bond that is cleaved upon UV-irradiation is indicated.

Since photolithography was conducted with a 405 nm laser, very high power densities were required when using nitrobenzene as a photosensitive moiety, which also lead to side reactions such as photo-destruction of tris-NTA. Although this problem was solved by using 1,4-benzoquinone as a free radical quencher, we expected that using 4,5-dimethoxy nitrobenzene would enable selective photo-fagmentation of the peptide even in the absence of the free radical quencher. In order to verify this hypothesis, we attempted photolithography of tris-NTA functionalized surfaces using this modified peptide (His$_{NVOC}$). The scheme for this experiment was the same as described in the last chapter (Figure 4.3): tris-NTA modified surfaces were loaded with Ni(II) and subsequently incubated under a solution of His_{NVOC} in order to completely saturate the remaining coordination sites of Ni(II) (I). Selected regions were then scanned with the 405 nm laser of a CLSM. His_{NVOC} in the irradiated regions was fragmented and therefore dissociated from the Ni(II) ions due to loss of multivalency (II). Ni(II) coordination sites were thus freed in order to bind His-tagged proteins from solution (III).

Very efficient targeting of His-tagged EGFP (H6-EGFP) was shown to be possible using this protocol (Figure 5.3). Thus, His_{NVOC} allowed us to pattern His-tagged proteins on tris-NTA functionalized surfaces without exposure to 1,4-benzoquinone.

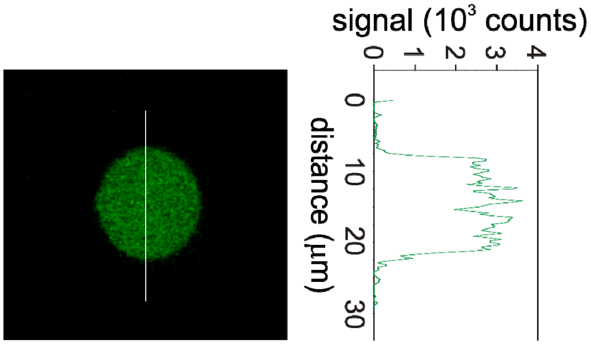

Figure 5.3 Patterning using His_{NVOC}. CLSM image of a tris-NTA surface blocked with His_{NVOC}, which was uncaged by irradiaton using a UV laser of a CLSM followed by incubation of H6-EGFP. The profile shows the fluorescence intensity across the indicated line.

Having this peptide in hand, we next optimized protocols for surface immobilization of proteins carrying the combined His-Halo and His-ybbR tags.

5.3.2 Surface immobilization of His-Halo-tagged proteins

Monomeric EGFP (mEGFP) with contiguous N-terminal hexahistidine and Halo-tags (H6-Halo-mEGFP) was used as a model to study the immobilization of His-Halo-tagged proteins on surfaces functionalized with tris-NTA and Halo-tag ligand (HTL) (Figure 5.4). RIf experiments using this protein showed significant binding to Ni(II) loaded surfaces (Figure 5.4a: top, Figure 5.4b: black curve). Moreover, negligible dissociation of the protein was observed even upon injection of 500 mM imidazole signifying that all the protein was immobilized covalently. Injection of EGFP carrying only a hexahistidine-tag (H6-EGFP) led to even higher amounts of bound protein, all of which was however removed upon injection of imidazole (Figure 5.4a: middle, Figure 5.4b: green curve).

While the higher binding was most probably due to the dimerization propensity of EGFP, this experiment incontrovertibly proved the necessity of the Halo-tag for covalent immobilization to the surface. Upon removal of Ni(II) ions from the surface in order to abolish the His-tag-tris-NTA interaction, and subsequent injection of H6-Halo-mEGFP, very little binding was observed (Figure 5.4a: bottom, Figure 5.4b: blue curve). This underlines the very low efficiency of protein immobilization when the Halo-tag is used as the sole targeting moiety.

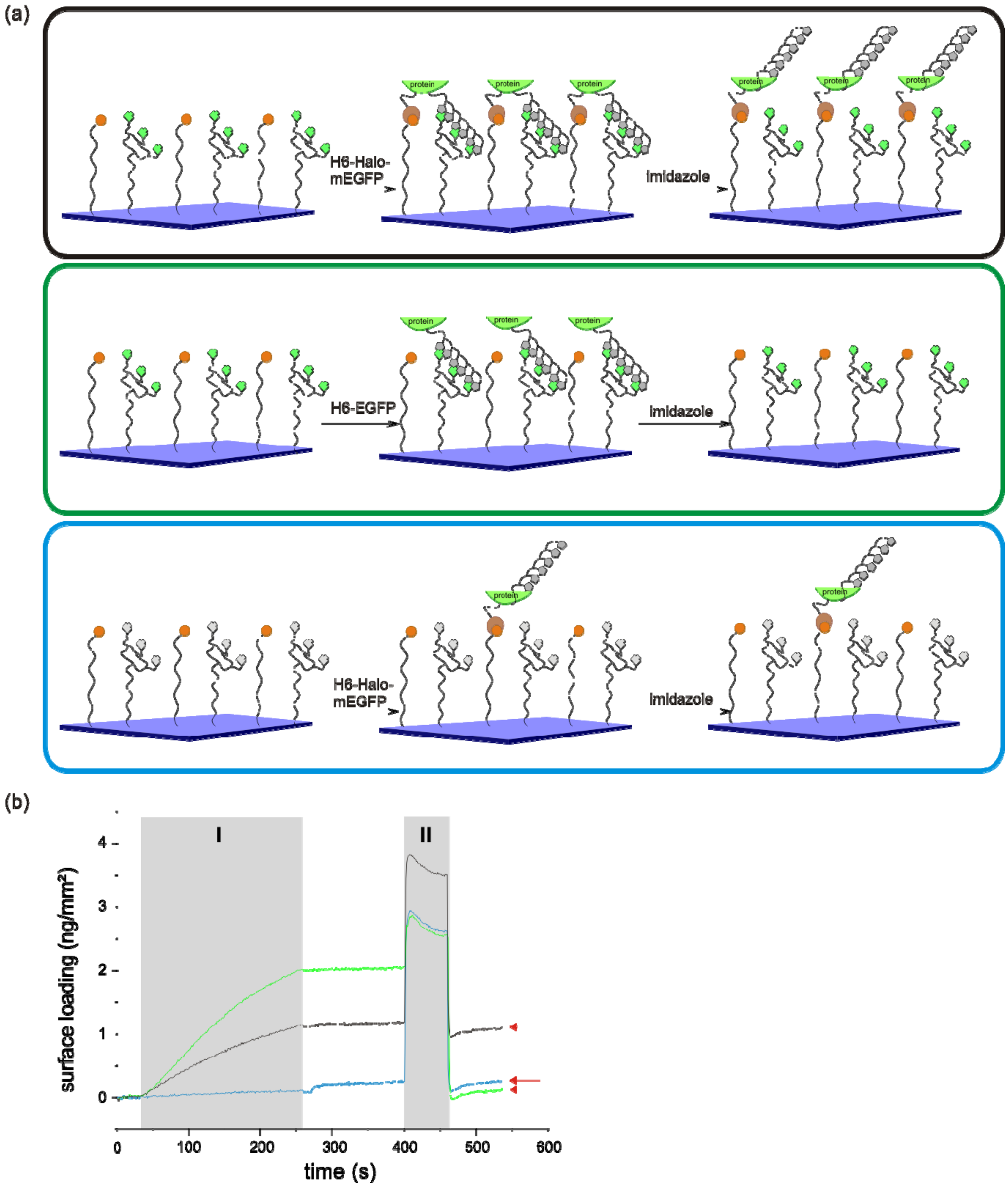

Figure 5.4 Immobilization of His-Halo-tagged proteins. (a) A cartoon representation of the experimental scheme. Surfaces functionalized with tris-NTA and HTL were used to capture H6-Halo-mEGFP (top panel) or H6-EGFP (middle panel) followed by wash with imidazole to remove the His-tag-tris-NTA interaction. H6-Halo-mEGFP was also bound to a similarly functionalized surface but that was devoid of coordinated Ni^{2+} ions (bottom panel). (b) Binding of 200 mM H6-Halo-mEGFP to Ni^{2+} loaded tris-NTA and HTL modified surface (black curve, I), followed by injection of 500 mM imidazole (II) as detected by RIf. As controls, H6-EGFP was injected (green curve, I) on a similar surface and H6-Halo-mEGFP was injected onto a tris-NTA and HTL functionalized surface without coordinated Ni^{2+} (blue curve, I). The grey bars mark the injection periods. The arrows indicate the protein levels after wash with imidazole.

In order to test the applicability of this system to pattern proteins using His_{NVOC}, H6-Halo-mEGFP was injected onto the surface after caging all tris-NTA groups with the peptide (Figure 5.5, red curve). Insignificant protein binding was observed in this case, indicating that the surface could be efficiently blocked by His_{NVOC}.

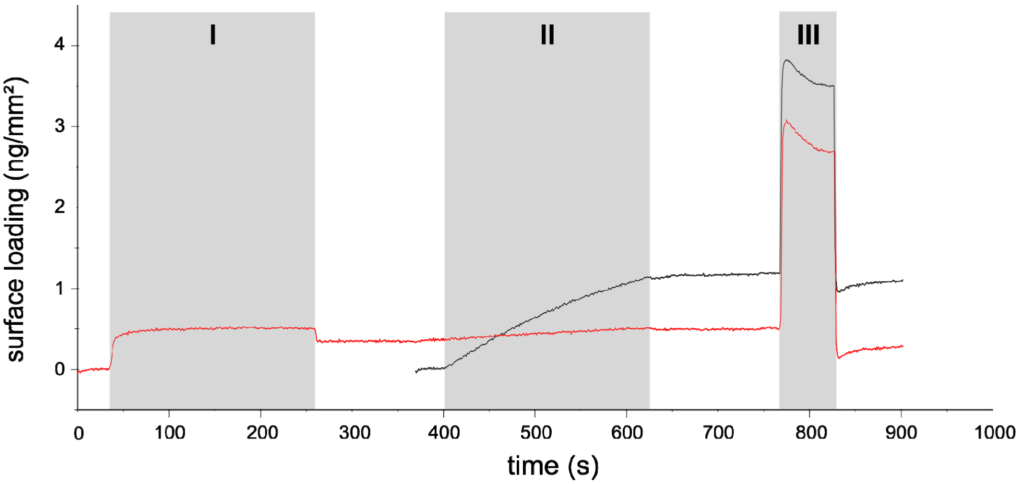

Figure 5.5 Caging efficiency of His_{NVOC}. Binding of His_{NVOC} to a Ni^{2+} loaded tris-NTA and HTL modified surface (red curve, I), followed by injections of 200 nM H6-Halo-mEGFP (II) and 500 mM imidazole (III) as detected by RIf. In comparison, the black curve shows the binding of 200 nM H6-Halo-mEGFP to the surface without prior blocking with the peptide.

5.3.3 Surface immobilization of His-ybbR-tagged proteins

Next, we investigated the immobilization of EGFP carrying an N-terminal hexahistidine-tag followed by a ybbR-tag (H6-ybbR-EGFP) on surfaces modified with tris-NTA and CoA (Figure 5.6). Injection of H6-ybbR-EGFP on a Ni(II) loaded surface in the presence of Sfp and Mg(II) led to significant binding of the protein (black curve). Upon washing with 500 mM imidazole, more than half the bound EGFP remained on the surface, indicating that it was covalently immobilized. In contrast, when EGFP carrying only an N-terminal hexahistidine tag (H6-EGFP) was injected in the presence of Sfp and Mg(II), a high intitial protein binding was observed, all of which was removed by imidazole (green curve). This proved the importance of the ybbR-tag for covalent surface immobilization. As another control, H6-ybbR-EGFP, together with Sfp and Mg(II), was injected onto a tris-NTA and CoA functionalized surface that however did not carry any Ni(II) ions (blue curve). Thus, the His-tag and tris-NTA interaction was abolished, and binding observed was only due to the reaction of ybbR-tag with CoA. Significantly reduced EGFP binding was observed in this case; however all of the bound protein remained on the surface even after washing with imidazole. From these experiments, we concluded that the combined tag leads to almost four times higher covalent immobilization of target proteins as compared to the ybbR-tag alone.

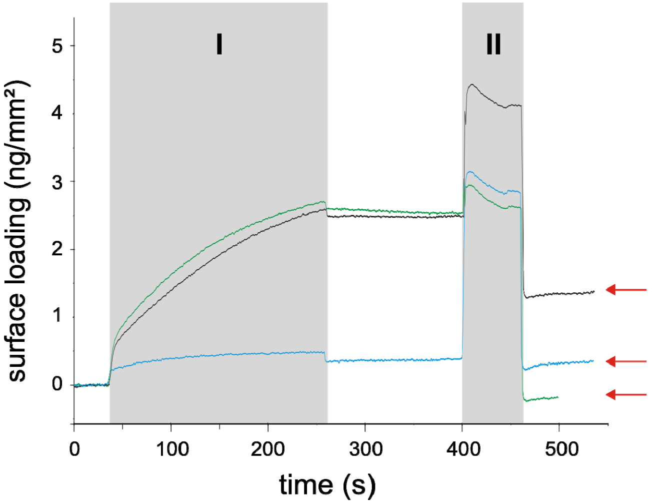

Figure 5.6 Immobilization of His-ybbR-tagged proteins. Binding of 200 mM H6-ybbR-EGFP in solution with 1 µM Sfp and 10 mM Mg^{2+} to a Ni^{2+} loaded tris-NTA and CoA modified surface (black curve, I), followed by injection of 500 mM imidazole (II) as detected by RIf. As controls, H6-EGFP with Sfp and Mg^{2+} was injected (green curve, I) on a similar surface and H6-ybbR-EGFP with Sfp and Mg^{2+} was injected onto a tris-NTA and CoA functionalized surface without coordinated Ni^{2+} (blue curve, I). The grey bars mark the injection periods. The arrows indicate the protein levels after wash with imidazole.

However, since significant protein binding was observed even in the absence of the His-tag-tris-NTA interaction (Figure 5.6, blue curve), this immobilization strategy was not useful for surface patterning using His_{NVOC}. Therefore, we tested if proteins carrying His-ybbR tags could be covalently immobilized in a two-step process: proteins were first captured by the His-tag binding to tris-NTA only. Subsequently Sfp and Mg(II) were injected so as to catalyze the reaction of the ybbR-tag to neighboring CoA moieties (Figure 5.7). This approach was found to be successful, and almost similar binding of H6-ybbR-EGFP was observed after removal of the non-covalently bound fraction with imidazole (black curve). In contrast, when the surface was covered with His_{NVOC}, negligible protein binding could be observed (red curve). Thus this approach to immobilize proteins carrying combined His-ybbR tags was not only useful for increasing the efficiency of protein capture on surfaces, but also promised applications for protein patterning.

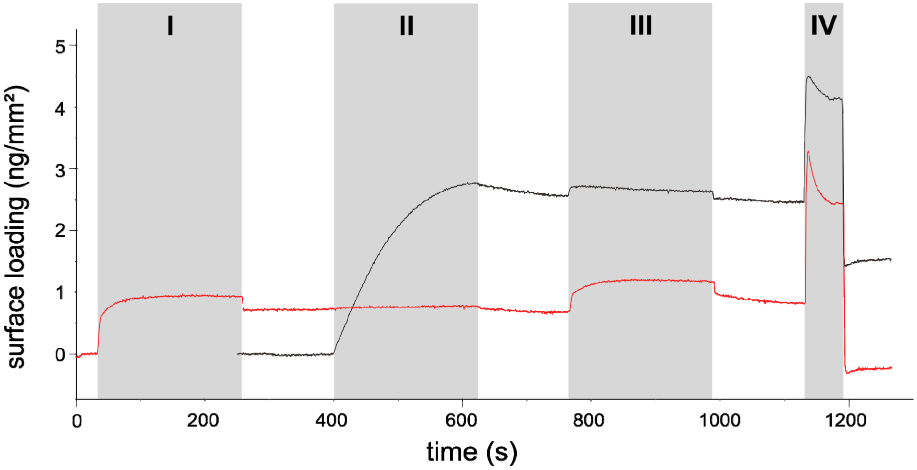

Figure 5.7 Two-step immobilization of His-ybbR tagged proteins. Binding of 200 mM H6-ybbR-EGFP to Ni^{2+} loaded tris-NTA and CoA modified surface (black curve, II), followed by injection of 1 µM Sfp with 10 mM Mg^{2+} (III) and 500 mM imidazole (IV). In order to confirm blocking efficiency of His_{NVOC}, the surface was first blocked with the peptide (red curve, I), followed by injections of H6-ybbR-EGFP (II), Sfp and Mg^{2+} (III) and imidazole (IV). The grey bars mark the injection periods.

5.3.4 Patterning of H6-Halo-mEGFP

Having confirmed the photo-fragmentation of His_{NVOC} in a CLSM, and optimized conditions for covalent immobilization of H6-Halo-mEGFP, we next proceeded to pattern this protein. A scheme similar to that in Figure 4.3 was adopted on surfaces functionalized with tris-NTA and HTL and blocked with His_{NVOC}. Upon scanning a region of interest (ROI) with a 405 nm laser in a CLSM, specific binding of H6-Halo-mEGFP to the region was detected (Figure 5.8a, upper circle). After removal of unbound protein and reblocking with His_{NVOC}, another ROI was scanned and H6-EGFP was bound to the surface (lower circle). Fluorescence signals could be observed in both ROIs, indicating successful protein binding. However, only H6-Halo-mEGFP was immobilized covalently as confirmed by the complete loss in fluorescence signal in the lower ROI upon incubation under imidazole (Figure 5.8b).

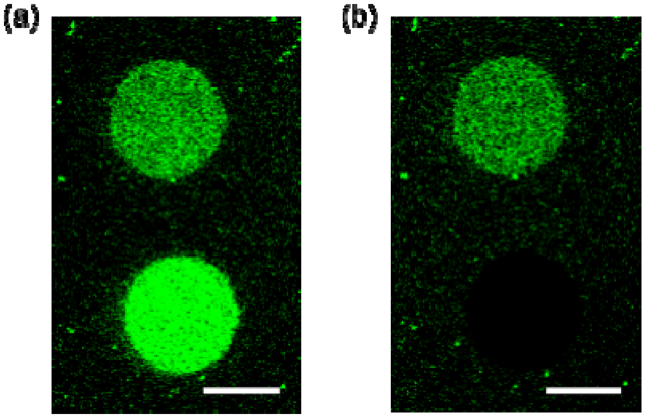

Figure 5.8 Patterning of H6-Halo-mEGFP. (a) CLSM image of a tris-NTA and HTL functionalized surface blocked with His$_{NVOC}$, which was sequentially uncaged by irradiation using a UV laser of a CLSM followed by immobilization of H6-Halo-mEGFP (top circle) and H6-EGFP (bottom circle). (b) The same region after incubation under 500 mM imidazole. Scale bars represent 10 μm.

5.3.5 Patterning of H6-ybbR-EGFP

For patterning H6-ybbR-EGFP on surfaces modified with tris-NTA ad CoA, the two-step immobilization protocol described above was adopted. H6-ybbR-EGFP was targeted to a ROI scanned with the 405 nm laser in a CLSM (Figure 5.9a, upper circle). After removal of unbound protein by washing with HBS, the immobilized protein was covalently bound to the surface by incubation under Sfp and Mg(II). As a control, free tris-NTA sites were again caged with His$_{NVOC}$ and the same protocol was followed for H6-EGFP (lower circle). At the end of these steps, fluorescent signals could be observed in both ROIs indicating protein immobilization in both cases. However, upon washing the surface with imidazole, fluorescence could be detected only in the upper ROI confirming that H6-ybbR-EGFP was immobilized covalently while H6-EGFP was not (Figure 5.9b).

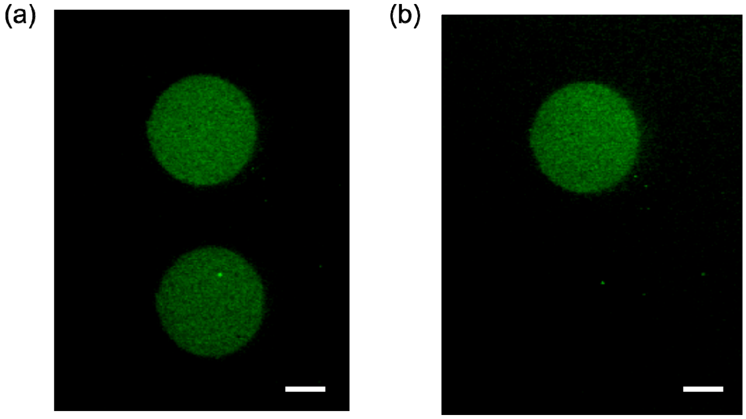

Figure 5.9 Patterning of H6-ybbR-EGFP. (a) CLSM image of a tris-NTA and CoA functionalized surface blocked with $\mathrm{His}_{\mathrm{NVOC}}$, which was sequentially uncaged by irradiation using a UV laser of a CLSM followed by immobilization of H6-ybbR-EGFP (top circle) and H6-EGFP (bottom circle). The two step immobilization protocol consisting of protein binding by His-tag and covalent immobilization via Sfp mediated CoA-ybbR tag reaction was followed. The surface was re-blocked with $\mathrm{His}_{\mathrm{NVOC}}$ between the two protein immobilization steps. (b) The same region after incubation under 500 mM imidazole. Scale bars represent 10 μm.

5.3.6 Functionality of patterned proteins

Having demonstrated the ability to pattern proteins with combined tags in a covalent manner using this strategy, we next proceeded to test the functionality of patterned proteins. For this, we used Interferonα2 receptor, Ifnar2, with an N-terminal ybbR-tag and a C-terminal decahistidine-tag (ybbR-Ifnar2-H10) as a test protein to test its interaction with its ligand. After patterning the protein using its His-tag, it was further covalently immobilized by incubating the surface under Sfp and Mg(II). Non-covalently-bound protein was then removed by washing the surface with imidazole. Binding of interferonα2 mutant-YNS fluorescently-labeled with OG488 ($\mathrm{IFNa2\text{-}YNS}^{\mathrm{OG488}}$) was observed only in the regions that had immobilized Ifnar2 thus confirming that the patterned protein was active (Figure 5.10a). Upon incubating the surface with unlabeled interferonα2, the fluorescence signal quickly diminished indicating that the interaction was specific (Figure 5.10b). This experiment, in addition to confirming protein activity also demonstrated that the two tags when placed at different termini of a protein can still achieve similar function as a contiguous tag.

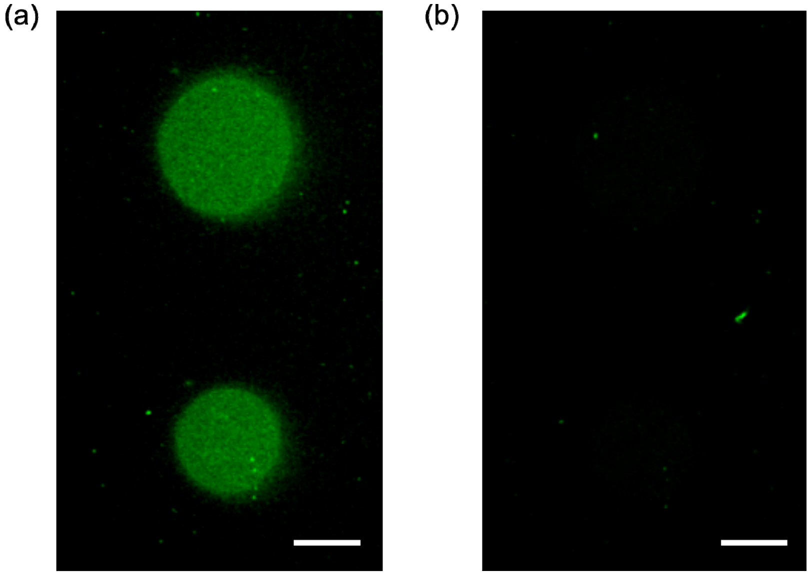

Figure 5.10 Activity of patterned protein. (a) IFNa2-YNS^{OG488} targeted to its receptor ybbR-Ifnar2-H10 patterned on a tris-NTA and CoA modified surface via the two-step immobilization scheme described above. (b) The same region after incubation under unlabeled IFNa2-YNS. Scale bars represent 10 μm.

5.3.7 Multiplexed protein patterning

Next, we attempted to pattern multiple proteins on surfaces in a sequential manner using the combined His-ybbR tag. The first ROI was scanned with the 405 nm laser, followed by immobilization of H6-ybbR-EGFP. Subsequently, the protein was covalently bound by incubating the surface under Sfp and Mg(II) (Figure 5.11a). After blocking free tris-NTA with His$_{NVOC}$, another ROI was scanned and H6-ybbR-mCherry was covalently immobilized in a similar manner. Upon visualization in the CLSM, the two circles with the targeted proteins could be observed (Figure 5.11b). Subsequently, the sequence was repeated again to immobilize H6-ybbR-EGFP in a new ROI to acquire the image shown in Figure 5.11c. Thus, repeated patterning of multiple proteins into flexible user-defined structures was possible using our strategy.

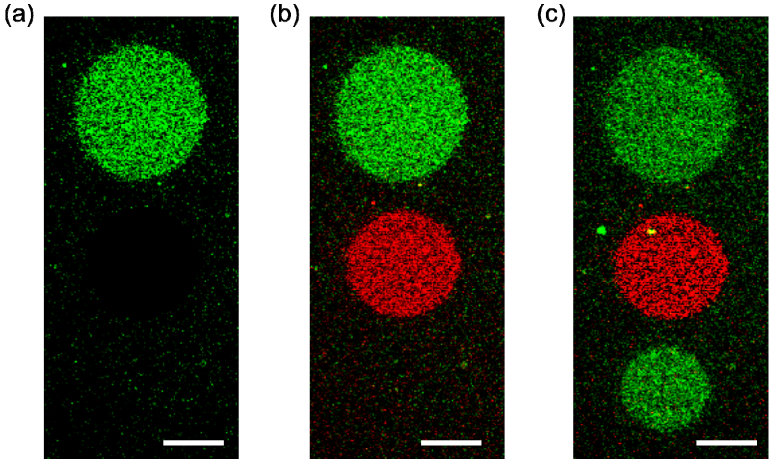

Figure 5.11 Multiplexed protein patterning. Sequential targeting of (a) H6-ybbR-EGFP, (b) H6-ybbR-mCherry followed by (c) H6-ybbR-EGFP again to a tris-NTA and CoA modified surface using the two step protocol described above. Scale bars represent 10 µm.

5.4 Conclusions

Through these experiments we demonstrated that the combination of the His-tag with the ybbR-tag and the Halo-tag allows the covalent immobilization of fusion proteins to suitably functionalized surfaces with much higher efficiencies as compared to the individual tags. This stategy can be further extended to almost all peptide tags, as well as to other protein immobilization approaches that suffer from low binding rate constants. We also took advantage of the His-tag to pattern fusion proteins with such combined tags on the surface using a photo-cleavable Histidine peptide. Rapid targeting of both His-ybbR- and His-Halo-tagged proteins to microstructures that could be flexibly defined with the UV laser of a CLSM was demonstrated. Due to the covalent nature of protein immobilization, multiplexed protein patterns were easily created using sequential irradiation and immobilization steps. Due to the flexibility of this approach with respect to the type of tags that can be used in conjunction with the His-tag, which itself is frequently used for affinity purification of proteins, we anticipate a huge potential for very generic application of this approach.

5.5 Summary

In this chapter we reported the combination of a His-tag with either a Halo- or ybbR-tag as a means to achieve rapid immobilization of fusion protein on surfaces in a covalent manner. The combined tags allowed the covalent immobilization of fusion proteins to suitably functionalized surfaces with much higher efficiencies than the individual tags. Furthermore, photo-fragmentable histidine peptides that had been developed for the patterning of His-tagged proteins on tris-NTA functionalized surfaces could also be used for the patterning of proteins carrying these combined tags. Local irradiation using a UV-laser of a CLSM allowed the creation of multiplexed protein patterns. Protein-protein interaction experiments confirmed that proteins immobilized into patterns retained a high degree of activity.

5.6 References

1. Lisse, D., et al., *Selective targeting of fluorescent nanoparticles to proteins inside live cells.* Angew Chem Int Ed Engl, 2011. **50**(40): p. 9352-5.
2. Los, G.V., et al., *HaloTag: a novel protein labeling technology for cell imaging and protein analysis.* ACS Chem Biol, 2008. **3**(6): p. 373-82.
3. Waichman, S., et al., *Functional immobilization and patterning of proteins by an enzymatic transfer reaction.* Anal Chem, 2010. **82**(4): p. 1478-85.
4. Wong, L.S., J. Thirlway, and J. Micklefield, *Direct site-selective covalent protein immobilization catalyzed by a phosphopantetheinyl transferase.* J Am Chem Soc, 2008. **130**(37): p. 12456-64.
5. Yin, J., et al., *Genetically encoded short peptide tag for versatile protein labeling by Sfp phosphopantetheinyl transferase.* Proc Natl Acad Sci U S A, 2005. **102**(44): p. 15815-20.
6. Lata, S., et al., *High-affinity adaptors for switchable recognition of histidine-tagged proteins.* J Am Chem Soc, 2005. **127**(29): p. 10205-15.
7. Lamken, P., et al., *Ligand-induced assembling of the type I interferon receptor on supported lipid bilayers.* J Mol Biol, 2004. **341**(1): p. 303-18.

8. Piehler, J. and G. Schreiber, *Biophysical analysis of the interaction of human ifnar2 expressed in E. coli with IFNalpha2.* J Mol Biol, 1999. **289**(1): p. 57-67.

9. Lata, S. and J. Piehler, *Stable and functional immobilization of histidine-tagged proteins via multivalent chelator head-groups on a molecular poly(ethylene glycol) brush.* Anal Chem, 2005. **77**(4): p. 1096 -1105.

10. You, C., et al., *Self-controlled monofunctionalization of quantum dots for multiplexed protein tracking in live cells.* Angew Chem Int Ed Engl, 2010. **49**(24): p. 4108-12.

11. Gavutis, M., et al., *Lateral ligand-receptor interactions on membranes probed by simultaneous fluorescence-interference detection.* Biophys J, 2005. **88**(6): p. 4289-302.

12. Gavutis, M., S. Lata, and J. Piehler, *Probing 2-dimensional protein-protein interactions on model membranes.* Nat Protoc, 2006. **1**(4): p. 2091-103.

13. Piehler, J. and G. Schreiber, *Fast transient cytokine-receptor interactions monitored in real time by reflectometric interference spectroscopy.* Anal Biochem, 2001. **289**(2): p. 173-86.

6 Conclusions

This thesis described the development of four different approaches to spatially organize proteins on surfaces. All four approaches utilized highly defined surface chemistry based on a biocompatible PEG polymer brush that has been previously shown to be very efficient at preventing non-specific protein adsorption and at protecting immobilized proteins from denaturation [1]. Protein immobilization was achieved by the use of protein and peptide tags that can be genetically fused to proteins of interest [2-4]. These tags ensured that surface bound proteins were homogenously oriented and active residues were unhindered from access to soluble ligands. The approaches described for surface patterning were all based on photolithography using UV light. All the techniques were compatible with readily available collimated light sources that use xenon or mercury lamps. More flexibility with respect to pattern geometry could be achieved by using a UV laser of a CLSM.

6.1 His-tagged protein patterning by photodestruction of tris-NTA

We utilized a photo-induced Fenton reaction for locally destroying tris-NTA moieties on a surface. This reaction was shown to be highly dependent on the type of transition metal ion that was coordinated to tris-NTA: Cu(I), Fe(II) and Co(II) were shown to be active catalysts while Ni(II) was not. Since the metal ion has to switch between oxidation states during the Fenton reaction, the availability of multiple oxidation states is a possible criterion for the metal ion selectivity [5-7]. The Fenton reaction generated hydroxyl radicals that oxidized and destroyed neighboring tri-NTA moieties thus rendering them incapable of binding His-tagged proteins in a stable manner. UV-irradiation of Co(II) loaded tris-NTA modified surfaces through a photomask allowed the patterning of His-tagged proteins onto non-irradiated regions. Photo-destruction of tris-NTA could also be achieved by scanning selected regions by a UV laser of a CLSM and this was used to flexibly modify a pattern previously acquired by irradiation through a photomask. Finally, this technique was used to pattern His-tagged kinesin on a surface and microtubules were shown to glide along the patterns with a high degree of fidelity in an ATP-dependent manner.

Despite the ease and efficiency of this approach, it is limited to only His-tagged proteins. Moreover, only one protein can be patterned at a time on the surface. As a solution to these drawbacks, we developed an approach based on photo-sensitive caging of the terminal amine groups of the PEG brush used for surface functionalization.

6.2 Binary protein patterning by NVOC-based caging

Surfaces were functionalized with a biocompatible dense PEG polymer brush that presented terminal amine groups for further functionalization. We demonstrated that these amine groups were very efficiently protected after reaction with nitroveratryloxycarbonyl (NVOC) [8]. Upon UV irradiation, up to 75% of the surface amines could be uncaged as confirmed by solid phase protein binding assays. Sequential irradiation through a photomask and reaction with biotin and coenzyme A (CoA) allowed the patterning of streptavidin and a ybbR-tagged protein on a surface [4]. Interaction assays between soluble interferon-α2 and its patterned receptor confirmed that proteins retained a high degree of activity even after patterning. Since the amine group can be further reacted to get diverse functional moieties on the surface, this approach should allow not only the patterning of proteins with different peptide tags, but also be applicable for patterning other biochemical molecules such as DNA and lipids, and even cells.

In spite of these advantages, this technique can be used to pattern at most two proteins on a surface. However, many applications require the organization of multiple proteins on the same surface. Furthermore, the patterned surface has to be functionalized with protein capturing groups prior to immobilization. Thus, it is not possible to have simultaneous temporal and spatial control over protein immobilization using this approach. In a bid to overcome these constraints, we developed a strategy based on photo-fragmentable His-tags as caging groups for tris-NTA modified surfaces.

6.3 Multiplexed protein patterning by photo-fragmentations of histidine peptides

A peptide with the sequence $(HHH\Phi)_3HHH$ where ‘Φ’ stands for 3-amino-3-(2-nitrophenyl)-propionic acid, was confirmed to be very efficient at protecting tris-NTA modified surfaces from the binding of His-tagged proteins. UV-irradiation of the peptide caused efficient fragmentation and loss in surface protection efficiency. UV-irradiation of a peptide caged surface under a photomask in the presence of a free radical quencher (1,4-benzoquinone) caused localized peptide-fragmentation and allowed the targeting of His-tagged proteins into the irradiated regions. In a CLSM, selected regions could be scanned with a 405 nm laser beam in order to pattern proteins with a high spatial and temporal control. Finally, sequential uncaging and protein binding allowed the creation of multiplexed protein microstructures on a surface.

Although this technique of laser lithography enabled the assembly of versatile, user-defined protein micropatterns under physiological conditions with a standard confocal laser-scanning microscope, its disadvantage was that proteins were bound in a non-covalent manner. Thus, protein binding stability was sensitive to transition metal ions and their chelators as well to other proteins with histidines. This caused problems for multiplexed protein patterning as the exposure of the surface to a new His-tagged protein led to partial displacement of previously immobilized proteins from the surface. Although several peptide and protein tags are available to immobilize proteins covalently and thus overcome this drawback, there is a lack for generic patterning approaches for multiplexed patterning of proteins fused to such tags. Furthermore, the reactions of almost all such tags with their specific ligands suffer from slow binding kinetics and thus require comparatively large protein concentrations for surface immobilization. All of these limitations were elegantly overcome by using combined tags comprising of a His-tag and another tag such as a ybbR- or Halo-tag for covalent protein patterning on suitably functionalized surfaces.

6.4 Combining peptide tags for improving immobilization efficiencies and micropatterning of proteins

On surfaces simultaneously modified with tris-NTA together with either Halo-tag ligand or CoA, proteins with combined His-Halo or His-ybbR tags could be covalently immobilized with much greater efficiencies as compared to proteins with the Halo-tag or the ybbR-tag alone. This is because the His-tag-tris-NTA interaction, which has a high association rate constant (~ 10^5 $M^{-1}s^{-1}$) [2], quickly increases the local protein concentration on the surface. Due to this, the rate of the second reaction that covalently binds the protein is significantly increased as compared to what it would be if the protein was in solution. Taking advantage of the His-tag, such proteins could also be patterned by using a photo-fragmentable peptide as previously described. Thus stable multiplexed protein patterns could be created that were resistant to all the agents mentioned above.

As protein immobilization based on the His-tag/Ni(II) interaction is bioorthogonal in nature, experiments to evaluate the suitability of this approach to covalently pattern fusion proteins from complex mixtures such as a cell lysate are planned in the future.

6.5 References

1. Piehler, J., et al., *A high-density poly(ethylene glycol) polymer brush for immobilization on glass-type surfaces.* Biosens Bioelectron, 2000. **15**(9-10): p. 473-81.

2. Lata, S., et al., *High-affinity adaptors for switchable recognition of histidine-tagged proteins.* J Am Chem Soc, 2005. **127**(29): p. 10205-15.

3. Los, G.V., et al., *HaloTag: a novel protein labeling technology for cell imaging and protein analysis.* ACS Chem Biol, 2008. **3**(6): p. 373-82.

4. Yin, J., et al., *Genetically encoded short peptide tag for versatile protein labeling by Sfp phosphopantetheinyl transferase.* Proc Natl Acad Sci U S A, 2005. **102**(44): p. 15815-20.

5. Ciesla, P., et al., *Homogeneous photocatalysis by transition metal complexes in the environment.* Journal of Molecular Catalysis a-Chemical, 2004. **224**(1-2): p. 17-33.

6. Leonard, S., et al., *Cobalt-mediated generation of reactive oxygen species and its possible mechanism.* Journal of Inorganic Biochemistry, 1998. **70**(3-4): p. 239-244.

7. Urbanski, N.K. and A. Beresewicz, *Generation of (OH)-O-. initiated by interaction of Fe2+ and Cu+ with dioxygen; comparison with the Fenton chemistry.* Acta Biochimica Polonica, 2000. **47**(4): p. 951-962.

8. Corrie, J.E.T., et al., *Photoremovable Protecting Groups Used for the Caging of Biomolecule.* Dynamic Studies in Biology. 2005, Wiley-VCH Verlag GmbH & Co. KGaA. p. 1-94.

7 Summary

My PhD research aimed to establish generic techniques based on photolithography which could be used to control the spatial as well as temporal organization of recombinantly expressed proteins on surfaces. This thesis describes in detail four strategies that I developed for achieving this goal. In the first approach a photo-induced Fenton reaction was used to selectively destroy tris(nitrilotriacetic acid) (tris-NTA) moieties on a surface. UV-irradiation through a photomask allowed localized photo-destruction and targeting of His-tagged proteins to non-irradiated regions. Photo-destruction could also be achieved by scanning selected regions with the UV laser of a confocal laser scanning microscope (CLSM) thus allowing flexible creation and modification of protein patterns. The second strategy was based on a photosensitive protection group- nitroveratryloxycarbonyl chloride (NVOC-Cl), which was used to cage amine groups on a surface. Sequential uncaging by UV-irradiation through a photomask followed by reactions with biotin and coenzyme A was used to pattern streptavidin and ybbR-tagged proteins into microstructures. In the third approach a photo-fragmentable Histidine peptide was used to block tris-NTA surfaces against binding of His-tagged proteins. UV-irradition through a photomask or by using a UV laser in a CLSM cleaved the peptide into short fragments which quickly dissociated from the surface due to loss in multivalency. His-tagged proteins could be efficiently targeted into irradiated regions even from a complex cell lysate. Sequential uncaging and immobilization allowed the construction of multiplexed protein patterns with a high degree of temporal control. The fourth strategy used combined peptide tags comprising of a His-tag as well as a Halo- or ybbR-tag to achieve rapid covalent immobilization of recombinant fusion proteins on surfaces functionalized with specific ligands. Furthermore, photo-fragmentable histidine peptides that had been used for the patterning of His-tagged proteins on tris-NTA functionalized surfaces could also be used for controlling the spatio-temporal organization of proteins carrying these combined tags.

Therefore, the techniques developed in this thesis enabled the photolithographical micropatterning of recombinant proteins on surfaces in a functional manner. Due to the generic nature of immobilization strategies, coupled with the ease of patterning, highly versatile applications of these methods both in fundamental as well as bio-technological research can be envisioned.

8 Appendix

8.1 Publications

1. Alvarez, M., et al., *Modulating Surface Density of Proteins via Caged Surfaces and Controlled Light Exposure.* Langmuir, 2011. **27**(6): p.2089-95.

2. Waichman, S., et al., *Maleimide photolithography for single-molecule protein-protein interaction analysis in micropatterns.* Anal Chem, 2011. **83**(2): p. 501-8.

3. Bhagawati, M., et al., *Native laser lithography of His-tagged proteins by uncaging of multivalent chelators.* J Am Chem Soc, 2010. **132**(17): p. 5932-3.

4. Waichman, S., et al., *Functional immobilization and patterning of proteins by an enzymatic transfer reaction.* Anal Chem, 2010. **82**(4): p. 1478-85.

5. Bhagawati, M., et al., *Organization of motor proteins into functional micropatterns fabricated by a photoinduced Fenton reaction.* Angew Chem Int Ed Engl, 2009. **48**(48): p. 9188-91.

6. You, C., et al., *Affinity capturing for targeting proteins into micro and nanostructures. Anal Bioanal Chem,* 2009. **393**(6-7): p. 1563-70.

8.2 List of figures and tables

FIGURE 1.1 SURFACE ARCHITECTURE. 3
FIGURE 1.2 ‘MUSHROOMS’ VERSUS ‘POLYMER BRUSHES’. 5
FIGURE 1.3 SCHEMATIC DEPICTION OF AN ALKYLSILOXANE SAM ON GLASS....6
FIGURE 1.4 BIOTIN/ STREPTAVIDIN-BASED IMMOBILIZATION. 10
FIGURE 1.5 HIS-TAG/ TRANSITION METAL ION-BASED IMMOBILIZATION. 11
FIGURE 1.6 HALOTAG/ HALOTAG LIGAND-BASED IMMOBILIZATION. 12
FIGURE 1.7 YBBR TAG/ COA-BASED IMMOBILIZATION. 14
FIGURE 1.8 JABLONSKI DIAGRAM. 17
FIGURE 1.9 STRATEGIES FOR PHOTOCHEMICAL PROTEIN PATTERNING. 20

FIGURE 1.10 PRINCIPLE OF RIFS DETECTION 23

FIGURE 1.11 CONFOCAL LASER SCANNING MICROSCOPY. 26

FIGURE 2.1 CHARACTERIZATION OF NTA-PHOTODESTRUCTION BY THE LIGHT-INDUCED FENTON REACTION. 41

FIGURE 2.2 SCHEMATIC ILLUSTRATION OF THE PATTERNING PROCESS. 42

FIGURE 2.3 FUNCTIONAL SURFACE MICROPATTERNING BY ILLUMINATION THROUGH A MASK. 43

FIGURE 2.4 SCHEMATIC ILLUSTRATION OF PATTERNING USING THE UV LASER OF A CLSM. 44

FIGURE 2.5 IN *SITU* PATTERNING OF TRIS-NTA SURFACES IN A CLSM. 45

FIGURE 2.6 COMBINING PHOTOMASK- AND CLSM- BASED PATTERNING. 46

FIGURE 2.7 TRANSPORT OF MICROTUBULES BY PATTERNED KINESIN. 47

FIGURE 3.1 CAGING OF SURFACE AMINES BY NVOC-CHLORIDE. 58

FIGURE 3.2 SCHEMATIC OF THE PATTERNING PROCESS. 59

FIGURE 3.3 BINARY PROTEIN PATTERNING. 60

FIGURE 4.1 THE PHOTOCLEAVABLE PEPTIDE. 69

FIGURE 4.2 BLOCKING OF TRIS-NTA FUNCTIONALIZED SURFACES BY THE □-HIS-PEPTIDE. 70

FIGURE 4.3 SCHEMATIC ILLUSTRATION OF THE PATTERNING METHOD. 71

FIGURE 4.4 PROTEIN PATTERNING BY UV IRRADIATION THROUGH A PHOTOMASK. 72

FIGURE 4.5 PROTEIN PATTERNING BY LASER LITHOGRAPHY. 73

FIGURE 4.6 PROTEIN PATTERNING BY LASER LITHOGRAPHY. 74

FIGURE 4.8 SEQUENTIAL PATTERNING OF MULTIPLE PROTEINS . 75

FIGURE 5.1 COMBINED PEPTIDE TAGS. 80

FIGURE 5.2 THE PHOTOCLEAVABLE PEPTIDE. 83

FIGURE 5.3 PATTERNING USING HIS$_{\text{NVOC}}$. 84

FIGURE 5.4 IMMOBILIZATION OF HIS-HALO-TAGGED PROTEINS. 86

FIGURE 5.5 CAGING EFFICIENCY OF HIS$_{\text{NVOC}}$. 87

FIGURE 5.6 IMMOBILIZATION OF HIS-YBBR-TAGGED PROTEINS. 88

FIGURE 5.7 TWO-STEP IMMOBILIZATION OF HIS-YBBR TAGGED PROTEINS. 89

FIGURE 5.8 PATTERNING OF H6-HALO-MEGFP. 90
FIGURE 5.9 PATTERNING OF H6-YBBR-EGFP. 91
FIGURE 5.10 ACTIVITY OF PATTERNED PROTEIN. 92
FIGURE 5.11 MULTIPLEXED PROTEIN PATTERNING. 93
TABLE 1.1 ATTRIBUTES OF THE DIFFERENT PROTEIN IMMOBILIZATION APPROACHES 14

8.3 Abbreviations

CLSM	confocal laser scanning microscopy
DAPEG	diamino poly(ethylene glycol)
DPN	dip pen nanolithography
ECM	extra cellular matrix
HTL	HaloTag ligand
HTP	HaloTag protein
mAb	monoclonal antibody
MCH	multivalent chelator head
MPA-NHS	3-(Maleimido)propionic acid N-hydroxysuccinimide ester
NVOC	nitroveratryloxycarbonyl
PCG	protein capturing group
PPT	phosphopantetheinyl transfer
RIf(S)	reflectometric interference (spectroscopy)
SAM	self assembled monolayer
SAv	streptavidin
SIP	surface initiated polymerization
TIRFS	total internal reflection fluorescence spectroscopy
tris-NTA	tris(nitrilotriacetic acid)

Curriculum Vitae

NAME	Maniraj Bhagawati
DATE OF BIRTH	30th October, 1984
CONTACT DETAILS	Department of Biophysics University of Osnabrueck Barbarastrasse 11 49076 Osnabrueck, Germany

EDUCATION

2007- Present PhD, Biophysics, University of Osnabrueck, Germany

Thesis title: “Photolithographic surface functionalization for spatio-temporal control over protein immobilization”

2003- 2007 BTech, Biotechnology, Indian Institute of Technology, Kharagpur, India

Thesis title: “Screening of small molecular weight compounds from edible mushrooms for anti-cancer properties”

HONOURS AND AWARDS

2010 Best poster award in the Division of Colloid and Surface Chemistry

239th ACS National Meeting and Exposition, San Francisco

2007- 2008 Graduate research fellowship

Center for Membrane Proteomics

Johann Wolfgang Goethe University, Frankfurt am Main, Germany

RESEARCH EXPERIENCE

2007- Present **Graduate Student**
University of Osnabrueck, Germany, with Professor Jacob Piehler

2006- 2007 Undergraduate Research Assistant

Indian Institute of Technology, Kharagpur India, with Professor T. K. Maiti

2006 **Summer Intern**
Institute of Genomics and Integrative Biology, New Delhi India, with Dr. Dwaipayan Bharadwaj

Declaration

I hereby declare that the presented thesis 'Photolithographic surface functionalization for spatio-temporal control over protein immobilization' was prepared entirely on my own and I have not used outside sources without declaration in the text. Any concepts or quotations applicable to these sources are clearly attributed to them. I have not attempted a promotion before.

Osnabrueck, 21st December 2011 Maniraj Bhagawati